SUPERCONDUCTIVITY AND THE STRUCTURAL PHASE TRANSITIONS IN PALLADIUM HYDRIDE AND PALLADIUM DEUTERIDE

BY

ROBERT WENDELL STANDLEY

B.S., California Institute of Technology, 1974
M.S., University of Illinois, 1975

THESIS

Submitted in partial fulfillment of the requirements
for the degree of Doctor of Philosophy in Physics
in the Graduate College of the
University of Illinois at Urbana-Champaign, 1980

Urbana, Illinois

DISCLAIMER

SUPERCONDUCTIVITY AND THE STRUCTURAL PHASE TRANSITIONS IN PALLADIUM HYDRIDE AND PALLADIUM DEUTERIDE

BY

ROBERT WENDELL STANDLEY

B.S., California Institute of Technology, 1974
M.S., University of Illinois, 1975

THESIS

Submitted in partial fulfillment of the requirements
for the degree of Doctor of Philosophy in Physics
in the Graduate College of the
University of Illinois at Urbana-Champaign, 1980

Urbana, Illinois

SUPERCONDUCTIVITY AND THE STRUCTURAL PHASE TRANSITIONS IN PALLADIUM HYDRIDE AND PALLADIUM DEUTERIDE

Robert Wendell Standley, Ph.D.
Department of Physics
University of Illinois at Urbana-Champaign, 1980

The results of two experimental studies of the superconducting transition temperature, T_c, of palladium hydride, PdH_x, and palladium deuteride, PdD_x, are presented.

In the first study, the superconducting transition temperature of $PdH_x(D_x)$ is studied as a function of H(D) concentration, x, in the temperature range from 0.2 K to 4 K. The data join smoothly with those reported previously by Miller and Satterthwaite at higher temperatures, and the composite data are described by the empirical relation $T_c = 150.8\ (x-x_o)^{2.244}$, where $x_o = 0.715$ for hydride samples and 0.668 for deuteride samples. The results, when compared with the theoretical predictions of Klein and Papaconstantopoulos, et al., raise questions about the validity of their explanation of the reverse isotope effect, which is based solely on a difference in force constants.

In the second study, the effect of the order-disorder structural transition associated with the "50 K anomaly" on the superconductivity of $PdH_x(D_x)$ is investigated. Samples were quenched to low temperatures in the disordered state, and their transition temperatures measured. The samples were then annealed just below the anomaly temperature, and the ordering process followed by monitoring the change in

sample resistance. The transition temperatures in the ordered state were then measured.

In a $PdD_{0.817}$ sample, the formation of a long-range ordered structure in the deuterium sublattice led to a 9.2% reduction in T_c. In a $PdH_{0.837}$ sample, the formation of a long-range ordered structure led to a splitting of the superconducting transition, roughly half of the transition being depressed by $\sim$ 9%, the other half remaining unchanged. This splitting is interpreted as arising from the coexistence of ordered and disordered domains. In a $PdD_{0.742}$ sample, long-range order did not develop, but an enhancement of short-range order occurred, which led to a 7.5% increase in T_c. In all cases the changes in the superconducting transitions were reversible, the transitions reverting to their original values when the samples were again disordered at the end of each run. These results are discussed in the framework of the "local structural excitation" model proposed by Ngai and Reinecke. In both studies, samples were prepared from Pd foils loaded with H(D) electrolytically. The superconducting transitions were monitored by measurement of the diamagnetic susceptibility of the samples, using an a.c. mutual inductance method.

ACKNOWLEDGMENTS

A great many people have contributed in a variety of ways to the work presented in this thesis, for which they have my gratitude.

I would particularly like to thank my research advisor, Dr. C. B. Satterthwaite, for his counsel and encouragement during the course of this work. Special thanks also go to Dr. T. O. Brun and Dr. D. M. Ginsberg for acting as my advisors during periods of Dr. Satterthwaite's absence.

The experimental work presented in Chapter III was done in collaboration with Dr. M. Steinback, whose knowledge of low temperature techniques, together with his sense of humor, greatly aided in the gathering of the data. I would like to thank Dr. A. C. Anderson for his cooperation in this phase of the experimental work, and also for the wealth of advice he provided me on several other occasions.

Much of the resistivity data presented in Chapter IV were collected with the able assistance of R. C. Potter and M. E. Misenheimer.

The neutron diffraction data on PdD_x were graciously supplied by Dr. M. H. Mueller and Dr. T. O. Brun of Argonne National Laboratory, and also by Dr. R. Klemencic of the Universitat der Wien. I enjoyed several stimulating discussions with these people in our attempts to understand the ordered phases of $PdH_x(D_x)$.

I enjoyed a lively exchange of information with fellow graduate students A. D. Bross, P. C. Allen, D. Alde, M. Jackson, T. E. Ellis,

L. E. Storm, R. C. Potter, J. Oberschmidt, J. Katerberg, B. W. Nedrud, my juggling partner G. L. Koos, and J. Legrange, who read part of this manuscript and made valuable comments on it.

For their warm friendship and moral support, I especially thank E. A. Dorsey, R. and K. Muniz, and A. D. Bross.

Most of all, I wish to thank my parents for their unwavering love, guidance, and encouragement, and without whom, ultimately, I would not have been possible.

This material is based upon work supported by the National Science Foundation under grants DMR 75-13083, DMR 77-08463 and DMR 77-23999. The experimental work in Chapter III was also supported in part by Department of Energy grant EY-76-C-02-1198.

TABLE OF CONTENTS

I. INTRODUCTION

The words "metal hydrides" encompass a broad variety of materials with diverse properties. In fact, the majority of metals in the periodic table, and numerous alloys, will react with hydrogen to form metal hydrides.[1/] While several of these metal-hydrogen systems were known in the last century, they aroused only limited scientific interest due to a lack of commercial and technological relevance. Within the last forty years, however, the metal hydrides have become important facets of several emerging technologies, and as such have become the focus of an extensive research effort.

The initial impetus to this effort arose from the need to understand the mechanism by which hydrogen embrittles certain metals, notably steels, degrading their mechanical properties. Hydrogen embrittlement remains a problem of great practical importance, and hence an area of active research. More recently, metal hydrides are playing an increasing role in many energy-related technologies. For instance, because many metal hydrides have very high proton densities (often higher than that of liquid H_2) and protons have large neutron scattering cross sections, metal hydrides have been considered for use as neutron moderators in nuclear fission reactors. In most of the current designs for controlled nuclear fusion reactors, the containment, or "first wall," material which contains the reacting plasma will be subjected to a high flux of deuterons and tritons, making it imperative to understand

the interactions between these hydrogen isotopes and the containment structure.

Another promising approach to many energy problems is the proposed "hydrogen-based energy economy" in which energy is used to generate hydrogen gas from water, coal or other sources. The hydrogen may then be stored or transported, and then recombined with oxygen to yield chemical energy when and where it is needed. By virtue of their large proton densities and modest hydrogen absorption-desorption temperatures and pressures, some metal hydrides may make ideal hydrogen storage media for certain applications, obviating the cryogenic equipment necessary for liquid hydrogen storage, and inherently safer and more energy efficient than storing hydrogen as a highly compressed gas.

The fact that the absorption and desorption pressures of metal hydrides are strong functions of temperature and alloy composition has also been utilized in several ingenious thermodynamic cycles, such as "solid state" heat engines, hydrogen compressors and methods of upgrading low grade waste heat to more useable temperatures. In all of these schemes, it will be necessary to know how hydrogen interacts with all of the metal components in the systems.

Discounting the technological stimuli, the basic properties of metal hydrides have proved worthy of study in their own right. For example, the masses of the various hydrogen isotopes differ by a factor of two or three, instead of a few percent, as is the case with the isotopes of heavier nuclei. Thus, when one isotope of hydrogen is substituted for another in a metal hydride, very large and often anomalous "isotope effects" can result. The small masses of the hydrogen isotopes also

lead to important "quantum crystal" effects, such as proton tunneling and delocalization, and large zero point motion amplitudes, all of which may have marked effects on the physical properties of the material.

Because interstitial metal hydrides can exist at substoichiometric compositions (i.e., not all interstitial sites are occupied by hydrogen atoms) and hydrogen in the lattice is very mobile, many metal hydrides exhibit order-disorder transformations, the material passing from a phase in which hydrogen atoms occupy interstitial sites at random into a phase in which they occupy a specific subset of interstitial sites with a lower crystal symmetry as the temperature is decreased.

Finally, in recent years it has been found that hydrogen can have a profound effect on the superconducting properties of the host metal. In most cases, the addition of hydrogen has a deleterious effect on the superconducting properties of the host material, yet in a few metals and alloys it greatly enhances superconductivity.

An excellent collection of review articles on the basic properties and applications of metal hydrides has recently appeared, to which the reader is directed for further information on these topics.[2/]

In many respects, palladium hydride, PdH_x, is a model metal-hydrogen system. Since the discovery, more than a century ago, that palladium absorbs large amounts of hydrogen gas,[3/] the Pd-H system has been intensively investigated; to date it is the most thoroughly studied metal-hydrogen system. While this abundant literature provides a solid foundation on which to build a theoretical understanding of PdH_x, it does not imply that such an understanding has already been reached. In the past twenty-five years, PdH_x has been found to exhibit nearly all of the

phenomena which are so intriguing in metal hydrides, viz. enhancement of superconductivity by the addition of hydrogen, order-disorder transformations involving the hydrogen atoms, and anomalous isotope effects in such properties as diffusion and superconductivity related to the quantum nature of the light atoms. An understanding of these phenomena is only recently emerging.

The aim of the experimental work presented in this thesis is to investigate more fully (1) the superconducting behavior of $PdH_x(D_x)$, in particular the "reverse" isotope effect when deuterium is substituted for hydrogen, and (2) the order-disorder transition associated with the "50 K anomaly" and its effect on the superconducting transition.

Chapter II presents an introduction to the basic physical properties of the Pd-H(D) system, in order to provide a framework for discussion of the experimental results in subsequent chapters.

After a brief survey of superconductivity in metal hydrides, Chapter III focuses on the superconducting properties of $PdH_x(D_x)$ and the various theoretical attempts to explain them. We then present the results of measurements of the superconducting transition temperature of $PdH_x(D_x)$ as a function of H(D) concentration in the temperature range from 0.2 K to 4 K and discuss how these results bear upon current theoretical treatments.

Chapter IV begins with an introduction to the empirical relationship between high superconducting transition temperatures and structural instabilities in metals. This is followed by a description of the nature of the structural phase transitions associated with the "50 K

anomaly" in $PdH_x(D_x)$. Measurements of the effects of these phase transitions on the superconducting transition temperature of $PdH_x(D_x)$ are then presented, followed by a discussion of mechanisms which might account for these effects.

Finally, Chapter V summarizes the results of this research and the conclusions drawn from them.

II. THE Pd-H(D) SYSTEM

Pure Palladium

Palladium is a group VIII transition metal which forms a face centered cubic (FCC) crystal with a lattice constant of 3.889 Å at room temperature.[4]

While atomic Pd has a $4d^{10}\ 5s^{0}$ electronic configuration (filled 4d-shell), deHaas-Van Alphen measurements on Pd demonstrate that, in the metallic state, the 4d-band is not filled, but contains about 0.36 holes per Pd atom.[5] Band structure calculations indicate that in Pd metal, the 5s- and 5p-states hybridize to form a broad s-p band which overlaps the narrow d-band and which is populated partly at the expense of the d-band.[6] This incomplete filling of the d-band has profound effects on the properties of Pd metal. The Fermi energy lies just below the top of the d-band, and just above a sharp peak in the d-band density of states, producing a large value of N(0), the electronic density of states at the Fermi level, as shown in Figure 3a. This large value of N(0), together with a strong exchange interaction between electrons, places Pd very close to the ferromagnetic instability; while long range ferromagnetic ordering in Pd is absent, neutron scattering data indicate a substantial short range ordering of electron spins, extending over distances of $\sim$ 10 Å.[7] These large spin fluctuations, or paramagnons, produce a large Stoner enhancement of the magnetic susceptibility, and also presumably account for the lack of superconductivity in pure Pd, as will be discussed more fully in the next chapter. Because of this

strong exchange interaction, Pd was considered a likely candidate for a triplet-state superconductor, in which the electrons form Cooper pairs in a triplet spin state, as do the nuclei in superfluid He^3, rather than a singlet spin state, as in other superconductors. A low temperature search for superconductivity in Pd showed no evidence of either singlet or triplet state superconductivity to temperatures as low as 1.7 mK.[8]

Structure of $PdH_x(D_x)$

When hydrogen (or deuterium) is introduced to palladium, it is readily dissociated and absorbed into the Pd lattice, which remains FCC but expands to a maximum lattice constant of 4.090 Å (4.084 Å) for stoichiometric PdH (PdD) at 77 K.[9] Neutron diffraction studies[10] reveal that the H(D) atoms occupy only the octahedral interstitial sites of the Pd lattice. Collectively, these octahedral sites form a second FCC lattice which interpenetrates the FCC Pd lattice, and at stoichiometry (all octahedral sites filled) PdH(D) has the simple NaCl (B1) structure.

$PdH_x(D_x)$ can exist at substoichiometric compositions also, by filling only a fraction, x (= the ratio of H(D) atoms to Pd atoms), of the octahedral sites. At high temperatures the fraction of octahedral sites occupied can be varied continuously from zero to one, but at temperatures below $\sim$ 300°C a miscibility gap occurs in the phase diagram, and samples of intermediate compositions will undergo a phase separation into regions of H(D)-poor material (the α-phase, with $x \sim 0.01$) and H(D)-rich material (the β-phase, with $x \sim 0.60$), as shown in Figure 1. For compositions greater than $\sim$ 0.60, a sample will be

Figure 1. High temperature phase diagram of the Pd-H system in the temperature-composition plane. The phase diagram of the Pd-D system is nearly identical, with slight differences in the location of the critical point.

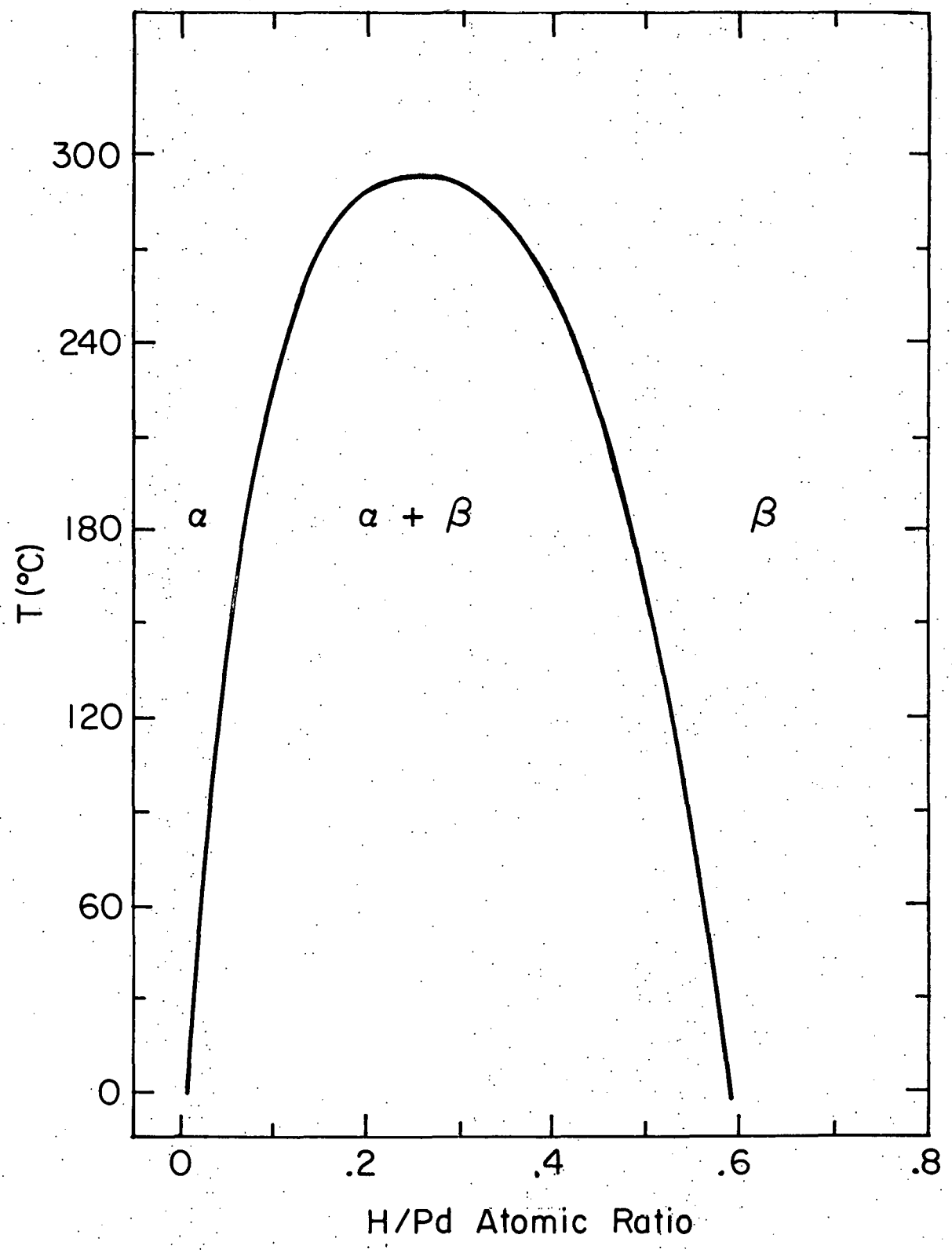
300
240
180
120
60
0
T (°C)
α
α + β
β
0
.2
.4
.6
.8
H/Pd Atomic Ratio

purely in the β-phase to low temperatures ($T \lesssim 100$ K) when new phases associated with the order-disorder transitions are encountered. The phenomena of interest in this thesis, superconductivity and the order-disorder transitions, are properties of the β-phase, so in subsequent discussion we will neglect the α-phase and two-phase regions of the phase diagram and restrict ourselves to the properties of samples with compositions between 0.6 and 1.0.

As previously mentioned, the uptake of H(D) results in an expansion of the FCC lattice. In the β-phase, the lattice constant of $PdH_x(D_x)$ increases nearly linearly with x from a value of 4.019 Å (4.016 Å) at $x \gtrsim 0.6$ to 4.090 Å (4.084 Å) at $x = 1.0$. The smaller lattice constant of the deuteride relative to a hydride of the same composition is attributed to the smaller zero-point motion amplitude in the lattice of the more massive deuteron.

Phonon Modes of $PdH_x(D_x)$

Changes in the phonon spectrum upon formation of β-phase $PdH_x(D_x)$ have been monitored by a variety of techniques. Low temperature specific heat measurements[11-15] on $PdH_x(D_x)$ indicate a Debye temperature, $\Theta_D \gtrsim 275$ K, which is nearly identical for that of pure Pd, at 271 K. That the long wavelength acoustic modes (of which Θ_D is a measure) of Pd and $PdH_x(D_x)$ are so similar is rather surprising in light of the substantial increase in lattice parameter; apparently the new H(D)-Pd bonding compensates for the decrease in Pd-Pd bonding due to lattice expansion. Inelastic neutron scattering measurements[16] on $PdD_{0.63}$ show a substantial softening (20-30%) of the acoustic modes near the Brillouin zone (B.Z.) boundary relative to pure Pd, however.

The inelastic neutron scattering experiments also yield the dispersion of the optic phonon modes of $PdD_{0.63}$ (pure Pd, of course, has no optic modes). These optic modes occur at very low frequencies ($\sim$ 38 meV for transverse optic (TO) phonons of $PdD_{0.63}$) compared with the optic mode frequencies of other metal hydrides, which are typically two to three times higher. The longitudinal optic (LO) modes show a large dispersion, implying strong first and second nearest neighbor D-D interactions. The phonon dispersion curves of $PdD_{0.63}$ and Pd are shown in Figure 2. The phonon dispersion relations of PdD_x samples at higher D concentrations (x = 0.88) are virtually identical to those of $PdD_{0.63}$.[17]

The linewidths of the neutron groups scattered from the $PdD_{0.63}$ optic modes show a strong increase with increasing temperature, which is attributed to anharmonicity of the potential well of the D atom.[16] Even at low temperatures the linewidths remain anomalously broad; this is due to the random distribution of D atoms in the FCC lattice of octahedral sites at substoichiometry, which in turn causes a distribution of LO modes with different dispersion, the LO mode dispersions being governed by the D-D interactions.[18]

As hydrogen is a strongly incoherent neutron scatterer, the phonon dispersion curves of PdH_x cannot be obtained by neutron scattering, however the phonon density of states is readily obtained by such measurements, and when these measurements are compared with the dispersion relations of PdD_x, several pieces of information may be extracted. Such density of states measurements on PdH_x show a strong peak at an energy of 56 meV[19,20] which, when compared with the data on PdD_x, must be

Figure 2. Phonon dispersion relations of $PdD_{0.63}$ (solid curves) and pure Pd (dashed curves) along directions of high symmetry (from reference 16).

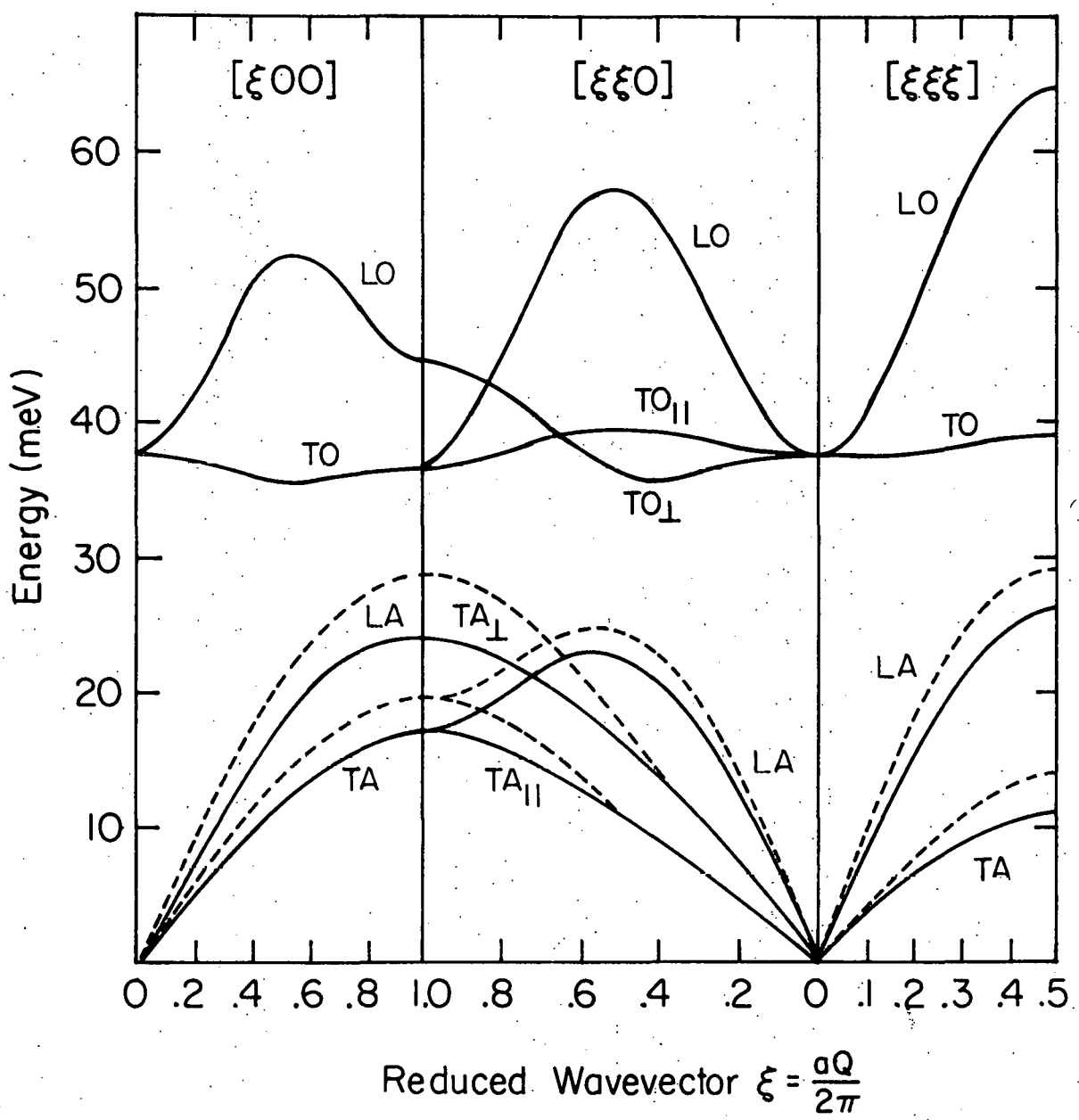
[ξ00]
[ξξ0]
[ξξξ]
60
50
40
30
20
10
Energy (meV)
LO
TO
LO
TO||
TO⊥
LO
TO
LA
TA⊥
TA
TA||
LA
LA
TA
0 .2 .4 .6 .8 1.0 .8 .6 .4 .2 0 .1 .2 .3 .4 .5
Reduced Wavevector ξ = aQ/2π

associated with the flat TO modes, which occurred at 38 meV in PdD_x. If the potential well in which the H or D atom vibrates were harmonic, then the ratio of these TO mode frequences should be

$$\omega_H/\omega_D \approx \sqrt{m_D/m_H} = \sqrt{2} \quad ,$$

($m_{H(D)}$ is the mass of the H(D) atom), but the observed ratio is 1.47, once again demonstrating the anharmonicity of this potential.

When a harmonic force constant model, fitted to the $PdD_{0.63}$ phonon dispersion curves, was used to fit the observed phonon density of states of $PdH_{0.63}$, it was found that the H-Pd force constant must be made $\sim$ 20% larger than the corresponding D-Pd force constant in order to obtain a good fit.[21] This is also interpreted in terms of anharmonicty; the proton, with a larger zero-point motion amplitude than the deuteron, feels the steeper, more anharmonic part of the potential more strongly, increasing its vibrational frequency (beyond the $\sqrt{2}$ increase due to the mass difference between H and D), which results in a larger effective force constant when interpreted in a harmonic model.

The major features of the PdD_x phonon spectrum appear in PdH_x also, viz. large dispersion in the LO modes, and smearing out of sharp features in the density of states due to the random distribution of H atoms at substoichiometry.[21] The acoustic mode spectra of PdH_x and PdD_x are virtually identical, as these modes are governed predominantly by the large mass of the Pd atoms and the Pd-Pd interactions.

Electronic Structure of $PdH_x(D_x)$

The electronic structure of Pd must necessarily be altered upon formation of $PdH_x(D_x)$ as each proton or deuteron entering the Pd lattice brings with it an electron. In a simple "protonic" model of $PdH_x(D_x)$, the H(D) atom enters the octahedral site and donates its electron to the Pd conduction band, thus increasing the Fermi energy, E_F, but producing no other changes. If such a simple rigid band model were valid, then one would expect the 0.36 holes/Pd in the d-band to be filled at a composition x = 0.36. In fact, low temperature specific heat[11] and magnetic susceptibility[22,23] measurements indicate that the d-band is not filled until $x \approx 0.63$, which corresponds to the low temperature β-phase boundary, so that some modification of the band structure must occur beyond a simple increase in E_F.

Band structure calculations on PdH[24-31] predict three changes in electronic structure, relative to pure Pd: (1) a slight lowering in energy of the Pd d-bands, (2) a substantial lowering of some of the s-p states (and, perhaps, d-states) of Pd, which combine with the H 1s-state to form a new bonding state ∿ 5eV below the Fermi energy, and (3) a slow increase in the Fermi energy with increasing H concentration. The bonding state involves a fraction of the H electron (statistically speaking), while the remaining fraction enters the conduction band, increasing E_F; this division of the H electron between bonding state and conduction band explains why the 0.36 holes/Pd in the d-band are not filled until a composition x = 0.63. The hydrogen-induced bonding states have been observed in photoemission studies of PdH_x,[32,33] but no detailed optical studies of $PdH_x(D_x)$ have been performed which might verify the other

predictions of the calculations. Such optical studies would be difficult at best, as the H(D) distribution in real samples is somewhat inhomogeneous, so that any sharp features of a property which depends sensitively on composition will be smeared out by compositional fluctuations. This smearing of fine details because of sample inhomogeneity occurs in measurements of many properties of $PdH_x(D_x)$, often complicating the interpretation of the results, and though the inhomogeneity can be minimized, it can never be eliminated.

In the absence of experimental verification, the details of the various band structure calculations, which often depend sensitively on the computational methods and initial assumptions, must be regarded skeptically. Even so, a few general remarks about the gross electronic structure of β-phase $PdH_x(D_x)$ can be made.

As previously mentioned, at the β-phase boundary the d-band is filled, and the Fermi level intersects the broad, low s-p band above the d-band. The drastic reduction of N(O), the density of states at the Fermi level, which accompanies the filling of the d-band, decreases the exchange enhancement of the susceptibility and quenches the spin fluctuations, so that the magnetic susceptibility, which was large and paramagnetic in pure Pd and α-phase $PdH_x(D_x)$, becomes small and diamagnetic in the β-phase.[22,23]

With additional increase in H(D) concentration, the Fermi energy slowly increases, while the density of states at the Fermi level remains nearly constant, as evidenced by the low temperature electronic specific heat coefficient,

$$\gamma = 2/3\ \pi^2 k_B^2\ N(0)\ (\ 1 + \lambda)\quad ,$$

which is nearly constant in the range $0.64 \leq x \leq 0.85$.[11-13] For $x > 0.85$ it has been reported that both γ and Θ_D drop sharply with increasing x,[14,15] however we believe that this drop is an artifact of the method of data analysis. This is the composition range in which the superconducting transition temperature, T_c, increases rapidly with x, and the values of γ and Θ_D are derived from extrapolation to T = 0 of the normal state specific heat, thus the extrapolation range increases with x, and the validity of the extrapolation becomes increasingly doubtful. It would be surprising if γ did decrease rapidly in the range where T_c is increasing, as a decrease in either N(0) or the electron-phonon coupling constant, λ, generally produces a decrease in T_c, although a decrease in Θ_D might partially compensate for this. Preliminary results on the specific heat of superconducting $PdH_x(D_x)$ driven normal by the application of a magnetic field suggest that the drops in γ and Θ_D are spurious.[34] It is reasonably safe to assume that N(0) remains essentially constant, or decreases only slowly throughout the range $0.64 \leq x \leq 1.0$, as predicted by the band structure calculations.

Though the total density of states, N(0), is relatively constant throughout the β-phase, the distribution of conduction electrons between H(D) sites and Pd sites may change with composition. The band structure calculations of Papaconstantopoulos, et al.,[30,31] predict that the density of states at the H(D) site increases rapidly with increasing E_F (and hence with increasing x), while that at the Pd site remains approximately unchanged. This implies that, as x increases, the

probability of finding conduction electrons at the H(D) site increases--a feature which is central to their theory of superconductivity in $PdH_x(D_x)$. There is some evidence for such a redistribution of conduction electrons from NMR measurements.[35] The calculated total and site-decomposed electronic densities of states of PdH(D) are shown in Figure 3.

Armed with this basic knowledge of the electron and phonon properties of β-phase $PdH_x(D_x)$ we may now address the problem of superconductivity in this system, which arises from the interaction of electrons with phonons.

Figure 3. Calculated electronic structure of pure Pd and $PdH_x(D_x)$:

(a) total density of states of pure Pd,

(b) total density of states of PdH(D),

(c) density of s-like states at H(D)-site in PdH(D),

(d) variation of the total density of states at the Fermi level with H(D) concentration,

(e) variation of the s-like density of states at the H(D)-site at the Fermi level with H(D) concentration.

All densities of states are in units of states per Ry-unit cell. Arrows indicate positions of Fermi energies, E_F. (Taken from references 30 and 31.)

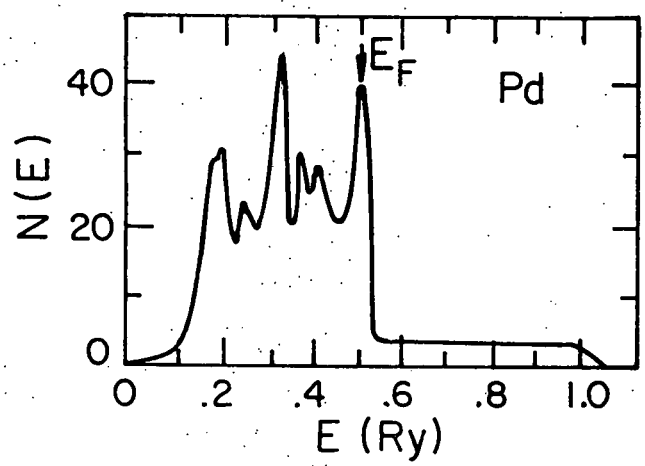
N(E)
40
20
0
E_F
Pd
0 .2 .4 .6 .8 1.0
E (Ry)

(a)

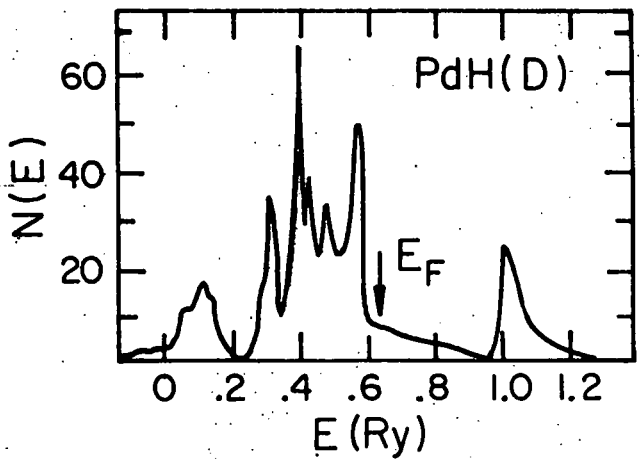
N(E)
60
40
20
PdH(D)
E_F
0 .2 .4 .6 .8 1.0 1.2
E(Ry)

(b)

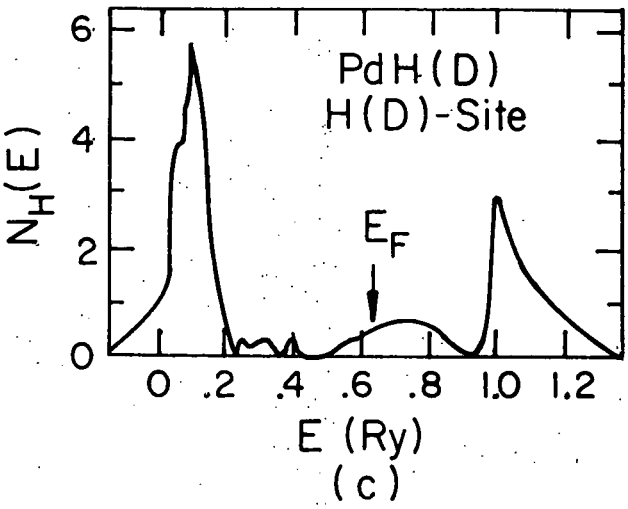
$N_H(E)$
6
4
2
0
PdH(D)
H(D)-Site
E_F
0 .2 .4 .6 .8 1.0 1.2
E (Ry)

(c)

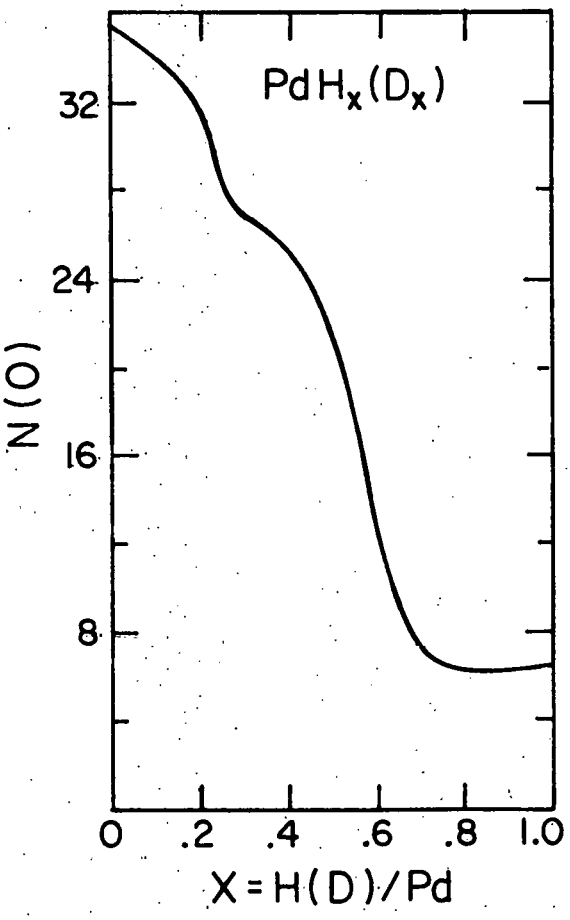
N(O)
32
24
16
8
$PdH_x(D_x)$
0 .2 .4 .6 .8 1.0
X=H(D)/Pd

(d)

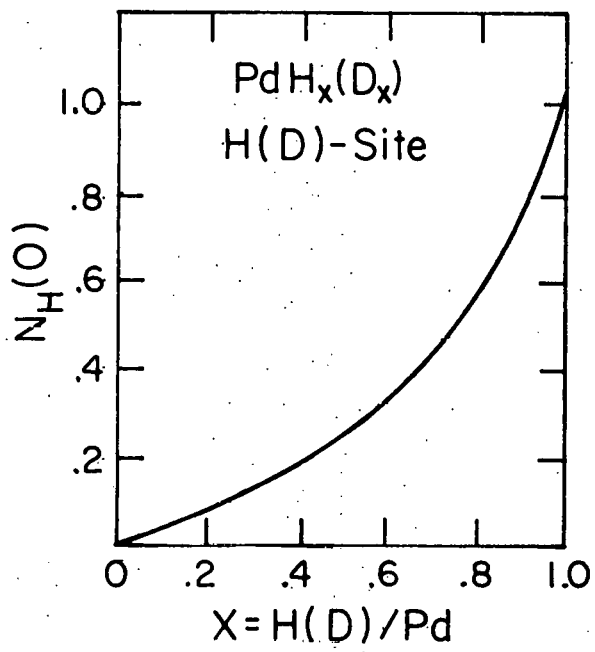
$N_H(O)$
1.0
.8
.6
.4
.2
$PdH_x(D_x)$
H(D)-Site
0 .2 .4 .6 .8 1.0
X=H(D)/Pd

(e)

III. SUPERCONDUCTIVITY IN $PdH_x(D_x)$

Superconductivity in Metal Hydrides

Since 1911, when Kamerlingh Onnes discovered superconductivity in mercury, an enormous amount of research has been directed at discovering a material with a superconducting transition temperature, T_c, which is high enough to dispense with liquid helium refrigeration. To date, superconductivity has been discovered in thousands of metals and alloys, yet only a few dozen of these materials have T_c's greater than 10 K, and the current record holder, Nb_3Ge, with T_c = 23 K, is still far below the temperature range accessible with liquid nitrogen refrigeration.

In the early days of research in superconductivity, a variety of empirical rules were formulated relating transition temperatures to physical properties of materials, but it was not until 1957, when Bardeen, Cooper and Schrieffer (BCS) developed a successful microscopic theory of superconductivity,[36] that the underlying relations between T_c's and material parameters were grasped.

The BCS theory evolved from Cooper's demonstration that, in the presence of an attractive interaction between electrons, the Fermi sea is unstable against the formation of bound "Cooper pairs" of electrons, regardless of how weak the interaction is. The direct, Coulomb interaction between electrons is always repulsive, and so cannot form Cooper pairs. Any additional "indirect" interaction between electrons which

is sufficiently strong to overcome the Coulomb repulsion will result in pair formation, and hence superconductivity.

In all known superconductors, this indirect interaction between electrons is mediated by the lattice vibrations (phonons); in essence, one electron will polarize the medium by attracting the positive ions of the lattice, and this polarization will attract the other electron. The essential features of this interaction may be perceived by considering the lattice to be a positively charged simple harmonic oscillator which is being driven by the motion of one electron, and which, in turn, drives the motion of a second electron. If the first electron moves with a frequency below the resonant frequency of the oscillator, then the oscillator will follow this motion, in phase with it. The second electron, following the oscillator motion, will thus follow the first electron, and the lattice-mediated interaction between electrons will be attractive. If the first electron moves with a frequency above the resonant frequency, then the oscillator responds 180° out of phase to the first electron, with an amplitude which decreases rapidly with increasing frequency. In this case, the second electron moves with a small amplitude, 180° out of phase to the first electron; the interaction has become weak and repulsive. Just below (above) resonance, the interaction is large and attractive (repulsive).

By replacing this complicated, frequency dependent interaction between electrons with an attractive potential which is a constant, V, up to some cutoff frequency, ω_o, and zero at higher frequencies, the BCS theory derives a simple expression for the transition temperature of a superconductor:

$$T_c = 1.13\ \omega_o \exp(-1/g) \qquad (1)$$

where $g = N(0)V$ is the "coupling constant," $N(0)$ is the electronic density of states at the Fermi level, and the cutoff frequency, ω_o, is a frequency characteristic of the lattice vibrations (expressed in units of temperature).

Equation (1) suggests that one approach to the problem of high temperature superconductivity is to find a material with high frequency lattice vibrations. Since $\omega_o \sim (k/m)^{\frac{1}{2}}$, where k is a force constant and m is the ion mass, it was suggested that the hypothetical metallic phase of hydrogen might be a high temperature superconductor, as it has the smallest possible ion mass. A variety of theoretical calculations on metallic H[37,38] have predicted transition temperatures ranging from 20 K to 200 K, depending on the assumptions made about the nature of metallic H. These predictions are tantalizing; however, the estimated pressure required to form metallic H, in excess of a megabar, is far above the hydrostatic pressures presently attainable in the laboratory. There is also no guarantee that metallic H, once formed, would remain stable if the applied pressure were removed. Metallic H would not seem to be a practical choice for a commercial high temperature superconductor!

The hydrides of the transition metals and early actinides behave in many ways as if they were simple binary alloys of the host metal and metallic hydrogen:[39] the metal hydrides remain metallic, the H enters the lattice in the atomic, rather than the molecular, state, and the H partial molar volumes and proton densities in the metal hydrides are comparable to those calculated for metallic H. Because of these similarities, it was hoped that these metal hydrides might mimic

certain properties of metallic H, including high temperature superconductivity.

A search for superconductivity in the hydrides of V, Nb and Ta,[40] Ti and Zr,[41] and La[42] yielded negative results above 1 K. These results were particularly disappointing, since Nb (T_c = 9.2 K), La (T_c = 6.0 K), V (T_c = 5.4 K) and Ta (T_c = 4.5 K) are among the best elemental superconductors, and the formation of the hydride phase suppressed their superconductivity.

In 1970, Satterthwaite and Toepke[43] discovered the first superconducting metal hydride, the higher hydride of thorium, Th_4H_{15}. Pure Th has a T_c of 1.38 K, and the dihydride phase, ThH_2, is not superconducting above 1 K, but in the higher hydride phase the transition temperature jumps to between 8 and 9 K. The role of the H atoms in the superconductivity of Th_4H_{15} is not clear; the transition temperature is independent of hydrogen concentration throughout the higher hydride phase, and the T_c of Th_4D_{15} is virtually the same as that of Th_4H_{15}.[44] It is possible that the hydrogen serves predominantly to stabilize the unusual crystal structure of Th_4H_{15}, which may be more favorable for superconductivity than the FCC structure of pure Th.

In 1972, Skoskiewicz[45] reported that a non-superconductor, Pd, became superconducting upon formation of the hydride phase, PdH_x, for hydrogen concentrations, x, in excess of $\sim$ 0.77. Subsequent investigations[46-49] revealed that the transition temperature increased strongly with increasing H concentration, reaching $\sim$ 9 K for PdH, and that substitution of D for H led to a large "reverse" isotope effect, the T_c of PdD_x being 1-2 K higher than that of PdH_x at the same composition (see

Figure 4). Clearly, the H(D) atoms are playing a central role in the superconductivity of this material. Further interest in this system was aroused when it was found that alloying Pd with Ag, Au or Cu and then hydrogenating produced transition temperatures ranging from 13 K to 17 K,[50] values which are rivalled by only a few other materials.

Since 1972, only a few other cases of enhancement of superconductivity by the addition of hydrogen have been reported, notably in Nb-Ru[51] and Nb-Pd[52] alloys, while several instances of degradation of superconductivity have been found.

Superconductivity in $PdH_x(D_x)$: Theory

The announcement of superconductivity in $PdH_x(D_x)$ spawned a legion of theoretical models. A successful model must address three key aspects of superconductivity in this system, namely: (1) why does superconductivity appear in $PdH_x(D_x)$ when it is absent in pure Pd, (2) why does the transition temperature increase strongly with increasing H(D) concentration, and (3) why is the isotope effect "reversed"? For a BCS superconductor, equation (1) predicts that a heavier isotope should have a lower T_c than a lighter isotope, by virtue of its lower phonon frequencies, yet PdD_x has a substantially higher T_c than PdH_x (thus the isotope effect is "reversed" from that which is normally observed). Equation (1) also predicts that a large value of N(O) should lead to a large coupling constant, g, and hence a large T_c, yet the hydrogenation of Pd leads to both a large decrease in N(O) and an increase in T_c. We must abandon the simple BCS theory in order to discuss superconductivity in the Pd-H(D) system.

A correct many-body treatment of superconductivity, involving the frequency dependent electron self-energies and dressed phonon and Coulomb interactions, presents a difficult problem.[53] Eliashberg[54] derived an approximate solution to this problem in the form of two coupled integral equations involving the complex, frequency dependent energy gap and electron self-energy as a function of electron and phonon structures and temperature. While these equations embody the "correct" solution to the problem of superconductivity, their predictions about transition temperatures enter in an indirect and rather opaque manner.

McMillan[55] numerically solved the Eliashberg equations for T_c for various values of the material parameters involved, and then fitted the results to an analytic, BCS-like expression. The resultant "McMillan equation," modified for d-band materials[56] is given by:

$$T_c = \frac{\Omega}{1.2} \exp\left[\frac{-1.04(1 + \lambda + \mu_p)}{\lambda - (\mu^* + \mu_p)(1 + 0.62\,\lambda)}\right] \qquad (2)$$

where λ is the electron-phonon coupling constant (or phonon mass enhancement), μ^* is the Coulomb pseudopotential, μ_p is the paramagnon mass enhancement, and Ω is a complicated factor related to the phonon frequencies.[57] The terms λ and μ_p are the contributions to the effective mass of the electron due to the "cloud" of lattice distortion and electron spin polarization which accompany it. The numerator of the exponent is the mass renormalization factor (the ratio of the effective to the band structure electron mass is $1 + \lambda + \mu_p$), which reduces the total electron-electron interaction. The denominator of the exponent plays the role of

the total electron-electron interaction strength, g, in equation (1). It consists of λ, which measures the strength of the attractive, phonon-mediated interaction between electrons, diminished by the combination of μ^*, which is a measure of the Coulomb repulsion, and μ_p, which reflects the fact that the exchange interaction favors a triplet spin state over the singlet spin state of the Cooper pair. If λ, the attractive part, is greater than $\mu^* + \mu_p$, the repulsive part, then Cooper pairs form, and $T_c > 0$; if the denominator vanishes (or is negative), then the repulsive interactions have "won," no pairing occurs, and $T_c = 0$. The numerical factors 1.04 and $(1 + 0.62\ \lambda)$ are "fudge factors" which make the expression fit the Eliashberg solutions. It must be emphasized that the McMillan equation was derived using a "Nb-like" phonon density of states, and so should not be used to make quantitative predictions of T_c for compounds with radically different phonon structure, such as $PdH_x(D_x)$. Values of T_c for $PdH_x(D_x)$ derived from equation (2) and from solution of the Eliashberg equations agree to within $\sim$ 10%,[30] so that equation (2) may be used to discuss trends in T_c and estimate the magnitudes of various effects.

Equation (2) indicates why pure Pd is not superconducting. The large value of N(0) in pure Pd is probably beneficial to λ (as in the simple BCS theory, where $g = N(0)V$); however it also leads to large values of μ^* and, in particular, μ_p. Thus the repulsive terms dominate, and superconductivity is absent. The drastic reduction of N(0) upon formation of β-phase $PdH_x(D_x)$ reduces μ^* and drives μ_p essentially to zero, so that in the β-phase the μ_p terms in equation (2) may be neglected.

An early theoretical treatment of superconductivity in the Pd-H(D) system, by Benneman and Garland,[58] ascribed the onset of superconductivity to this "quenching" of μ_p, which supposedly allowed the incipient superconductivity of the Pd lattice to manifest itself. The increase of T_c with x was explained as being due to a continuing decrease of N(0), and hence μ^*, while the isotope effect was attributed to the difference in lattice constants of PdH_x and PdD_x. This theory failed on all three counts. The band structure calculations and low temperature specific heat measurements indicated that N(0) is relatively constant in the β-phase, so that μ^* should not vary much. Lattice constant measurements showed a much smaller difference between hydride and deuteride than was estimated by the authors. The experimental work we present in a later section demonstrates that, while μ_p vanishes at $x \approx 0.63$, superconductivity does not appear until appreciably higher H(D) concentrations. Finally, the d-band of Pd may also be filled, and μ_p quenched, by alloying with Ag, yet Pd-Ag alloys do not exhibit superconductivity, even at 10 mK.[59] While the quenching of paramagnons is necessary for superconductivity in Pd, it is not sufficient.

Another early theory, by Auluck,[60] suggested that PdH_x was the first example of superconducting metallic H. In this model, the Pd matrix played a passive role, serving only to create an environment in which "metallic H" could form. This was the opposite point of view from that of Benneman and Garland, who argued that the H atoms played a passive role, while the Pd matrix was responsible for superconductivity. Auluck's theory, while in keeping with the original ideas which motivated the research on superconducting metal hydrides, is not supported by experiment.

The model could not explain the reverse isotope effect, and also predicted an increase in T_c under application of hydrostatic pressure, while experimentally it was found that T_c decreases with applied pressure.[61,62]

A semi-quantitative model proposed by Ganguly[63] marked a turning point in the understanding of superconductivity in the Pd-H(D) system. By making a comparison with Nb (which has nearly the same values of T_c and Θ_D as PdH), Ganguly argued that the quenching of μ_p could not possibly account for the observed T_c of $\sim$ 9 K in PdH, even in the extreme case of $\mu^* = 0$, unless there were also a large enhancement of λ over that of pure Pd. He proposed that the additional contribution to λ was due to coupling of the electrons to the high frequency optic phonon modes, and demonstrated that if these modes were anharmonic, then a reverse isotope effect was possible.

In order to demonstrate Ganguly's arguments, we differentiate equation (2) to obtain:

$$\frac{\Delta T_c}{T_c} = \frac{\Delta\Omega}{\Omega} + \frac{1.04(1 + 0.38\ \mu^*)\ \lambda}{\left(\lambda - \mu^*(1 + 0.62\ \lambda)\right)^2}\ \frac{\Delta\lambda}{\lambda} \qquad (3)$$

where Δ symbolizes the change in a quantity on substitution of a heavy isotope for a light one (e.g., $\Delta T_c = T_c$ of $PdD_x - T_c$ of PdH_x). $\Delta T_c/T_c < 0$ thus corresponds to a normal isotope effect. The first term on the right, $\Delta\Omega/\Omega$, is negative, as heavier ions have lower frequency phonon modes. If the term $\Delta\lambda/\lambda$ is sufficiently positive, then the second term on the right-hand side can be large enough to compensate for the negative $\Delta\Omega/\Omega$ and produce a reverse isotope effect, $\Delta T_c/T_c > 0$

(the factor which multiplies $\Delta\lambda/\lambda$ is always positive, as λ and μ^* are positive by definition).

The calculation of λ involves the phonon frequencies and phonon polarization vectors, which depend implicitly on ion mass, as well as explicit factors of ion mass. It can be shown on quite general grounds that these quantities enter into λ in such a way that the aggregate may be replaced by the inverse of the force constant matrix,[64] so that λ depends not on the masses, but on the force constants between atoms, and an increase in force constant produces a decrease in λ. Force constants depend on electronic structure, which is normally independent of isotope, so that for most materials, $\Delta\lambda = 0$ and the isotope effect enters only through $\Delta\Omega$, producing a normal isotope effect.

Ganguly separated the electron-phonon coupling constant into contributions from the acoustic and optic modes, $\lambda = \lambda_{ac} + \lambda_{op}$. He reasoned that $\Delta\lambda_{ac} \approx 0$, because the Debye temperatures and lattice constants (and hence Pd-Pd distances) of PdH_x and PdD_x are nearly identical. He also noted that the proton should have a much larger zero-point motion amplitude than the deuteron, but that the octahedral cages of Pd atoms surrounding the proton and deuteron are nearly identical in size, because of the similarity in lattice constants. Thus the H is, on time average, in closer proximity to the surrounding Pd's than is the D, and if the H(D)-Pd interaction is anharmonic, then the H will feel this anharmonicity more strongly. In a harmonic analysis of the optic phonon frequencies, even-order anharmonicity will thus produce an effective H-Pd force constant which is stiffer than the D-Pd force

constant, as mentioned in chapter II. The force constant difference then gives $\lambda_{op}(D) > \lambda_{op}(H)$, i.e., $\Delta\lambda_{op} > 0$, and a reverse isotope effect results.

Ganguly's model qualitatively explained all of the observed features of superconductivity in $PdH_x(D_x)$. It demonstrated that the suppression of paramagnons was not sufficient for superconductivity, but that additional electron-phonon coupling was needed. By ascribing this extra coupling to the optic modes, he showed that the reverse isotope effect was a natural consequence of a force constant difference due to zero-point motion consideration. The application of hydrostatic pressure should lead to a further stiffening of the H(D)-Pd force constant, and so lead to a reduction of T_c, as observed experimentally. Because of the large mass difference between H(D) atoms and Pd atoms, the optic modes are basically modes of H(D) atom vibrations. Thus λ_{op}, and hence T_c, should depend on the number of H(D) atoms available to couple to the electrons, producing the observed x-dependence.

Experimental evidence in support of Ganguly's ideas accumulated quickly. Thermodynamic analyses[65] and inelastic neutron scattering data[21] indicated that the H-Pd force constant is greater than the D-Pd force constant by 7% and 20% respectively. Resistivity measurements[66] implied a strong electron-optic phonon coupling. More importantly, superconducting tunneling measurements,[67,68] the most powerful probe of the electron-phonon interaction in metals, showed pronounced structure in the conductance curves at energies corresponding to the optic mode frequencies of $PdH_x(D_x)$. This phonon-induced

structure is a direct confirmation that the optic modes contribute strongly to the pairing interaction. Unfortunately, the tunneling data are not good enough to permit a quantitative determination of λ_{ac} and λ_{op} at this time.

The Model of Klein and Papaconstantopoulos, et al.

In a series of papers,[69-71,30,31] Klein and Papaconstantopoulos, et al., have developed a quantitative model (hereafter referred to as the KP model) of superconductivity in $PdH_x(D_x)$ based on the concepts advanced by Ganguly. They made ab initio band structure calculations and used the PdD_x phonon density of states (d.o.s.) obtained from neutron scattering experiments to calculate $\lambda = \lambda_{ac} + \lambda_{op}$ and T_c of PdH_x and PdD_x for several values of x.

In order to perform the calculations, the authors needed to make several simplifying assumptions: (1) the acoustic phonon d.o.s. of PdH_x and PdD_x were assumed to be identical, while the optic mode d.o.s. of PdH_x was derived by shifting that of PdD_x upward in energy by an amount consistent with the 20% increase in force constant, (2) the x-dependence of the phonon d.o.s. and lattice constants was ignored, (3) the electronic structure of PdH_x and PdD_x were assumed to be identical, and (4) the acoustic mode contribution, λ_{ac}, was assumed to be due to coupling of the electrons to the low frequency motions of the Pd atoms only, while the optic mode contribution, λ_{op}, was assumed to be due to the coupling of electrons to the high frequency motions of the H(D) atoms only. This last assumption enabled the authors to use a modified "constant-α^2" approximation which greatly simplified the computations.[70]

The calculations predict that λ_{ac} is nearly independent of x in the superconducting range ($0.7 \leq x \leq 1.0$), while λ_{op} increases strongly with x, from a value comparable to λ_{ac} to a value 2-3 times greater, producing the increase in T_c. The reason for the increase in λ_{op} is twofold. First, and more obvious, the number of H(D) atoms to which the electrons can couple is increasing. Second, the band structure calculations predict that the (site-decomposed) electronic density of states at the H(D)-site increases with increasing x (see Figure 3e), even though the total density of states decreases somewhat. This increases the likelihood of finding an electron at the H(D)-site, enhancing λ_{op}. The force constant difference ensures that $\lambda_{op}(D) > \lambda_{op}(H)$, producing the reverse isotope effect. The force constant difference is solely responsible for the reverse isotope effect in this model.

The results of the KP model are in reasonably good agreement with experiment. At stoichiometry, the model predicts T_c's of 10.4 K and 9.0 K for PdD and PdH respectively,[31] while the highest T_c's observed experimentally are 11.59 K and 9.49 K for samples with composition $x = 0.995 \pm 0.005$.[35] The KP model also predicts that the transition temperatures of PdH_x and PdD_x should vanish at the same composition, $x \approx 0.73$.[72]

Miller and Satterthwaite[49] measured T_c vs. x for PdH_x and PdD_x in the temperature range from 1.5 K to 10 K. They found that by rigidly shifting the PdD_x data to the right along the composition axis by about 0.05, it could be made to coincide with the PdH_x data. In other words,

they found that PdD_x had the same transition temperature as $PdH_{x+\delta}$, where $\delta \approx 0.05$. They hypothesized that the reverse isotope effect was due to a difference in the electronic structures of PdH_x and PdD_x, caused by the difference in zero-point motion amplitudes. They reasoned that the H atom, being closer to its neighboring Pd atoms (on average) than a D atom, would be more tightly bound in the lattice. That is, the H would contribute a larger fraction of its electron to the H-Pd bonding state, and hence a smaller fraction to the conduction band, than the D, so that the Fermi energy of PdH_x would lie slightly below that of PdD_x. If the Fermi energy of PdD_x were equal to that of $PdH_{x+\delta}$, then the BCS equation (1) would approximately reproduce the rigid shift behavior they observed. They cited the observed differences in dissociation pressures and heats of absorption between hydride and deuteride as evidence of such a bonding difference. Their model is also consistent with the pressure dependence of T_c, as compressing the lattice would increase the bonding, thus decreasing the Fermi energy and T_c. They attribute the force constant difference to this bonding difference, and not to anharmonicity. Ganguly assumed that the potential wells in which the H and D atoms vibrated were identical, and that the anharmonicity of this potential, which is sampled more strongly by the H atom, produced the force constant difference. Miller and Satterthwaite adopted the view that the potential well of the H atom was deeper and steeper than that of the D atom, because it was more tightly bound, resulting in the force constant difference.

We have seen that the BCS equation (1) is not adequate for discussing superconductivity in $PdH_x(D_x)$, so that the quantitative argument

of Miller and Satterthwaite regarding T_c's must be viewed skeptically. However, a difference in electronic structures of PdH_x and PdD_x induced by the difference in zero-point motions is distinctly possible. Such a difference could make an additional contribution to the reverse isotope effect, beyond that of the force constant difference invoked in the KP model.

The ideal test of the KP model would be a comparison of values of λ calculated from the model with those derived from tunneling measurements. Unfortunately, the present tunneling data do not allow a quantitative evaluation of λ due to the experimental difficulties in preparing high quality tunnel junctions from $PdH_x(D_x)$. A simpler, though less rigorous, test of the KP model is the measurement of the H(D) concentration dependence of T_c in the regime of vanishingly small T_c. If the force constant difference (due either to anharmonicity or a bonding difference) is solely responsible for the reverse isotope effect, as it is in the KP model, then the transition temperatures of PdH_x and PdD_x should vanish at the same composition, as the KP model predicts. If the transition temperatures of hydride and deuteride do not vanish at the same composition, then we may argue that there is an additional contribution to the reverse isotope effect which has been excluded from the KP model by the assumptions upon which it is based. Thus we set out to measure the transition temperatures of PdH_x and PdD_x in the temperature regime from 0.2 K to 4 K.

T_c vs. x: Experiment

Samples for this work were prepared from "Marz" grade Pd foil.[73] Spectroscopic analysis of the foil showed the major magnetic impurities to be Fe (∿ 20 ppm atomic) and Ni (∿ 15 ppm atomic). The foil was cut into strips measuring approximately 25.4 mm × 4.8 mm × 0.05 mm (∿ 65 mg of Pd), which were cleaned and etched, and then annealed in vacuo at ∿ 830°C for 18 hours.

The Pd foils were loaded with H(D) electrolytically. The Pd foil cathode and a Pt foil anode were immersed in an electrolyte of three parts 38% HCl (DCl) in H_2O (D_2O) to seventeen parts CH_3OH (CH_3OD). The deuterated compounds were 99+% isotopically pure. The foils were charged for 3-15 minutes (depending on the concentration desired) at a current of ∿ 200 mA (current density ∿ 80 mA/cm^2). With the electrolyte at room temperature, H(D) concentrations saturated at $x \lesssim 0.82$ (0.80). To reach higher concentrations, the samples were first charged to saturation at room temperature, and then transferred to fresh electrolyte which was cooled in a dry ice-acetone bath to about -78°C. The charging process was then continued for 1-3 hours at this low temperature, with the charging current reduced to ∿ 80 mA to avoid heating the electrolyte.

The dissociation pressure of $PdH_x(D_x)$ increases rapidly with increasing H(D) concentration in the β-phase. Samples with concentrations in the superconducting range are unstable at room temperature, and will spontaneously evolve $H_2(D_2)$. To prevent this loss of H(D), the samples were transferred to liquid nitrogen immediately after charging, and then stored in a dry ice-acetone bath until they were required.

Mounting of a sample into the dilution refrigerator and subsequent cool-down required about twenty minutes, during which time the sample was at room temperature. To prevent the loss of H(D) during this period, the samples were immersed for ten minutes in a potassium iodide-iodine (KI-I) solution[74] before mounting. This poisoned the Pd surface and reduced the outgassing rate by 2-3 orders of magnitude. For concentrations below about 0.8, the KI-I treated samples lost virtually no H(D) even after several hours at room temperature, while at higher concentrations the outgassing problem grew progressively worse (although still far better than in untreated samples). The apparatus used for T_c measurements between 1 K and 4 K allowed the samples to be kept cold during mounting, so that the KI-I treatment was not necessary; however, we measured several treated, as well as untreated, samples in this apparatus to check that the KI-I was not affecting the superconducting transitions. There were no discernable differences between treated and untreated samples.

The H(D) concentrations of the samples were determined by thermal decomposition of the samples and volumetric measurement of the $H_2(D_2)$ evolved. The samples were heated to $\sim$ 450°C, and the evolved gas was collected in a calibrated volume, while the gas pressure was monitored by a quartz Bourdon tube pressure gauge which had been calibrated against a Hg manometer. From the pressure, volume and temperature of the gas, the number of moles of $H_2(D_2)$ evolved was calculated from the ideal gas law. This number was then doubled to get the number of moles of H(D) in the sample. The degassed Pd foil was then weighed to determine the number of moles of Pd, and the ratio of moles of H(D) to moles of Pd

gave the value of x. The concentration determinations are accurate to 0.5%, corresponding to an uncertainty in x of about ± 0.005. The concentration analysis system is described in detail elsewhere.[75]

Just prior to each T_c measurement, the sample was cut in half, and one half was analyzed for H(D) content immediately. The other half was used for the determination of T_c, and was analyzed for H(D) content immediately after the T_c measurement. This routine checked that the sample had not lost H(D) during the course of the T_c measurement; data were acceptable only if the two concentration determinations were in close agreement ($\Delta x \lesssim 0.01$). The concentration of the half used for the T_c measurement was used as the sample concentration in the data analysis.

Transition temperature measurements in the range 0.2 K to 1 K were performed in a He^3-He^4 dilution refrigerator. The sample foil was daubed with Apiezon N grease and embedded in a brush of fine copper wires which were thermally anchored to the mixing chamber of the refrigerator. The superconducting transition was monitored inductively; the sample was surrounded by a pair of mutual inductance coils, and as the sample passed into the perfectly diamagnetic superconducting state the mutual inductance of the coil pair decreased. The superconducting transitions of $PdH_x(D_x)$ are rather broad, due to compositional inhomogeneity. If the transition were monitored resistively, the high concentration, high T_c parts of the sample would become superconducting at higher temperatures and tend to short out the regions which had not yet become superconducting, leading to an overestimate of the mean transition temperature. For this reason we chose the inductive technique,

which is more sensitive to the entire volume of the sample. The mutual inductance of the coils was monitored with a mutual inductance bridge, operating at 400 Hz. The sample temperature was determined by a Ge resistance thermometer. The thermometer resistance was measured by a four terminal a.c. resistance bridge, which eliminated errors due to lead resistances and thermal EMF's. The thermometer calibration was checked against superconducting fixed points and found to be accurate to ± 1 mK.

For measurements in the range from 1 K to 4 K, a pumped He^4 cryostat was used. Two identical pairs of mutual inductance coils were wired together with their primaries in series and their secondaries in series opposition, and the coils were balanced so that the induced voltages in the secondaries cancelled each other. The sample was placed in one of the coil pairs, and when it became superconducting, it unbalanced the coils, and an induced a.c. signal appeared across the secondaries. The signal across the secondaries was detected by a lock-in amplifier, the analog output of which was connected to the y-axis of an x-y recorder. The inductance measurements were made at 202 Hz. Again, a Ge resistance thermometer was used to determine the temperature. The resistance was measured by a four terminal d.c. technique; the ohmic voltage drop across the thermometer was measured with a nanovoltmeter, the analog output of which was displayed on the x-axis of the x-y recorder. The entire assembly of coils, sample and thermometer was immersed directly in the He^4 bath, and as the temperature was lowered by pumping on the bath, the transition was traced out on the x-y recorder. Because a d.c. method was used to measure the thermometer resistance, thermal

EMF's in the thermometer voltage leads could lead to erroneous resistance readings. For this reason, three superconducting fixed points (In, Th and Al) were included in each run, as a check of the thermometry. The thermometry was found to be accurate to ± 20 mK.

For all samples, we adopted the convention of Miller and Satterthwaite, defining T_c as the temperature at which the diamagnetism was 50% of its maximum value, and the breadth of the transition (shown as vertical error bars in Figure 4) as the temperature interval between 20% and 80% of maximum diamagnetism.

Experimental Results

The resulting T_c vs. H(D) concentration data for both hydrides and deuterides are shown in Figure 4, along with the previous data of Miller and Satterthwaite at higher concentrations. The present data join smoothly with the data of Miller and Satterthwaite, and we found that the composite data were well fitted by the empirical relation:

$$T_c = 150.8\ (x - x_o)^{2.244} \qquad (4)$$

where x_o, the concentration at which $T_c = 0$, is 0.715 for hydride samples and 0.668 for deuteride samples. This empirical relation (shown as the solid curves in Figure 4) also provides a good description of the T_c vs. x data obtained from specific heat[13-15] and resistivity[47,76] studies. In less satisfactory agreement are the T_c vs. x data of Schirber and Northrup,[48] which show much less curvature than the present data, lying about 0.5 K above our empirical relation

Figure 4. Superconducting transition temperatures as a function of H(D) concentration for PdH_x(▲) and PdD_x(●). Data at higher concentrations for PdH_x(△) and PdD_x(○) are taken from reference 49. Solid curves are empirical fits to the data, as described in text.

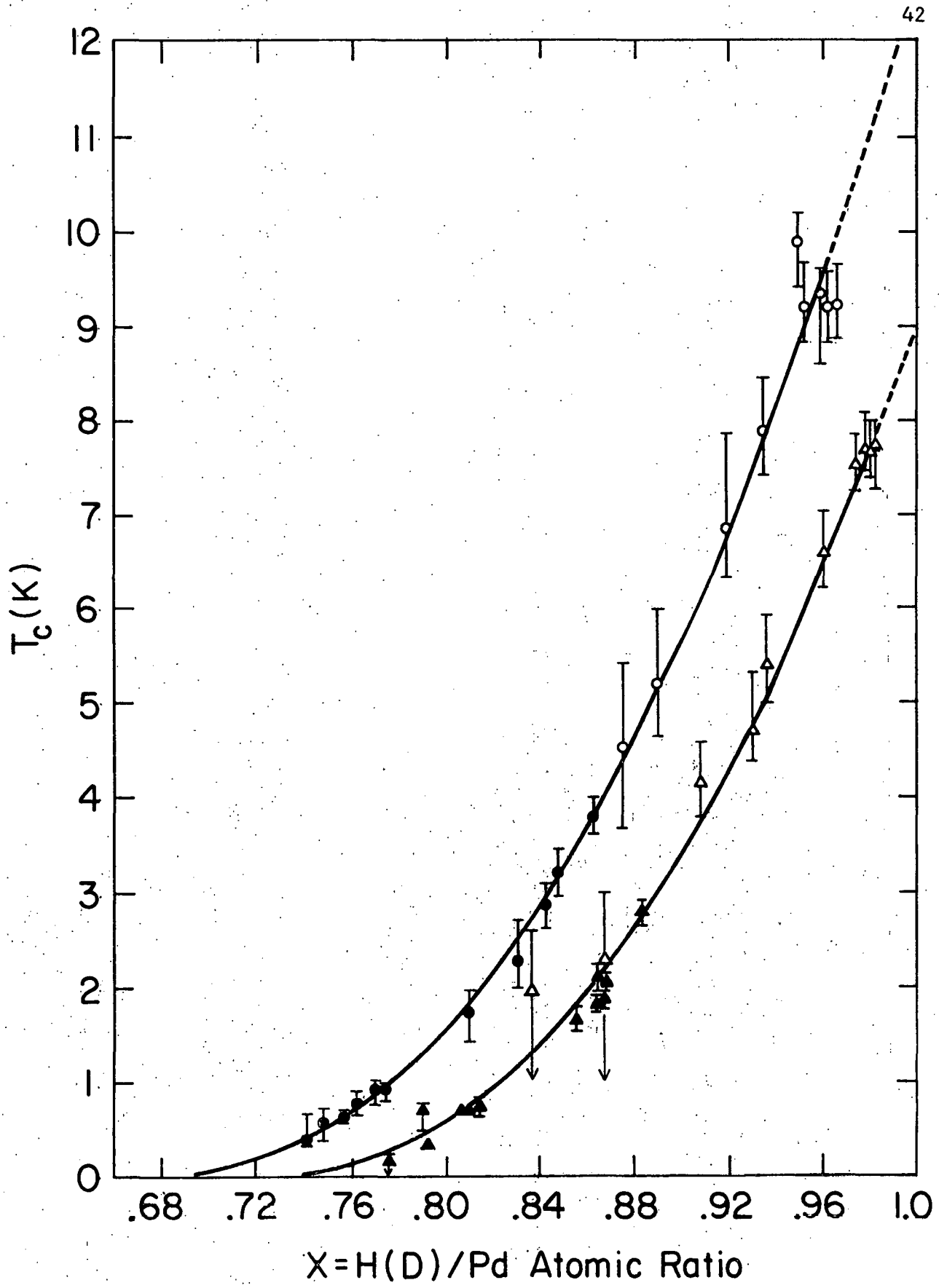
12
11
10
9
8
7
6
5
4
3
2
1
0
T_c(K)
.68
.72
.76
.80
.84
.88
.92
.96
1.0
X=H(D)/Pd Atomic Ratio

at low concentrations (T_c = 1-3 K) but then crossing and lying about 1 K below it at higher concentrations (T_c = 7-10 K). We can point to no obvious cause for this discrepancy, but the agreement with specific heat and resistivity data makes us confident that the present work is correct.

At stoichiometry, our empirical relation for T_c extrapolates to 9.02 K for PdH and 12.70 K for PdD, as compared with the highest observed values of 9.49 K and 11.59 K. Because of the power law nature of the empirical relation, the predicted values of T_c near stoichiometry are very sensitive to small changes in the fitting parameters, so that the predicted values of T_c for $x \gtrsim 1.0$ must be taken with a grain of salt. However, for H(D) concentrations below 0.98, the empirical relation gives good agreement with experiment.

The superconducting transitions of the present investigation are several times narrower than those observed by Miller and Satterthwaite, indicating that the H(D) distribution in our samples is much more homogeneous. There are two probable causes for this improved homogeneity. The first is that we charged our foils to saturation at room temperature, where the H(D) diffusion is rapid, before charging at low temperatures, while Miller and Satterthwaite charged their samples entirely at low temperatures, where the incoming H(D) atoms would have trouble diffusing from the surface to the interior of the foil. Second, Miller and Satterthwaite did not anneal their Pd foils before charging, while we thoroughly annealed our foils and took great pains to avoid bending or crimping them during subsequent handling. It is known that H atoms will concentrate at regions of high negative stress (dislocations,

etc.) in α-phase PdH_x;[77] we speculate that this kind of stress-induced inhomogeneity may occur in the β-phase also.

Discussion of Results

The most important fact to emerge from this experimental investigation is that the relation first noted by Miller and Satterthwaite, that the T_c of PdD_x is the same as that of $PdH_{x+\delta}$, is valid down to the lowest temperatures measured (0.2 K). This is reflected in the functional form of the empirical relation, equation (4), which gives a value for δ of 0.047, in good agreement with the value δ = 0.044 reported by Miller and Satterthwaite.

The present data for PdH_x extrapolate to $T_c = 0$ at a concentration $x_o = 0.715$, in fairly good agreement with the value $x_o = 0.73$ derived from the KP model. We find that superconductivity in PdD_x persists to much lower concentrations ($x_o = 0.668$), in contradiction to the KP model prediction that T_c of PdD_x should also vanish at $x_o = 0.73$. On the basis of this discrepancy, we question the assumption that the observed H(D)-Pd force constant difference is solely responsible for the reverse isotope effect. We believe that there is an additional contribution to the reverse isotope effect which has been omitted from the KP model because of the simplifying assumptions made in performing the calculations.

Further support for an additional contribution comes from predictions about the transition temperatures of stoichiometric PdH and PdD. Near stoichiometry, the KP model should be most reliable, because the computational difficulties of treating the random distribution of vacancies in the H(D) sublattice vanish. The KP model predicts the

magnitude of the isotope effect at stoichiometry to be 10.4 K - 9.0 K = 1.4 K ($\Delta T_c/T_c$ = 0.156), while experimentally it is found to be substantially larger, 11.59 K - 9.49 K = 2.1 K ($\Delta T_c/T_c$ = 0.221). In fact, the KP model underestimates the magnitude of the isotope effect at all compositions. Prior to the KP calculations, Brown[78] also calculated the magnitude of the isotope effect at stoichiometry. He assumed that the transition temperatures of PdH was 9.0 K, and then used the observed force constant difference to predict a T_c for PdD of 10.5 K ($\Delta T_c/T_c$ = 0.167). In a similar calculation, Singh, et al.,[79] assumed that T_c = 9.1 K for PdH, and then attempted to explicitly calculate the effect of anharmonicity on the optic phonon frequencies, arriving at a value of T_c = 10.1 K for PdD ($\Delta T_c/T_c$ = 0.110). All of these calculations, based only on the difference in H(D)-Pd force constants, consistently underestimate the magnitude of the reverse isotope effect, suggesting that the force constant difference is responsible for most, but not all, of the reverse isotope effect.

The most likely additional contribution to the reverse isotope effect stems from differences in the electronic structures of PdH_x and PdD_x induced by the difference in zero-point motions of proton and deuteron. Indirect evidence for such a difference may be found in the isotope dependence of several properties of $PdH_x(D)_x$, viz. $H_2(D_2)$ absorption-desorption pressures, heats of formation and the H(D)-Pd force constant, as noted by Miller and Satterthwaite. All of these properties are intimately related to the chemical interactions between H(D) atoms and Pd atoms, which are, in turn, governed by the nature of the electronic structure.

Very recently, direct confirmation of an isotopic effect on the electronic structure of $PdH_x(D_x)$ has been found in NMR and de Haas-van Alphen measurements. Wiley and Fradin[35] have performed NMR measurements of the spin-lattice relaxation time, T_1, in stoichiometric PdH and PdD. At low temperatures, the H(D) longitudinal spin relaxation is dominated by coupling to the conduction electrons via the Fermi contact interaction, which is directly proportional to the conduction electron spin density at the H(D)-site. The measurements reveal that the conduction electron spin density at the D-site is about 2% greater than that at the H-site. Venema, et al.,[80] have measured the de Haas-van Alphen effect in α-phase $PdH_{0.01}$ and $PdD_{0.01}$, and report small differences in the band structures from which they conclude that the Fermi energy of PdD_x is slightly higher than that of PdH_x, as hypothesized by Miller and Satterthwaite.

A theoretical treatment of the effect of zero-point motions on electronic structure is very difficult. The rigorously correct approach requires replacing the standard "rigid lattice" type of band structure calculation with the self-consistent electron-phonon problem, which is far too complex a problem for current theoretical means to attack. Jena, et al.,[81,82] have developed a much simpler, though less exact, approach to studying the effect of zero-point motion. They use a molecular cluster model to calculate how the displacement of the H(D) atom away from its octahedral site affects the electron distribution around the H(D). They then take an average over all displacements, weighted by the probability that the zero-point motion will produce

such a displacement. Their results indicate that, because the H spends more time in the region of high electron density surrounding the Pd's, it is more effectively screened from the conduction electrons than is the D. This increased screening will cause a decrease in $\lambda_{op}(H)$ relative to $\lambda_{op}(D)$ beyond that due to the force constant difference, thus making an additional contribution to the reverse isotope effect.

A difference in Fermi energies, as suggested by Miller and Satterthwaite, can also make a contribution to the reverse isotope effect. In the framework of the KP model, part of the increase in λ_{op} with increasing x is due to the increase in the (site decomposed) electronic density of states at the H(D)-site with increasing Fermi energy. Thus if the Fermi energy of PdH_x is slightly lower than that of PdD_x, this will result in a slightly lower electronic density of states at the H-site compared to the D-site, decreasing $\lambda_{op}(H)$ even beyond the decrease caused by the force constant difference.

A difference in Fermi levels caused by zero-point motions is also consistent with the observed lack of an isotope effect in the Pd-noble metal-H(D) alloys. The large T_c values in the Pd-(Ag, Au, Cu)-H(D) alloys are probably due, at least in part, to the raising of the Fermi energy up to the local maximum in the electronic density of states at the H(D)-site (located at an energy of about 0.75 Ry in Figure 3c). Because the slope of the density of states vs. energy curve is zero at this maximum, a small difference in the Fermi energies of hydride and deuteride will produce no difference in their respective densities of states at the H(D)-site, and hence no electronic contribution to the isotope effect.

The KP model slightly underestimates the T_c of PdH_x and more seriously underestimates the T_c of PdD_x. The electronic differences cited above will not increase the T_c estimates of PdD_x, but will instead decrease the T_c estimates of PdH_x (the rigid lattice approach of the KP model should be more correct for PdD_x, as the deuteron has the smaller zero-point motion). These electronic differences will thus lead to better estimates of the magnitude of the isotope effect, but will cause the KP model to underestimate T_c's of both hydride and deuteride. This does not imply that the arguments in favor of an electronic contribution to the reverse isotope effect are invalid. Rather, we feel that this underestimation of T_c is caused by another of the simplifying assumptions made in the KP model, namely, that the electrons do not couple to the acoustic mode vibrations of the H(D) atoms.

Because of the large mass difference between the H(D) atoms and the Pd atoms, the Pd atoms are nearly at rest in the optic mode vibrations throughout the Brillouin zone, so that the coupling of electrons to the optic mode vibrations of the Pd's can be ignored, as is done in the KP model. However, the H(D) atoms have significant vibrational amplitudes in the long wavelength acoustic modes, and only come to rest near the zone boundary, so it is not clear that the coupling of the electrons to these low frequency H(D) vibrations can be ignored, as it is in the KP model. Simple model calculations[64,83] have shown that the light atoms of a PdH-like compound can make a significant contribution to the acoustic mode electron-phonon coupling. The omission of this contribution in the KP model may account for the underestimation of T_c. The

acoustic modes are governed primarily by the Pd-Pd force constant and the large Pd mass, so that the difference between H-Pd and D-Pd force constants should not have much effect on the acoustic mode contributions of the H vs. D atoms, that is, $\lambda_{ac}(H) \approx \lambda_{ac}(D)$. Differences in the electronic structures of the H-site and D-site can result in a decrease of $\lambda_{ac}(H)$ relative to $\lambda_{ac}(D)$, just as in the optic mode case, providing still another possible contribution to the reverse isotope effect.

In summary, the results of this experiment indicate that an explanation of the reverse isotope effect in $PdH_x(D_x)$, based on a force constant difference alone, is too superficial. Careful investigation of the effects of zero-point motion on the electronic structure is needed, on both the experimental and theoretical fronts, as these effects may play a significant role in the isotope effect in $PdH_x(D_x)$.

This experiment also revealed that superconductivity in the Pd-H(D) system persists well into the concentration regime of the structural phase transitions associated with the "50 K anomaly." We thus proceeded to investigate the effects of these phase transitions on the superconducting transition, as described in the next chapter.

IV. SUPERCONDUCTIVITY IN THE ORDERED PHASES OF $PdH_x(D_x)$

Structural Instabilities and High T_c's

It has long been recognized that there is a relationship between the crystal structures of intermetallic compounds and their superconducting properties.[84] Certain crystal structures seem to virtually guarantee superconductivity; an excellent example of this is the A15 (or β-tungsten) structure, which includes the materials with the highest known T_c's, such as Nb_3Ge (T_c = 23 K), Nb_3Sn (T_c = 18 K) and V_3Si (T_c = 17 K). Other crystal structures, such as the B2 (or CsCℓ) structure, rarely produce a superconductor with T_c greater than 1 K. In the last decade, however, it has been found that it is not the structure, so much as instability in the structure, that gives rise to high transition temperatures.

Nearly every high T_c ($T_c \gtrsim 10$ K) superconductor exhibits some sort of instability in its crystal structure, though the types of instabilities are varied. Often, the high T_c materials are characterized by the existence of more than one phase (as a function of temperature and/or composition), with either actual or incipient transitions between phases present. The phonon properties of these materials may exhibit anomalous behavior, such as large anharmonicities or "soft modes" which are often precursors to a structural phase transition. In extreme cases, the high T_c phase of a material may be thermodynamically unstable or metastable, and can be stabilized only by the introduction of defects, such as impurities, disorder or nonstoichiometry, or by special

nonequilibrium preparation techniques, such as sputtering or quenching from high temperatures, etc. To illustrate the relationship between structural instabilities and high T_c's, we cite a few examples.

It was in the A15 class of materials that the relation of high T_c's to lattice instabilities was first recognized, and it is in the A15's that this relationship has been most thoroughly investigated.[85] Several A15's exhibit a martensitic transformation (either actual or incipient) from a cubic phase to a tetragonal phase at a temperature somewhat above the superconducting T_c. A large degree of anharmonicity and a substantial softening of the shear mode related to the tetragonal distortion appear as precursors to this transformation. A15's which demonstrate this instability, such as Nb_3Sn and V_3Si, have T_c's in excess of 15 K, while A15's in which this instability is absent have T_c's of a few Kelvins. The addition of a small amount of H to Nb_3Sn suppresses this instability, and reduces T_c from 18 K to less than 4.2 K. In the A15's with the highest T_c's, Nb_3Ge and, theoretically, Nb_3Si, the instability is so severe that these materials do not readily form in the cubic A15 phase. In fact, in the case of Nb_3Si, the cubic A15 structure does not form at all unless stabilized by a large defect concentration, which suppresses the instability completely, and consequently results in a low T_c. It is thought that if a technique were found for forming cubic A15 phase Nb_3Si without suppressing the instability, a T_c as high as 30 K might result.

The alloys ZrV_2, HfV_2 and $Zr_{1-x}Hf_xV_2$ exhibit the highest T_c's ($\sim$ 8 - 9 K) of any of the C15 (or Laves phase) compounds. These alloys also display a structural transition from a cubic to a rhombohedral or

orthorhombic phase, accompanied by soft phonon modes and perhaps an electronic instability.

As mentioned previously, the B2 (or CsCl) structure seems particularly unsuited for superconductivity, and no known B2 compound has a T_c in excess of 3 K (most are not superconducting at 1 K). The B2 alloy $V_{1-x}Ru_x$ is an exception to this; the T_c of $V_{1-x}Ru_x$ peaks sharply at 5.5 K for x = 0.445, at which composition a cubic to tetragonal structural transition appears.

Several interstitial compounds of the B1 (NaCl) structure also fit into this scheme. Examples of these compounds include some of the transition metal carbides and nitrides, such as NbC_x, NbN_x and TaC_x, as well as $PdH_x(D_x)$ and Pd-(Ag, Au, Cu)-$H_x(D_x)$. There are many similarities between these materials. The host metals form FCC lattices in which the non-metal atoms occupy the octahedral interstitial sites. These compounds all exist at substoichiometry ($0.6 < x < 1.0$), and appear to be unstable at full stoichiometry. These materials are all superconducting, with T_c's which increase rapidly with increasing non-metal atom concentration, reaching large values near stoichiometry ($T_c \sim 10 - 18$ K). NbC_x and TaC_x, which are good superconductors, show soft acoustic phonon modes, while in nonsuperconducting ZrC_x and HfC_x these soft modes are absent. NbC_x also exhibits an order-disorder transformation of the vacancies in the carbon sublattice. MoC_x and TaN_x, also good superconductors (T_c's $\sim 10 - 14$ K), exist in several noncubic phases as well as the cubic B1 phase. The optic modes of $PdH_x(D_x)$ are very soft throughout the Brillouin zone, and it has recently been found that the vacancies in the H(D) sublattice undergo a variety of order-disorder transitions.

These transitions and their effects on the superconductivity of $PdH_x(D_x)$ constitute the remainder of this chapter.

By citing these examples we do not mean to imply that structural instability in a material automatically leads to a high superconducting T_c. A good counter-example is sodium, which exhibits a structural phase transition accompanied by a soft shear mode, but which is not superconducting. Rather, the condition which is favorable to a high T_c, namely a strong electron-phonon interaction, will often lead to a structural instability. Phillips[86] has stated this connection in a very general way, which we paraphrase here. A structural distortion, by changing some ion-ion distances, results in an increase in the ion-ion interaction energy, which acts as a restoring force opposing the distortion. When we confine ourselves to materials with very high T_c's, we are selecting only those materials which have a strong electron-ion interaction, and a strong electron-ion interaction is capable of screening the ion-ion interaction, reducing the restoring force, and thus creating an instability, which may lead to a soft phonon mode or a structural change.

Having established that the strong electron-ion interaction which produces a high T_c may also destabilize the lattice, we now ask how the resulting structural change will affect T_c. Testardi[87] postulates that "The conditions for high T_c superconductivity are just those which occur because the high T_c compounds are headed toward structural instability. Any mechanism which relieves the instability at low temperatures will lead to a serious reduction in the superconducting transition temperature." In other words, the strong electron-ion interaction

produces a lattice instability which results in a structural change to a new, stable configuration. To remove the instability, the electron-ion interaction in the new, stable phase must be reduced, thereby decreasing T_c. The trick to producing a high T_c superconductor then, is to create an unstable lattice but inhibit the transformation which restores stability.

Beyond these qualitative arguments, the theory of instabilities and superconductivity is in a fairly early stage of development. The number of materials in which superconductivity can be investigated both before and after the occurrence of the structural transformation is rather small at present, and it is not clear what kinds of instabilities are most beneficial to high T_c's. The nature of the structural transformations in $PdH_x(D_x)$ makes this system well suited to studying the effects of these transformations on the superconducting transition temperature.

Structural Changes Associated with the "50 K Anomaly" in $PdH_x(D_x)$

In 1957, Nace and Aston[88] reported an anomalous peak in the specific heats of $PdH_{0.49}$ and $PdD_{0.48}$ samples at a temperature of about 55 K. Further specific heat studies demonstrated that the anomalous behavior persisted over a wide range of compositions ($0.1 \lesssim x \lesssim 0.8$). Since 1957, a vast amount of experimental and theoretical work on the nature of the 50 K anomaly has appeared. Excellent reviews of this literature may be found in references 2 and 89, and we will only summarize the results briefly.

Besides specific heat, anomalous behavior in the temperature range from 50 K to 70 K was found in resistivity, internal friction, and Hall constant of $PdH_x(D_x)$. No anomalies were found in the magnetic susceptibility, elastic constants, or Raman spectra. The anomaly was found to be a property of the β-phase; the temperature at which the anomaly occurred increased from ∿ 55 K for $x \leq 0.63$ to ∿ 80 K for $x \geq 0.75$, while the magnitude of the anomalous behavior decreased with increasing x, vanishing by $x = 0.89$.[89]

The anomalies in the various properties showed marked dependence on the thermal history of the sample, the heating/cooling rates and time. These dependences often led to apparent discrepancies among the studies, and confused or complicated their interpretation. It did seem clear that the anomalous behavior involved the H(D) atoms, and explanations involving the clustering of H(D) atoms or their migration from octahedral to tetrahedral sites were advanced. Neutron and x-ray diffraction experiments disproved these models; in fact, no change in structure was found upon cooling samples through the anomaly temperature.

By the 1970's it was well established that the nonstoichiometric hydrides and deuterides of the BCC transition metals V, Nb, and Ta exhibit a large variety of structural phase transitions. These order-disorder transitions are from high temperature phases, in which the H(D) atoms (or, alternatively, the vacancies in the H(D) sublattice) randomly occupy the tetrahedral sites, to phases in which they occupy specific subsets of sites, lowering the crystal symmetry and producing a larger unit cell. The resulting ordered structures depend on the H(D) concentration and temperature. Such order-disorder transformations seemed a

likely explanation for the 50 K anomaly in $PdH_x(D_x)$, but the diffraction studies revealed no new "superlattice" reflections which must necessarily accompany the symmetry change produced by the ordering.

The clue to the case of the missing superlattice lines in $PdH_x(D_x)$ was discovered in 1977 by Satterthwaite, et al.[90] Prompted by the report of a long time constant in the time dependence of the Hall coefficient, they studied the effects of long term annealing, at temperatures just below the anomaly temperature, on the electrical resistance of a $PdH_{0.795}$ sample. They found that the resistance stayed relatively constant or increased slightly in the first several hours, but then dropped precipitously after a very long time span (hundreds of hours). The large drop (20 - 40%) in resistance was due to a decrease of the residual resistance, the most likely explanation of which was a decrease in scattering from the vacancies in the H sublattice when these vacancies ordered to form a periodic array. This implied that the 50 K anomaly was associated with an order-disorder transition, but one which was exceedingly sluggish. No superlattice lines were observed in the previous diffraction experiments because the samples had not been given sufficient time to develop long range order.

Shortly after this announcement, new neutron diffraction studies were undertaken. Anderson, et al.,[92,93] found that in $PdD_{0.64}$ and $PdD_{0.67}$ crystals, superlattice reflections appeared at the points belonging to the (1, ½, 0) star in reciprocal space (i.e., the W points of the Brillouin zone) after annealing for 48 hours at 50 K, and disappeared when the sample temperature was raised above 50 K. They named this ordered phase the γ-phase, and proposed that the ordered structure

belonged to the space group $I4_1/amd$, which would be stoichiometric at $PdD_{0.50}$ (see Figure 5a).

Almost simultaneously, Ellis, et al.,[94] reported the appearance of superlattice reflections at the points of the (4/5, 2/5, 0) star in a $PdD_{0.76}$ crystal annealed at 70 K for 100 hours. The increase in intensity of the superlattice line was shown to correlate with the decrease in resistance, demonstrating that the ordering process was responsible for the anomalous behavior in PdD_x. The authors proposed that the ordered structure was the interstitial analog of the Ni_4Mo structure, space group I4/m (shown in Figure 5b), which is stoichiometric at $PdD_{0.80}$. We shall refer to this as the δ-phase.

Since this time, additional neutron diffraction work at Argonne National Laboratory[95] and Institut Laue-Langevin,[96-98] combined with resistivity studies performed here,[89,95] have "filled in the blanks" to the point where a coherent picture of the ordered phases of $PdH_x(D_x)$ is emerging, which we summarize below.

The ordered states of PdD_x may be described as deuteron density waves forming along the [4, 2, 0] directions, with wavelengths which depend on composition. Figure 6a shows the Brillouin zone of an FCC lattice, and Figure 6b shows the $q_z = 0$ plane of reciprocal space, divided into the various Brillouin zones. The dashed line in Figure 6b indicates a typical [4, 2, 0] direction, and the open circle and open triangles show respectively the locations of the (1, ½, 0) and (4/5, 2/5, 0) superlattice reflections lying along that [4, 2, 0] direction. Figures 7, 8, and 9 show neutron diffraction data for neutron momentum transfers lying along the dashed line in Figure 6b.

Figure 5. Ordered structures of PdD_x. The dashed lines show the unit cells of the FCC lattice of octahedral interstitial sites. The solid lines show the new unit cell of the ordered structure. Solid circles represent D atoms, while the open circles represent vacancies. For the sake of simplicity, the Pd atoms are not shown. (a) shows the structure of the γ-phase, stoichiometric at x = 0.50, while (b) shows the structure of the δ-phase, stoichiometric at x = 0.80.

(a)

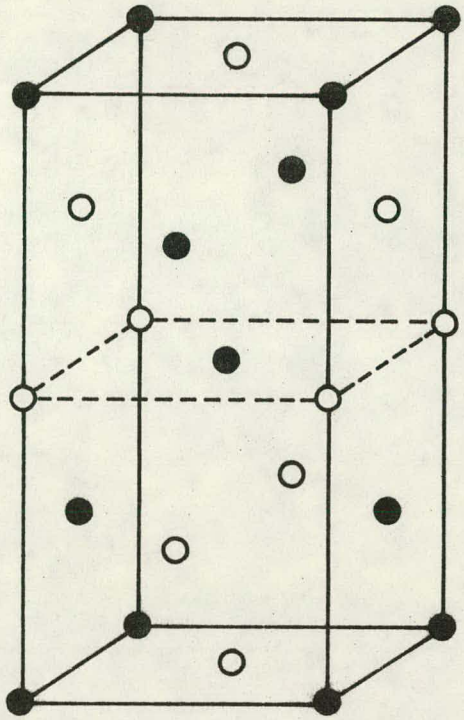

(b)

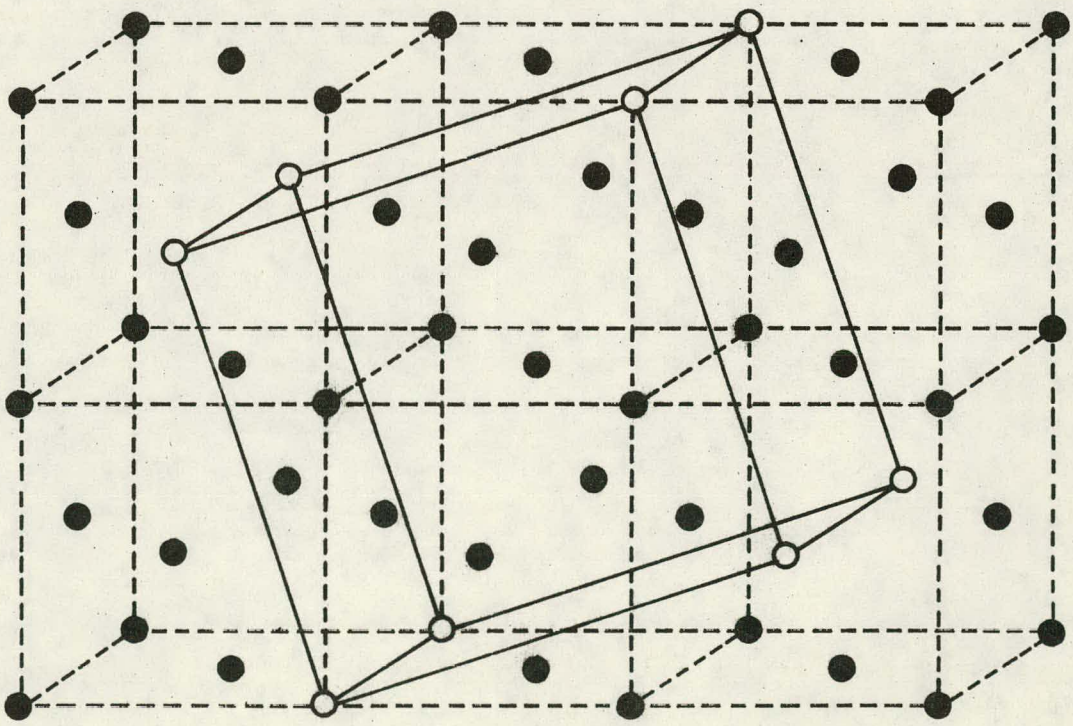

Figure 6. (a) The FCC Brillouin zone, showing locations of four different points of high symmetry in the $q_z = 0$ plane.

(b) The $q_z = 0$ plane of reciprocal space, divided into the various Brillouin zones. The solid squares at the zone centers mark the allowed reflections from the FCC lattice. The dashed line indicates the [4, 2, 0] direction along which the neutron diffraction scans of Figures 7, 8, and 9 were taken. The open circle and open triangles mark the positions of the (1, ½, 0) and (4/5, 2/5, 0) type superlattice reflections, respectively.

(a)

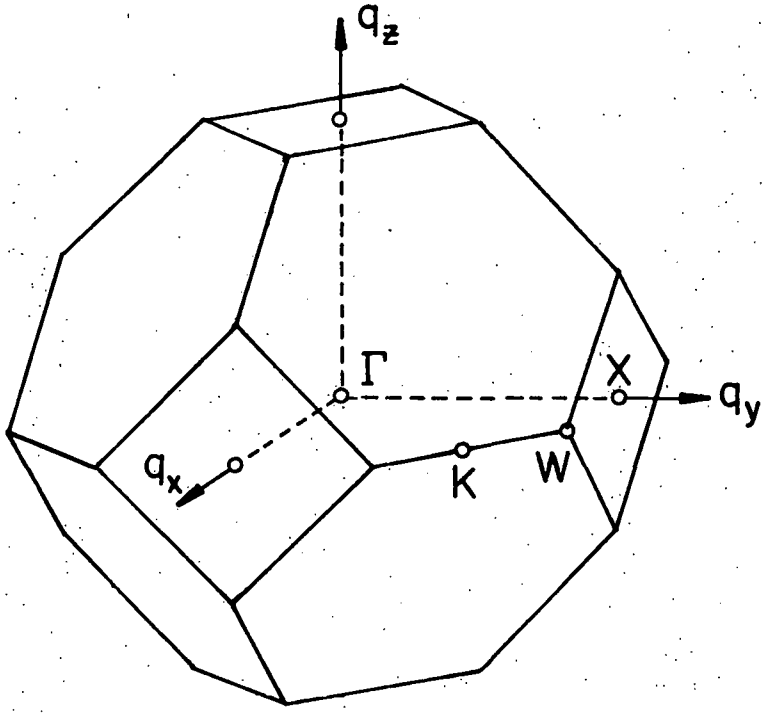

(b)

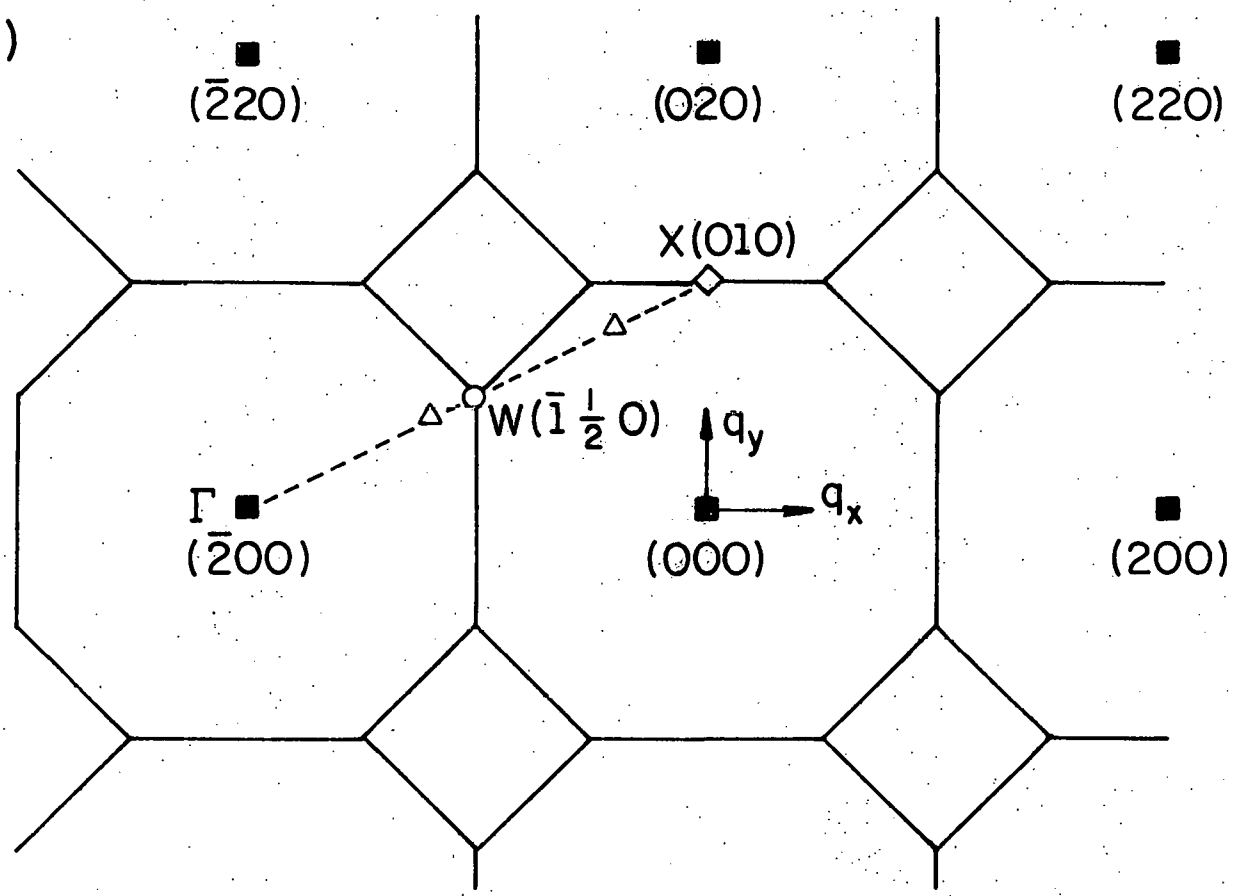

Figure 7. Neutron diffraction data on γ-phase PdD_x, for neutron momentum transfers in a [4, 2, 0] direction, showing the superlattice reflection at (1, ½, 0). From reference 100.

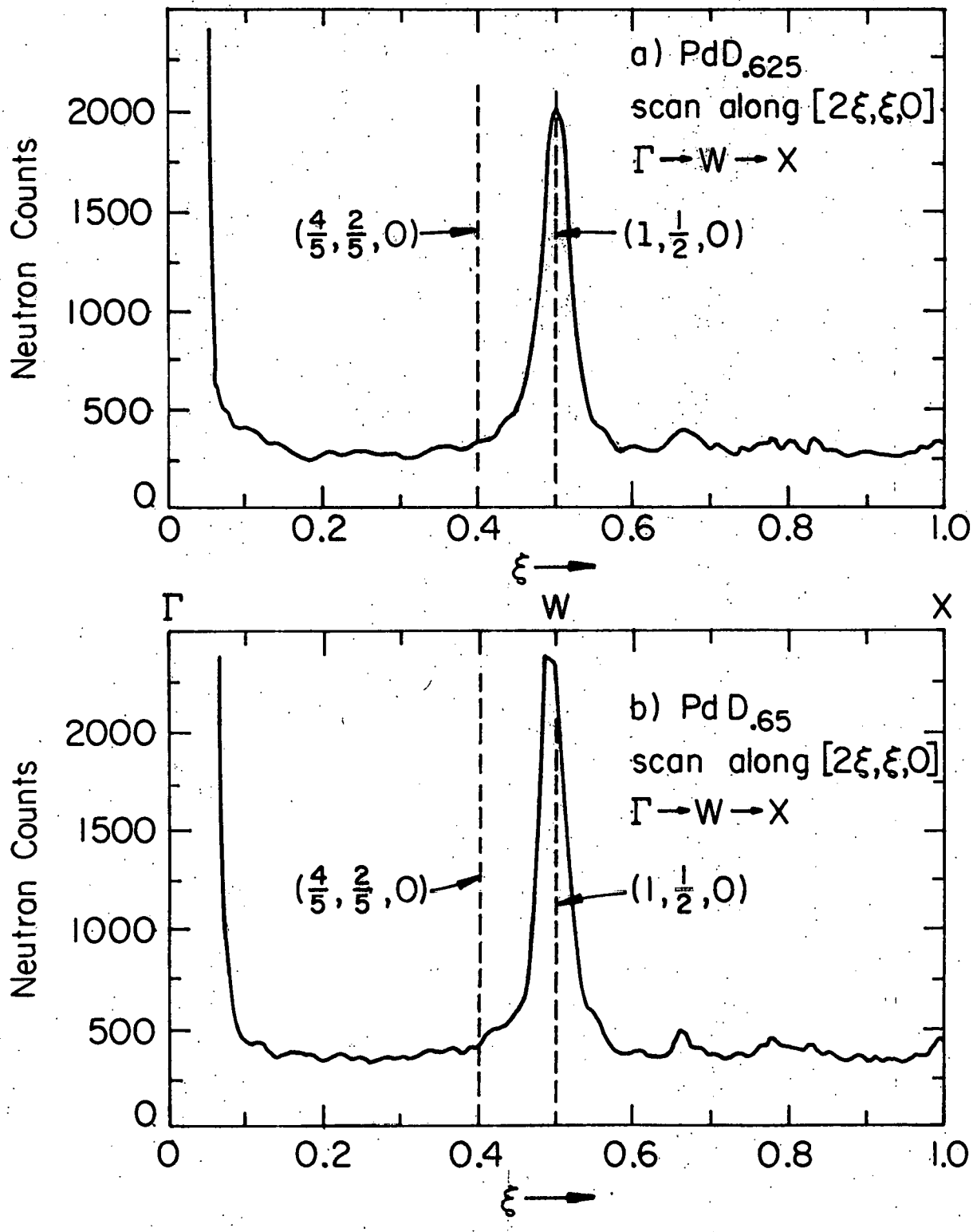
a) PdD.625
scan along [2ξ,ξ,0]
Γ → W → X
(4/5, 2/5, 0)
(1, 1/2, 0)
Neutron Counts
2000
1500
1000
500
0
0
0.2
0.4
0.6
0.8
1.0
ξ →
Γ
W
X
b) Pd D.65
scan along [2ξ,ξ,0]
Γ → W → X
(4/5, 2/5, 0)
(1, 1/2, 0)
Neutron Counts
2000
1500
1000
500
0
0
0.2
0.4
0.6
0.8
1.0
ξ →

Figure 8. Neutron diffraction data on SRO-phase $PdD_{0.73}$, from reference 100.

(a) Diffuse peak for neutron momentum transfers along a [4, 2, 0] direction.

(b) Neutron intensity contour map for momentum transfers in the $q_z = 0$ plane in the vicinity of (1, ½, 0), showing splitting of the diffuse peak.

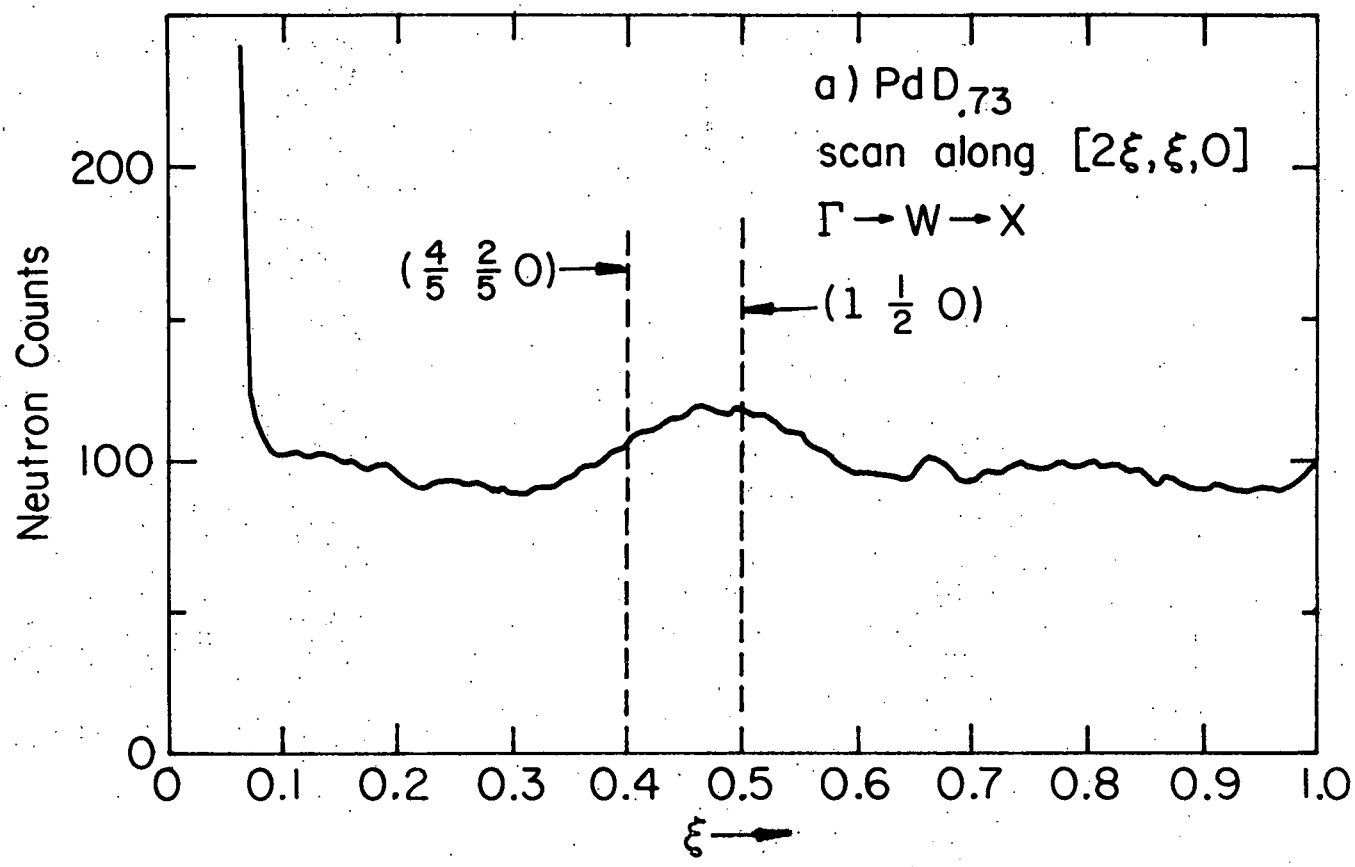
a) PdD.73
scan along [2ξ,ξ,0]
Γ → W → X
(4/5 2/5 0)
(1 1/2 0)
Neutron Counts
200
100
0
0 0.1 0.2 0.3 0.4 0.5 0.6 0.7 0.8 0.9 1.0
ξ →

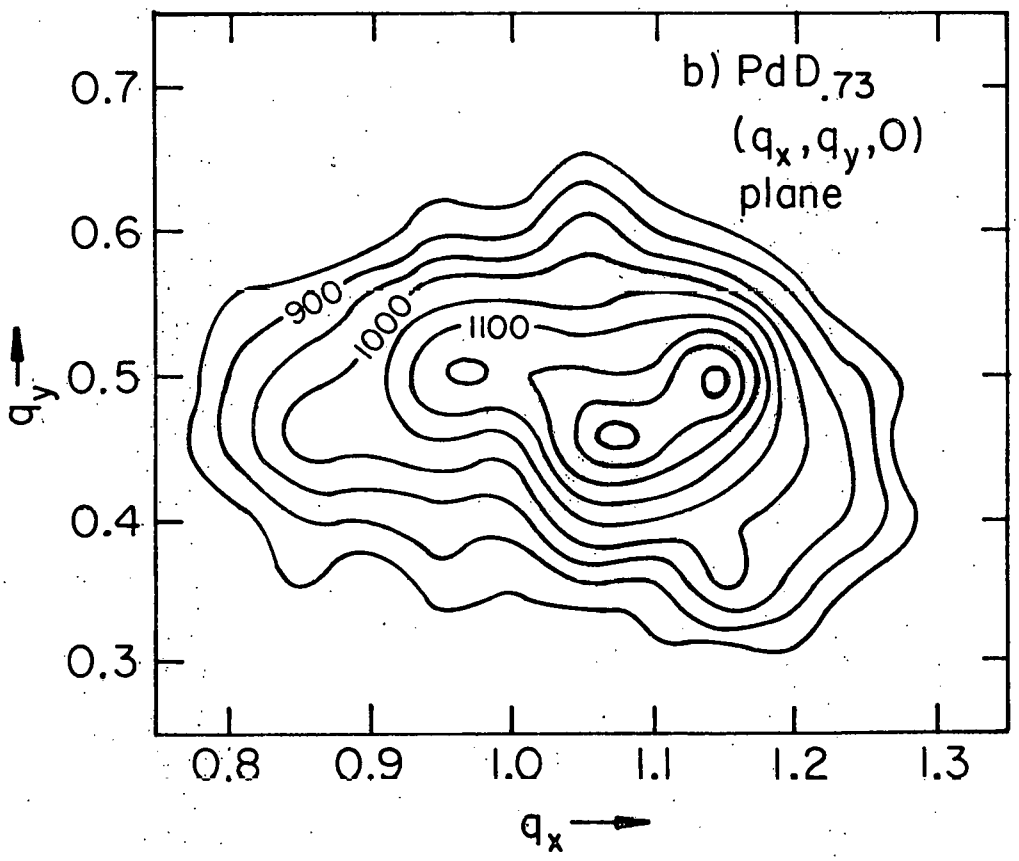
b) PdD.73
(qx, qy, 0)
plane
900
1000
1100
0.7
0.6
0.5
0.4
0.3
qy
0.8 0.9 1.0 1.1 1.2 1.3
qx →

Figure 9. Neutron diffraction data on δ-phase $PdD_{0.76}$ for neutron momentum transfers in a [4, 2, 0] direction, showing the superlattice reflection at (4/5, 2/5, 0). From reference 94.

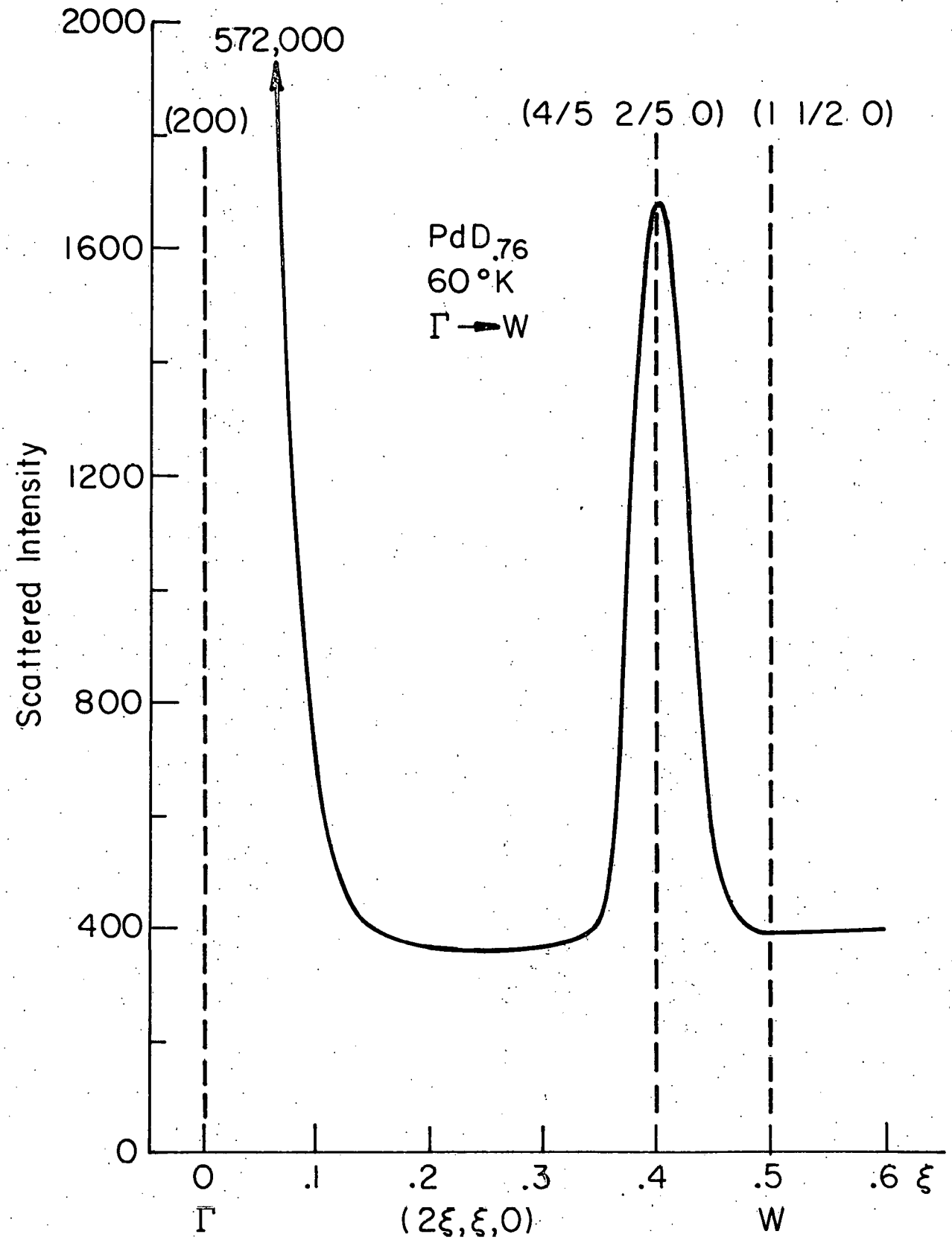
2000
1600
1200
800
400
0
572,000
(200)
(4/5 2/5 0)
(1 1/2 0)
PdD.76
60°K
Γ → W
Scattered Intensity
0
.1
.2
.3
.4
.5
.6 ξ
Γ
(2ξ, ξ, 0)
W

At low concentrations (x = 0.625, 0.64, 0.65, 0.67), PdD_x orders in the γ-phase, producing superlattice reflections at (1, ½, 0) and equivalent points (see Figure 7a, b). While this structure is stoichiometric at x = 0.50, the actual formation of the stoichiometric compound is prevented by the α-β phase separation which occurs for $x \lesssim 0.60$.

If samples in this composition range are annealed below 56 K, their resistance will show a small (∿ 3 - 6%) decrease after a time span of 20 - 40 hours, indicating the onset of long range order (LRO). By annealing a sample at low temperatures (∿ 47 K), and then warming it up in steps, allowing the resistance to equilibrate at each step, an "equilibrium" resistance vs. temperature curve can be obtained, such as those shown in Figure 10. These curves show a broad, shallow minimum in the resistance between 80 K and 100 K, followed by an increase which peaks at ∿ 56 K. Below 56 K, the resistance drops off rather sharply. The increase in resistance which occurs from 100 K to 56 K is probably due to the nucleation of short range order (SRO), while the development of LRO for temperature less than 56 K produces the drop in resistance as well as the (1, ½, 0) superlattice lines. The size of the resistance drop is rather small because the ordered structure is highly defected, being far from stoichiometry. As x increases from ∿ 0.63 to ∿ 0.70, the ordered structure apparently undergoes some distortion due to the increasing defect concentration. In the resistance vs. temperature data, this distortion decreases the magnitude of the drop-off below 56 K for increasing x (see Figure 10). The distortion is also evident in the neutron diffraction data; the (1, ½, 0) peak

Figure 10. Equilibrium resistance ratio vs. temperature for several samples of γ-phase and one sample of SRO-phase $PdH_x(D_x)$.

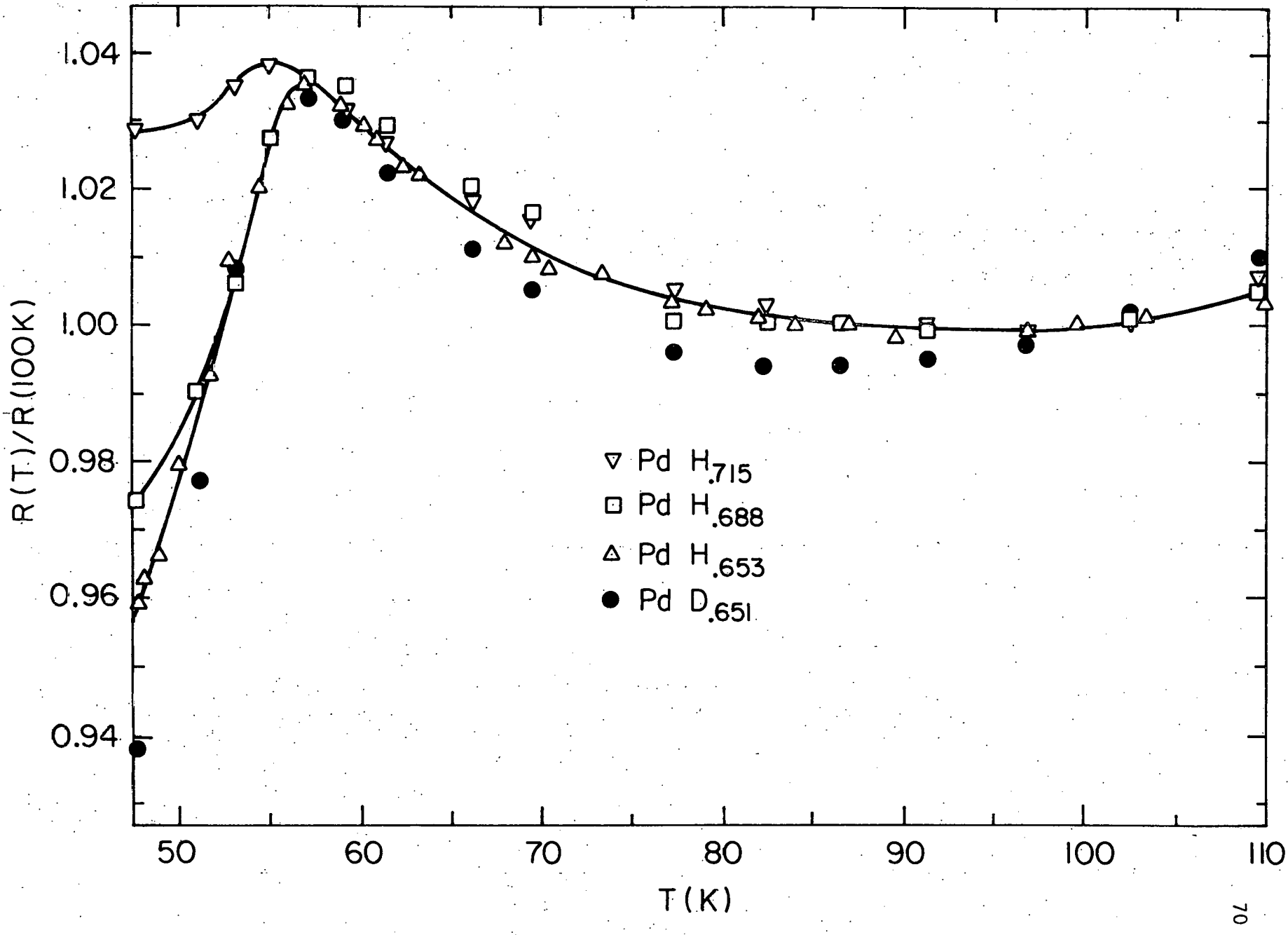
1.04
1.02
1.00
0.98
0.96
0.94
R(T)/R(100K)
50
60
70
80
90
100
110
T(K)
Pd H.715
Pd H.688
Pd H.653
Pd D.651

is shifted slightly toward the (4/5, 2/5, 0) position (see Figure 7) and the neutron intensity distribution around (1, ½, 0) in the $q_z = 0$ plane changes from nearly axially symmetric to very anisotropic.[100]

For D concentrations greater than about 0.71, this distortion is great enough to suppress the formation of LRO, and the γ-phase does not form. For $0.71 \lesssim x \lesssim 0.75$, the sharp superlattice line at (1, ½, 0) is replaced by a broad, diffuse peak which straddles both (1, ½, 0) and (4/5, 2/5, 0), as shown in Figure 8a. This sort of diffuse scattering is characteristic of SRO with no LRO present. Such an interpretation is also consistent with the resistance vs. temperature data, where the data for all samples are identical for T > 56 K (where only SRO is present), but the decrease in resistance below 56 K is absent in the high concentration sample (x = 0.715) where LRO is also absent (see Figure 10).

Blaschko, et al.,[99] interpret this diffuse pattern as arising from the coexistence of microdomains of DO_{22} tetragonal structure, stoichiometric at x = 0.75, with those of the Dl_a (Ni_4Mo) structure which occurs in the δ-phase, and is stoichiometric at x = 0.80. They hypothesize that there is a competition between these two structures which prevents either one from dominating and establishing LRO. In $PdD_{0.73}$ the diffuse scattering is split into three weak peaks, as shown in Figure 8b. Blaschko, et al.,[98] suggest that this is due to the modulation of the DO_{22} microdomains by a periodic distribution of antiphase boundaries (APB's). The details of the splitting of the diffuse intensity vary with D concentration implying that the distribution of APB's varies through this region of SRO.

The DO_{22} and Dl_a structures are closely related, in that both may be described as a periodic modulation of the occupancy of the (4, 2, 0) planes of the FCC lattice of octahedral sites. In the DO_{22} structure, this modulation consists of three fully occupied (4, 2, 0) planes followed by one vacant (4, 2, 0) plane, while in the Dl_a structure it consists of four fully occupied planes followed by one vacant plane. Certain types of antiphase boundaries can convert regions of one of these structures into the other, as has been shown to occur in the early ordering stages of the Ni_4Mo system.[101] The situation in PdD_x for $0.71 \lesssim x \lesssim 0.75$ may be similar to that in the early ordering stages of Ni_4Mo. The resistance behavior of $PdH_x(D_x)$ in this concentration range has not been studied. This is the concentration range in which the anomaly temperature increases from the γ-phase value of ∿ 56 K to the δ-phase value of ∿ 80 K.[89] We would not expect annealing to produce a large drop in the resistance in the absence of LRO.

For concentrations greater than ∿ 0.75, PdD_x orders in the Dl_a structure of the δ-phase (see Figure 5b), which produces a superlattice reflection at (4/5, 2/5, 0) and equivalent points, as shown in Figure 9. The Dl_a structure is stoichiometric at x = 0.80, as described previously. The δ-phase structure has been observed in neutron diffraction studies of $PdD_{0.76}$[94] and $PdD_{0.78}$.[99] Resistance studies[89] indicate that the δ-phase persists over the concentration range $0.75 \leq x \leq 0.82$, while higher concentrations have not been studied, other that an x = 0.89 sample which showed no anomaly. When samples in this range are annealed at temperatures below about 80 K, the resistance stays constant or increases by $\lesssim$ 3% during the first several tens of hours. After a

period ranging from 60 hours to several hundred hours, the resistance shows a precipitous drop, amounting to 20 - 40% of its initial value, as LRO develops. If an ordered sample is warmed up in steps to obtain an equilibrium resistance vs. temperature curve, the result, shown in Figure 11, is quite different from that of the γ-phase, shown in Figure 10. The decrease in resistance below the anomaly temperature is much larger in the δ-phase than in the γ-phase, because the δ-phase concentrations are near ideal stoichiometry. Also, the strong precursor effects which create the peak in the resistance of the γ-phase are absent or much reduced in the δ-phase.

Because of the large incoherent neutron scattering cross section of the proton, all of the neutron diffraction work on the ordered structures has been performed on PdD_x samples. There is one exception, a neutron and gamma-ray diffraction study of $PdH_{0.73}$[96] which shows the same type of diffuse scattering as occurs in $PdD_{0.73}$. The resistive behavior of hydride and deuteride samples are very similar. There is an isotopic difference in the ordering kinetics, particularly in the γ-phase, where the resistance of hydride samples decreases more rapidly than that of deuteride samples during the annealing process. The equilibrium resistance vs. temperature curves of both hydride and deuteride samples are nearly identical, however, as may be seen in Figure 10. The compositional ranges in which the various phases occur are also identical for both hydride and deuteride, within the rough limits in which they have been sketched out. We cannot rule out minor isotopic differences in the phase diagrams until the phase boundaries can be

Figure 11. Equilibrium resistance ratio vs. temperature for a δ-phase $PdD_{0.762}$ sample, compared with that for a quenched, disordered $PdD_{0.743}$ sample. From reference 89.

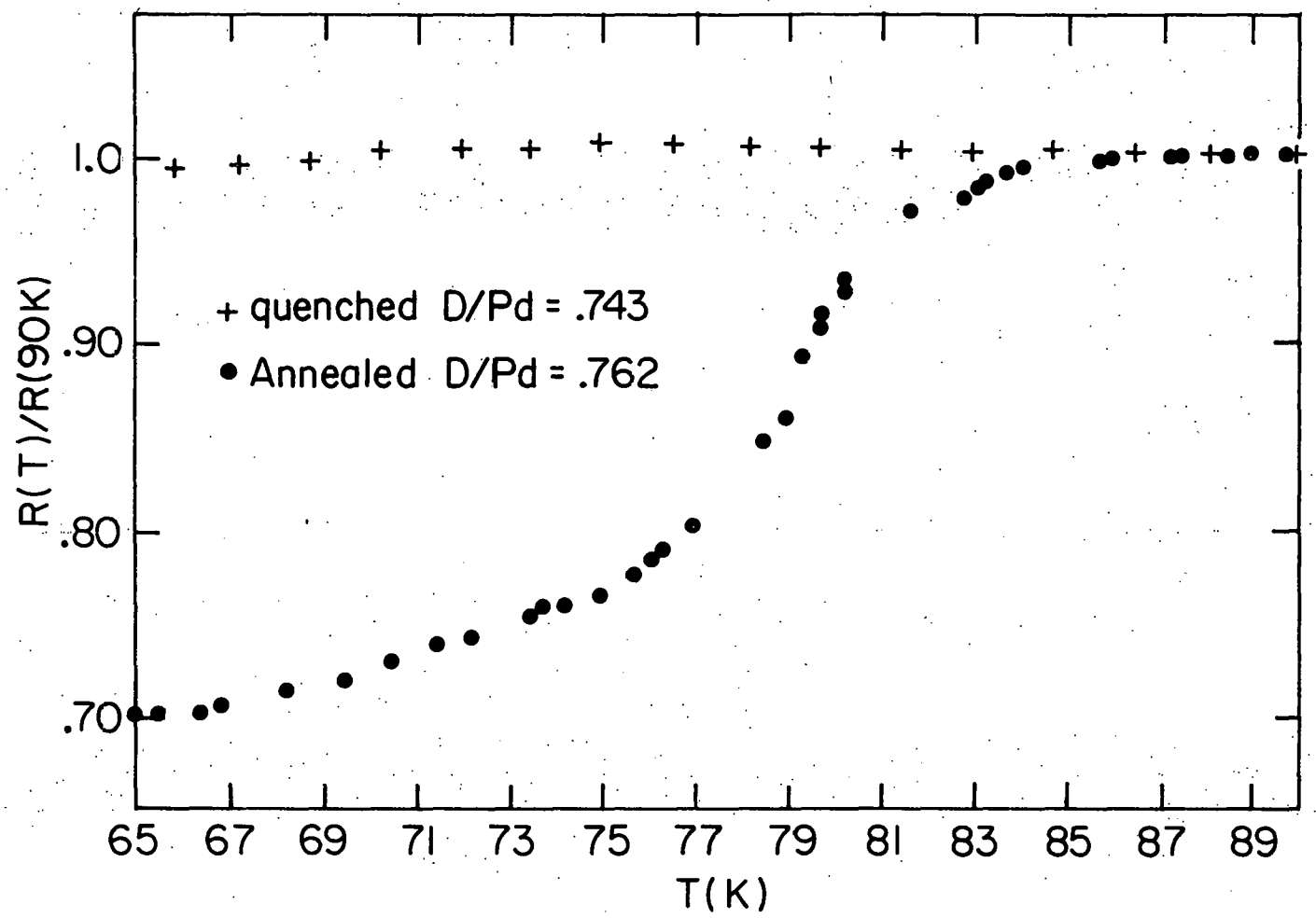
1.0
.90
.80
.70
R(T)/R(90K)
+ quenched D/Pd = .743
• Annealed D/Pd = .762
65
67
69
71
73
75
77
79
81
83
85
87
89
T(K)

more accurately determined. Such differences are known to occur in the Group V hydrides.[2/]

$PdH_x(D_x)$ is a nearly ideal system for studying the effects of the ordering process on T_c. Because the ordering process is so slow (taking hundreds of hours), samples may be quenched from high temperatures to liquid He temperatures, freezing in the disorder, to study superconductivity in the disordered state. In fact, the T_c measurements of Chapter III, and all previous work on the superconducting transition, were made on disordered β-phase material. The samples may then be annealed and the ordering process monitored resistively. The process is slow enough that it may be arrested at any desired stage by again quenching to liquid He temperatures to measure the ordered state T_c, after which the ordering process may be resumed by rewarming the sample to the annealing temperature and continuing to anneal. The only drawback to the $PdH_x(D_x)$ system is that the time scale for ordering is so long that one is never sure whether the process has reached equilibrium at a given temperature, or just slowed down to an almost imperceptible rate. This uncertainty, together with the simple problem of measuring several concentrations of both isotopes when each measurement takes more than a month, are the reasons why the properties of the ordered states are not well known as of yet.

Ordered State T_c's: Experiment

The work presented in Chapter III demonstrated that with a pumped He^4 cryostat it was possible to study superconductivity in the δ-phase of PdD_x and, possibly, PdH_x. By using a He^3 cryostat, temperatures to

0.3 K can be obtained, permitting the observation of superconductivity in the SRO-phase of PdD_x as well. In the γ-phase, the superconducting T_c's of both PdH_x and PdD_x are vanishingly small.

Samples for this work were prepared and analyzed in the manner described in Chapter III. A $PdD_{0.742}$ sample was prepared from the same Marz grade Pd foil used in the previous work. $PdD_{0.817}$ and $PdH_{0.837}$ samples were prepared from ultrahigh purity Pd foil which contained less than 1 ppma Fe.[102] Foils measured approximately 25.4 mm × 5.5 mm × 0.05 mm. The samples were all treated with the KI-I solution to retard H(D) loss during mounting in the He^3 cryostat.

Because He^3 has a much higher vapor pressure than He^4, much lower temperatures can be reached by evaporative cooling, e.g., ∿ 0.3 K for He^3 vs. ∿ 1.0 K for He^4. For this reason, we assembled a He^3 cryostat for these measurements, so that both the δ-phase and SRO-phase might be studied. Figure 12 shows the details of the He^3 refrigerator, while Figure 13 shows the external equipment associated with it.

The He^3 pot, sample, thermometers, etc., were housed in a stainless steel vacuum can which was immersed in the liquid He^4 bath. An indium o-ring provided the vacuum seal between can and flange. The vacuum can could be evacuated through a 9.5 mm O.D. thin wall stainless steel tube.

The He^3 pot, machined from OFHC copper, had an internal volume of about 7 cm^3. A layer of copper beads approximately 5 mm deep was sintered into the bottom of the He^3 pot to increase the surface area in thermal contact with the He^3. A 6.4 mm long, threaded (¼-20) copper stud was provided on the bottom side of the pot, for attachment of the

Figure 12. Details of the He^3 cryostat insert.

A. vacuum can pumping line

B. epoxy-sealed electrical feedthrough

C. optical baffle

D. indium o-ring

E. stainless steel vacuum can

F. He^3 pot (cutaway view)

G. heater windings

H. Ge resistance thermometer

I. Pt resistance thermometer

J. epoxy sample clamp (cross-section)

K. mutual inductance coils (cross-section)

L. He^3 pumping line

M. electrical lead (others not shown)

N. sintered copper beads

O. thermal grounding pin

P. Ge-Au resistance thermometer

Q. sample stage

R. sample

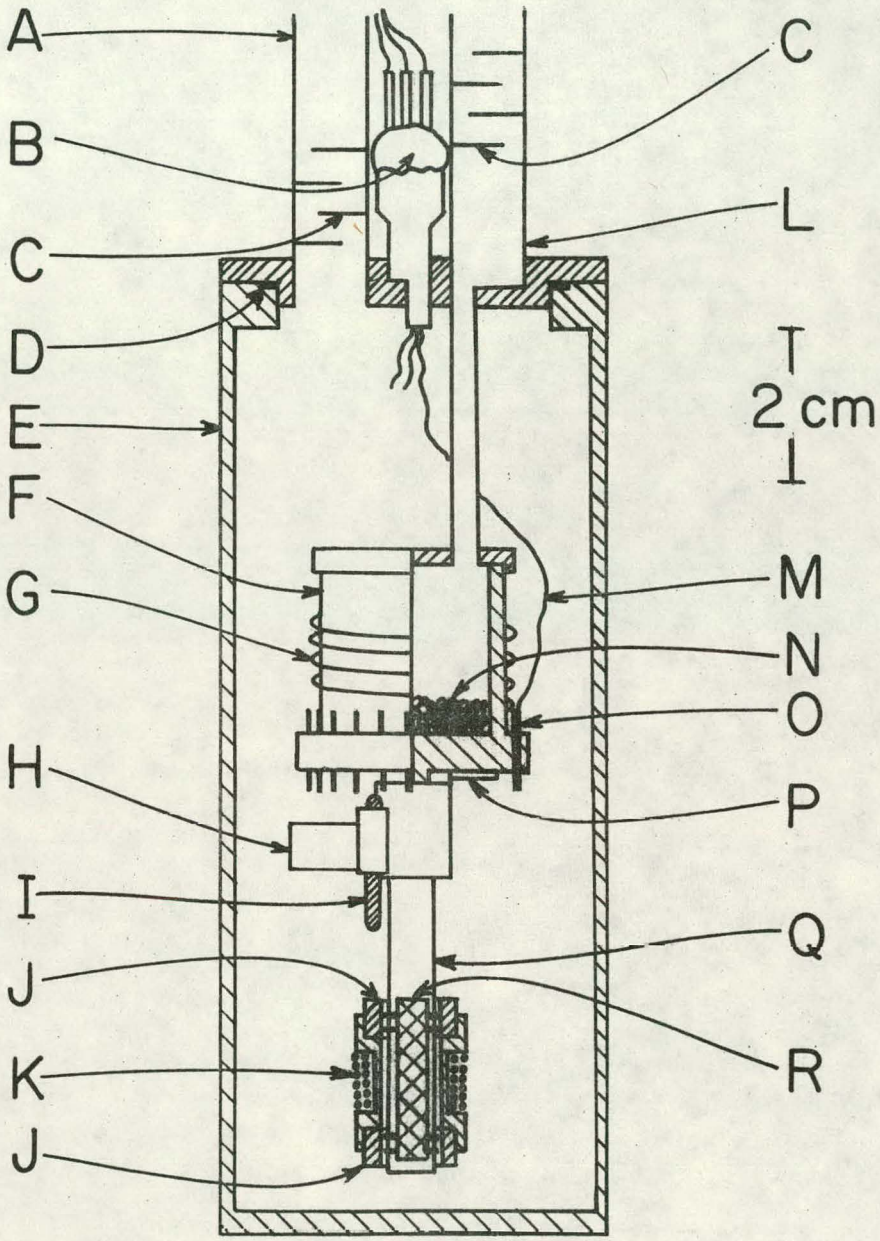
A
B
C
D
E
F
G
H
I
J
K
J
C
L
2 cm
M
N
O
P
Q
R

Figure 13. Schematic diagram of He^3 cryostat and He^3 gas handling system.

A. glass dewar vessels

B. liquid nitrogen

C. vacuum can pumping line

D. He^3 pumping line

E. pumped liquid He^4 bath

F. stainless steel vacuum can

G. He^3 pot

H. sample stage

I. throttling valves

J. 0-50 torr mechanical vacuum gauge

K. thermocouple vacuum gauge

L. diffusion pump

M. compound vacuum-pressure mechanical gauge

N. He^3 storage tank

O. mechanical vacuum pump

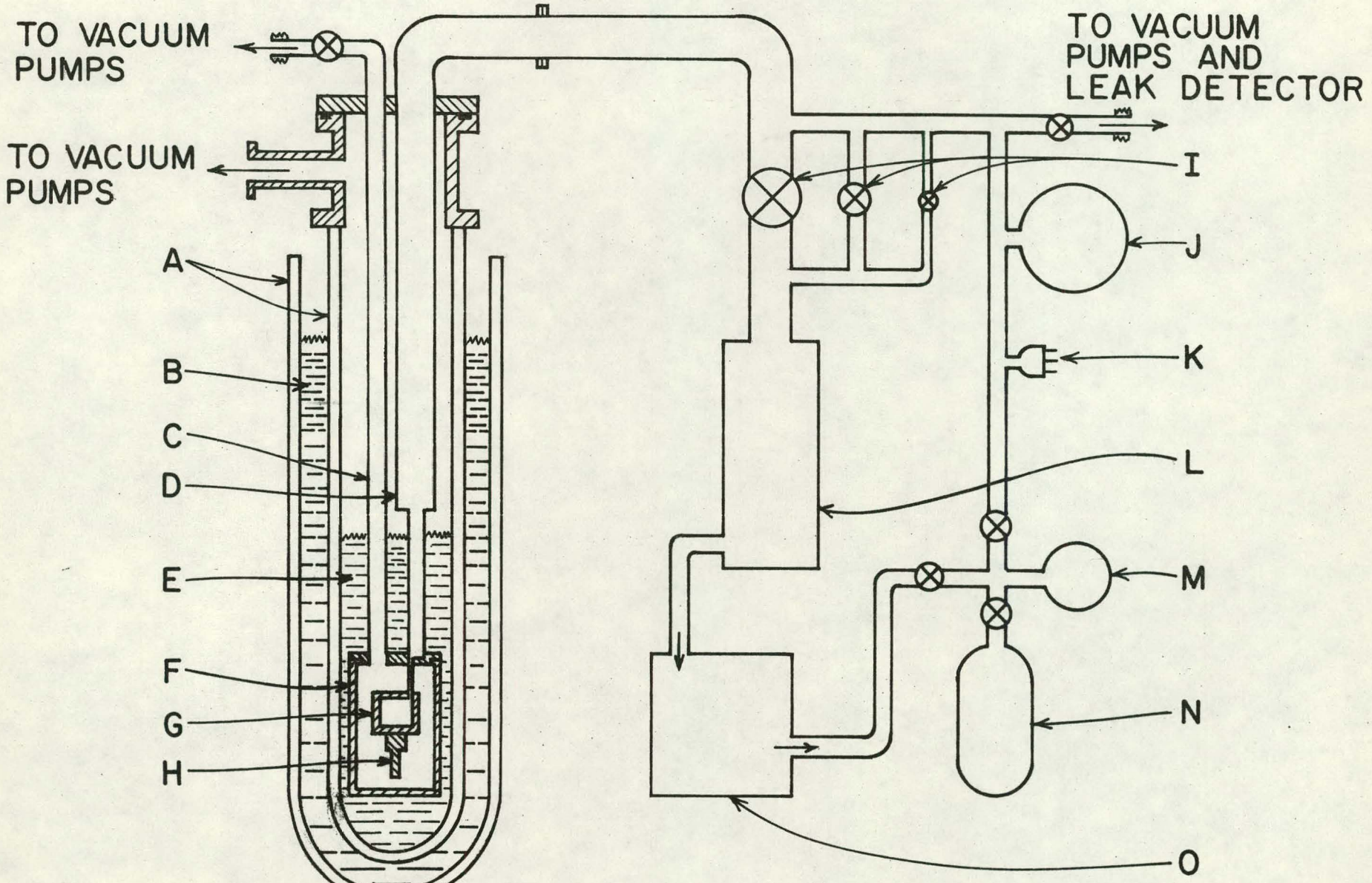
TO VACUUM PUMPS
TO VACUUM PUMPS
TO VACUUM PUMPS AND LEAK DETECTOR
A
B
C
D
E
F
G
H
I
J
K
L
M
N
O

sample apparatus. Twenty-four evenly spaced holes were drilled through the flange at the base of the pot, and short lengths of #18 insulated copper wire were epoxied into these holes to provide thermal grounding pins for all electrical leads. The sides of the pot were electrically insulated with a layer of cigarette paper and adhesive varnish, and 450 Ω of #40 manganin wire were wound bifilarly around the pot, to act as heater windings for the temperature controller. The heater windings were covered with another layer of cigarette paper and varnish to protect them. The He^3 pot was evacuated through a 3.2 mm O.D. thin wall stainless steel tube, which widened to 9.5 mm O.D., and ultimately, 25.4 mm O.D. thin wall stainless steel tube outside the vacuum can.

Thirty electrical leads (six bundles of five wires each) of #36 varnished manganin wire were brought into the vacuum can through an epoxy-sealed feedthrough. Twenty-one of these leads were needed for the experiment, with nine spares provided in case of breakage, etc. The wire bundles were sheathed in teflon tubing at the epoxy seal to provide strain relief.

The sample stage consisted of a long, flat OFHC copper finger which extended down from the bottom of the He^3 pot. The finger was coated by an electrically insulating layer of cigarette paper and varnish, and two pairs of bare copper wire electrodes were varnished in place across the finger, to form the electrical contacts for measuring the sample resistance. The voltage electrodes were spaced about 15 mm apart. A foil sample was laid across the two electrode pairs, and pressed firmly onto them by means of two epoxy clamps and set screws. These epoxy clamps also served to hold in place the

mutual inductance coils which surrounded the sample. These coils consisted of 83 turns of superconducting Cu-clad Nb wire as the primary, and 1400 turns of #40 Cu wire as the secondary, wound on a coil form 10 mm long and 10 mm in outer diameter.

Three thermometers were needed for the experiment. A factory calibrated Ge resistance thermometer,[103] mounted on the sample stage, was used for temperature measurements in the range from 0.3 K to 4.2 K. A Pt resistance thermometer,[104] also mounted on the sample stage, was used in the temperature range from 20 K to 100 K. A third resistance thermometer, consisting of a thin film of Ge-Au alloy evaporated onto a glass substrate,[105] was mounted on the bottom of the He^3 pot, and was used as the temperature sensor for the temperature controller. The R vs. T characteristics of the Ge-Au thermometer were such as to provide good sensitivity from 0.3 K to 100 K.

The necessary electronics for this experiment are shown schematically in Figure 14.

The superconducting transitions were monitored inductively, as in Chapter III, using a mutual inductance bridge[106] operating at 155 Hz to measure the change in mutual inductance of the coil pair surrounding the sample. The resolution of the bridge was $\sim$ 0.7% of the total change in mutual inductance produced when the sample became superconducting. The magnetic field applied to the sample by the coils was about 0.5 gauss.

The resistance of the Ge thermometer was measured by a simple, home-built, four-terminal a.c. resistance bridge, operating at 17 Hz. The bridge had an accuracy of 0.1%, leading to an accuracy in the

Figure 14. Block diagram of electronics associated with the ordered state T_c measurements.

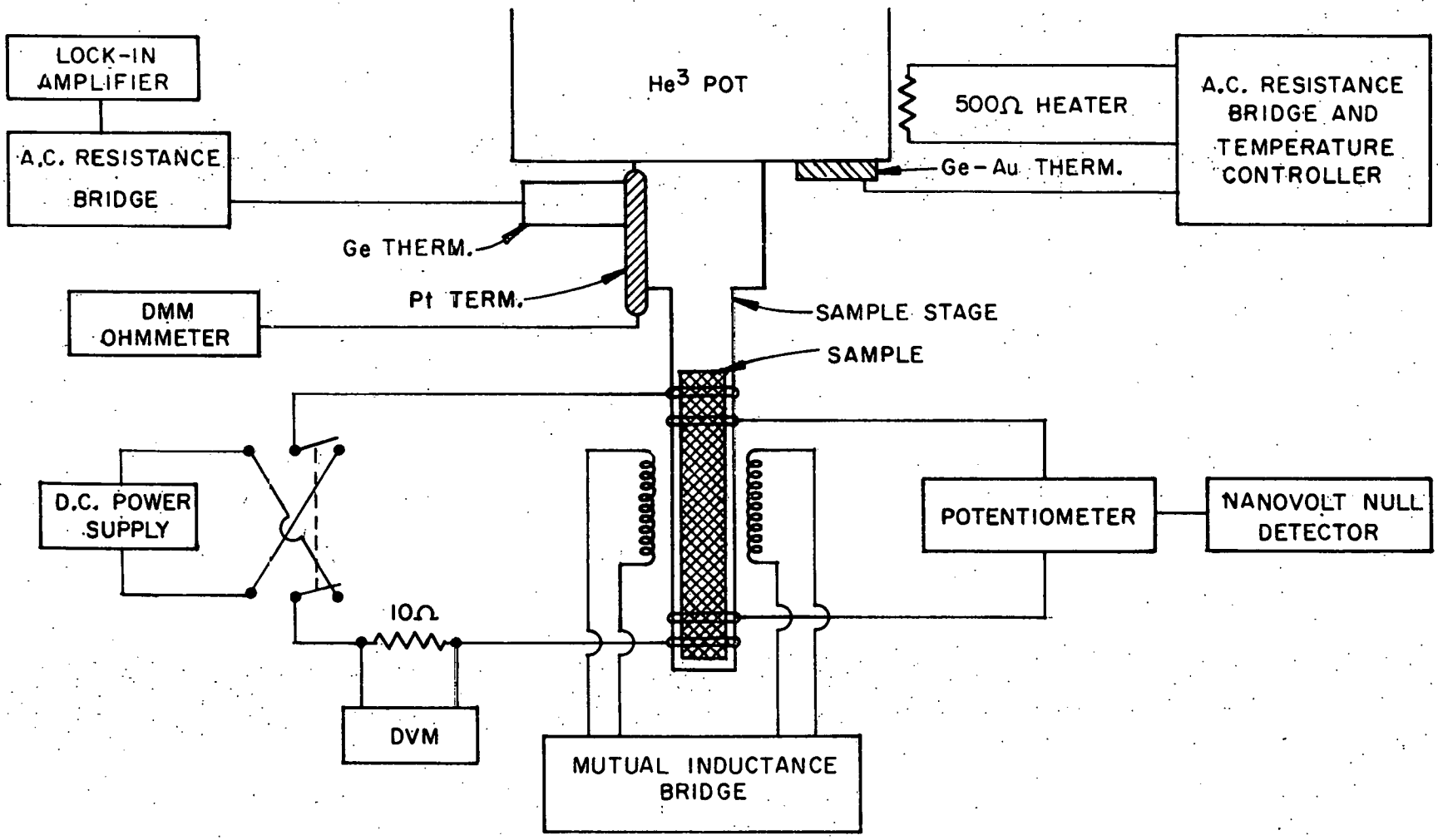
LOCK-IN AMPLIFIER
A.C. RESISTANCE BRIDGE
Ge THERM.
Pt TERM.
DMM OHMMETER
He3 POT
500Ω HEATER
Ge-Au THERM.
A.C. RESISTANCE BRIDGE AND TEMPERATURE CONTROLLER
SAMPLE STAGE
SAMPLE
D.C. POWER SUPPLY
10Ω
DVM
MUTUAL INDUCTANCE BRIDGE
POTENTIOMETER
NANOVOLT NULL DETECTOR

temperature determination of slightly better than 0.1% for 1 K $\leq$ T $\leq$ 4 K, and an accuracy of 1 mK for T < 1 K. The thermometer calibration was checked against the T_c of Al and found to be accurate to 1 mK at T $\approx$ 1 K. The Pt thermometer resistance was measured by a digital multimeter[107] operating in a four-terminal d.c. resistance mode. Temperature resolution was about 0.05 K in the temperature range from 25 K to 100 K.

Sample resistance was determined by a four-terminal d.c. technique. Current through the sample was determined by measuring the ohmic voltage drop across a 10 Ω standard resistor placed in series with the sample, using a digital voltmeter.[107] The ohmic voltage drop across the sample was measured by a six dial potentiometer[108] and nanovolt null detector.[109] Resistance measurements were made with the current flow in each direction and then averaged together to eliminate errors due to thermal EMF's anywhere in the circuit. The resolution of the resistance measurements was 4 - 5 μΩ out of a total of 5 - 9 mΩ, or somewhat better than 0.1%, with a sample current of 25 mA.

For T_c measurements above 1 K, a small amount of He^4 exchange gas was admitted to the vacuum can, and the sample was cooled by pumping on the He^4 bath in which the can was immersed. To obtain temperatures below 1 K, the vacuum can was left evacuated, and the He^4 bath was pumped down to a temperature of $\sim$ 1.1 K. He^3 was then admitted to the pot, where it rapidly condensed (He^3 normal boiling point = 3.19 K). The condensed He^3 was then pumped on, rapidly cooling the pot and sample stage to an ultimate temperature of about 0.28 K. The four

liter-atm. of He^3 gas (about 5 cm^3 of liquid) were sufficient to maintain a temperature of 0.3 K for about eight hours under normal operating conditions.

Coarse temperature control was obtained by varying the pumping rate on the He^4 bath or, below 1 K, the He^3 pot, by means of throttling valves. Fine temperature control was effected by a three-terminal a.c. resistance bridge and feedback temperature controller,[110] using the Ge-Au resistor as a sensor.

The procedure followed for each sample was as follows. The electrolytically charged sample foil was removed from storage in a dry ice-acetone bath and transferred to the KI-I solution for 10 minutes. From there it was mounted on the sample stage and, after checking the electrical contacts to the sample, the vacuum can was sealed and the assembled insert was placed in the precooled dewars. The vacuum can was evacuated and then back-filled with a small amount of He^4 exchange gas in order to cool the sample. Approximately forty minutes lapsed between placing the sample in the KI-I solution and cooling of the sample and cryostat to $\sim$ 100 K, during which time the high concentration samples lost a small amount of H(D) ($\Delta x \lesssim 0.1$).

Once the sample had cooled, the vacuum can was evacuated and the sample temperature was stabilized at 100 K for 48 hours in order to ensure that the sample was disordered, and the effects of previous thermal history erased. The sample resistance was also measured several times to check that it was not changing at this temperature. The sample was then quenched to 4.2 K, freezing in the disorder, and the T_c of the disordered state was measured. Following this, the sample

was again heated to 100 K for 48 hours, prior to starting the annealing process.

The sample temperature was lowered to 72 K at the start of each annealing run, and the resistance of the sample was measured at intervals of several hours to monitor the ordering process. The annealing temperature was changed periodically, to find a temperature at which the sample would order rapidly; the actual heat treatments varied from sample to sample.

In the $PdD_{0.817}$ and $PdH_{0.837}$ samples, the annealing process was interrupted by quenching the sample to liquid He temperatures in order to measure T_c during an intermediate stage of ordering. After this measurement, the sample was rewarmed to the annealing temperature and the annealing was continued.

After about 650 hours of annealing, the sample was again quenched to liquid He temperatures and the T_c of the ordered state was determined. Following this, the sample was warmed to 100 K for 48 hours to disorder it again, and the sample resistance was measured several times to check that it returned to its initial value. The sample was then quenched to 4.2 K and the disordered state T_c was remeasured to check that any changes in the superconducting transition upon ordering were reversible. The sample was then removed from the cryostat and analyzed for H(D) content.

Experiment Results

The results of this phase of the experiment are shown in Figures 15 through 22, and are summarized in Table 1.

The $PdD_{0.817}$ sample demonstrated annealing behavior fairly typical of the β-phase samples observed by Ellis[89] at lower concentrations ($x < 0.80$). At 72 K, after an initial increase of ∿ 2%, the resistance began to decrease sharply about 50 hours into the anneal, indicating the establishment of LRO (see Figure 15). When the resistance ratio, R(T)/R(100 K), had declined to a value of about 0.80, the sample was quenched to 4.2 K and T_c was measured. The ordering was found to have depressed T_c by about 7%, from its disordered state value of 2.211 K to a new value of 2.056 K (see Figure 17). The high concentration, high T_c parts of the sample were depressed somewhat more, and the low concentration, low T_c parts were depressed somewhat less, as evidenced by the changes in T_{20} and T_{80}, the temperatures at which the sample attained 20% and 80% of maximum diamagnetism, respectively (see Table 1).

After this T_c measurement, the sample was warmed to 68 K to continue the annealing. In the concentration range $0.75 < x < 0.80$, Ellis observed that decreasing the temperature of annealed samples produced additional decreases in resistance. In the present $PdD_{0.817}$ sample, dropping the temperature from 72 K to 68 K, and then 65 K, produced little change in the resistance, as shown in Figure 15. However, increasing the temperature to 78.5 K led to an additional decrease in resistance which was larger than that produced by annealing at 72 K, as shown in Figure 16. When the resistance ratio had decreased to a value of approximately 0.57, the sample was again quenched to 4.2 K to measure T_c. The transition temperature was depressed by a further 2% by the additional ordering (see Figure 17), and the difference

Figure 15. Resistance ratio of $PdD_{0.817}$ sample during annealing process. Sample temperature is recorded along top of graph. R(100 K) = 9.057 mΩ.

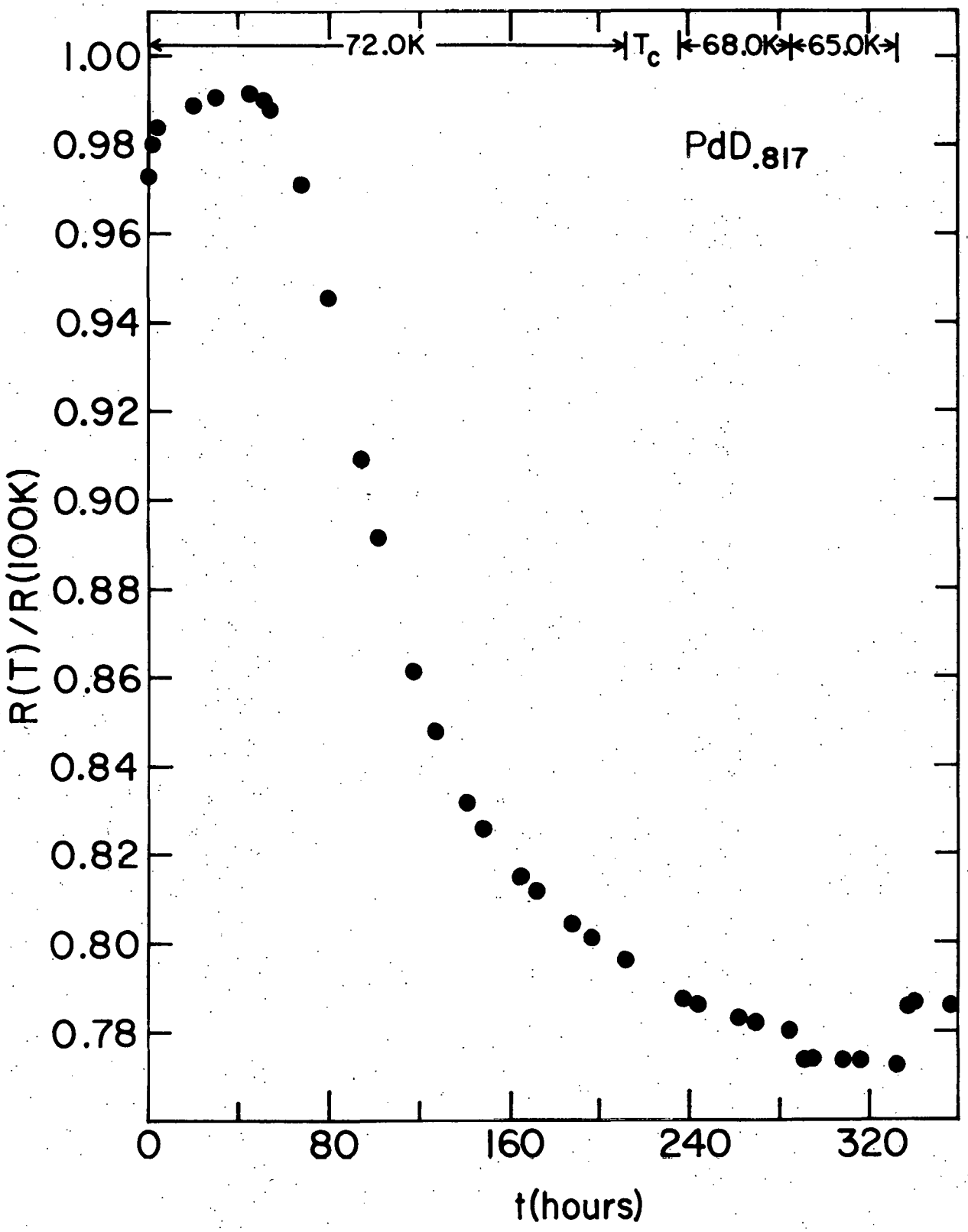
72.0K
T_c
68.0K
65.0K
$PdD_{.817}$
R(T)/R(100K)
1.00
0.98
0.96
0.94
0.92
0.90
0.88
0.86
0.84
0.82
0.80
0.78
0
80
160
240
320
t(hours)

Figure 16. Further annealing of $PdD_{0.817}$ sample.

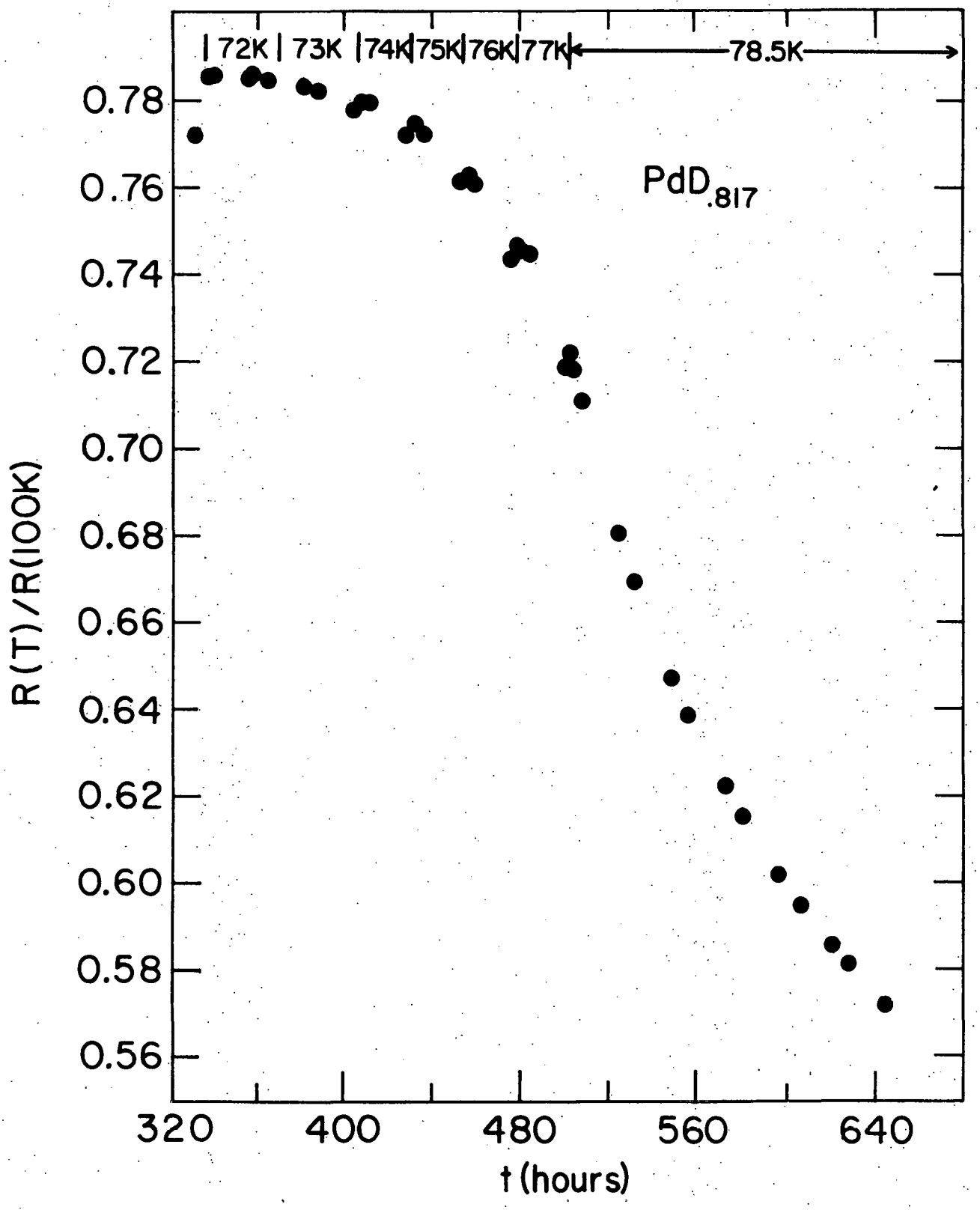
72K
73K
74K
75K
76K
77K
78.5K
PdD.817
R(T)/R(100K)
0.78
0.76
0.74
0.72
0.70
0.68
0.66
0.64
0.62
0.60
0.58
0.56
320
400
480
560
640
t (hours)

Figure 17. Superconducting transitions of $PdD_{0.817}$ in the disordered and ordered states.

(●) initial disordered T_c

(■) ordered T_c, R/R(100 K) $\approx$ 0.80

(▼) ordered T_c, R/R(100 K) $\approx$ 0.57

(▲) final disordered T_c.

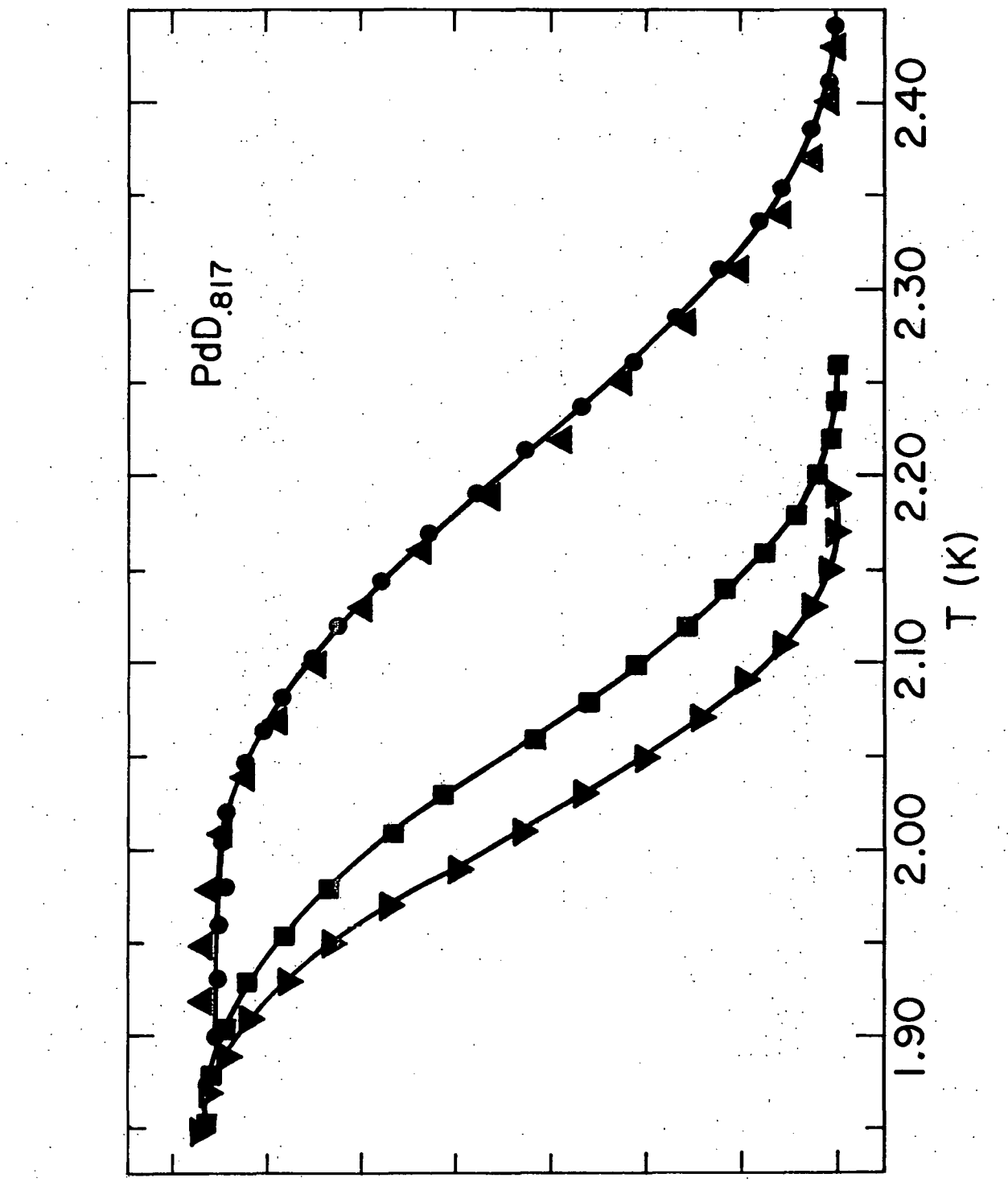
PdD.817
1.90
2.00
2.10
2.20
2.30
2.40
T (K)
DIAMAGNETIC SUSCEPTIBILITY (arbitrary units)

in the degree of depression of T_{20} and T_{80} was more pronounced, as indicated in Table 1.

Following this, the sample was warmed to 100 K to disorder it, and was then quenched again to remeasure the T_c of the disordered state. The transition temperature was restored to its original value, demonstrating that the ordering process is responsible for the change in T_c, and that the change is reversible, as is the ordering process itself. This second disordered transition lies slightly below the original disordered transition at high temperatures, and slightly above it at low temperatures, as shown in Figure 17. This may be due to a slight redistribution of D atoms during the ordering process, resulting in a slightly improved homogeneity. The difference in the two disordered state transitions is comparable to the experimental uncertainties in the data, however, so that this effect may be spurious. No such effect was seen in the other two samples.

When the $PdH_{0.837}$ sample was annealed at 72 K, the resistance rose initially, as seen in other δ-phase samples, but did not drop off again, as did the $PdD_{0.817}$ sample. Rather, the resistance levelled off, as shown in Figure 18. We quenched the sample from this level region to 4.2 K to determine the effect of SRO (which presumably causes the initial increase in resistance) on T_c. The resulting superconducting transition was identical to that of the disordered state, as shown in Figure 19.

Following this measurement, the sample temperature was again raised to continue the annealing. Raising the temperature to above 77 K resulted in a decrease in resistance, the rate of which increased

Figure 18. Resistance ratio of $PdH_{0.837}$ during annealing process. R(100 K) = 7.362 mΩ.

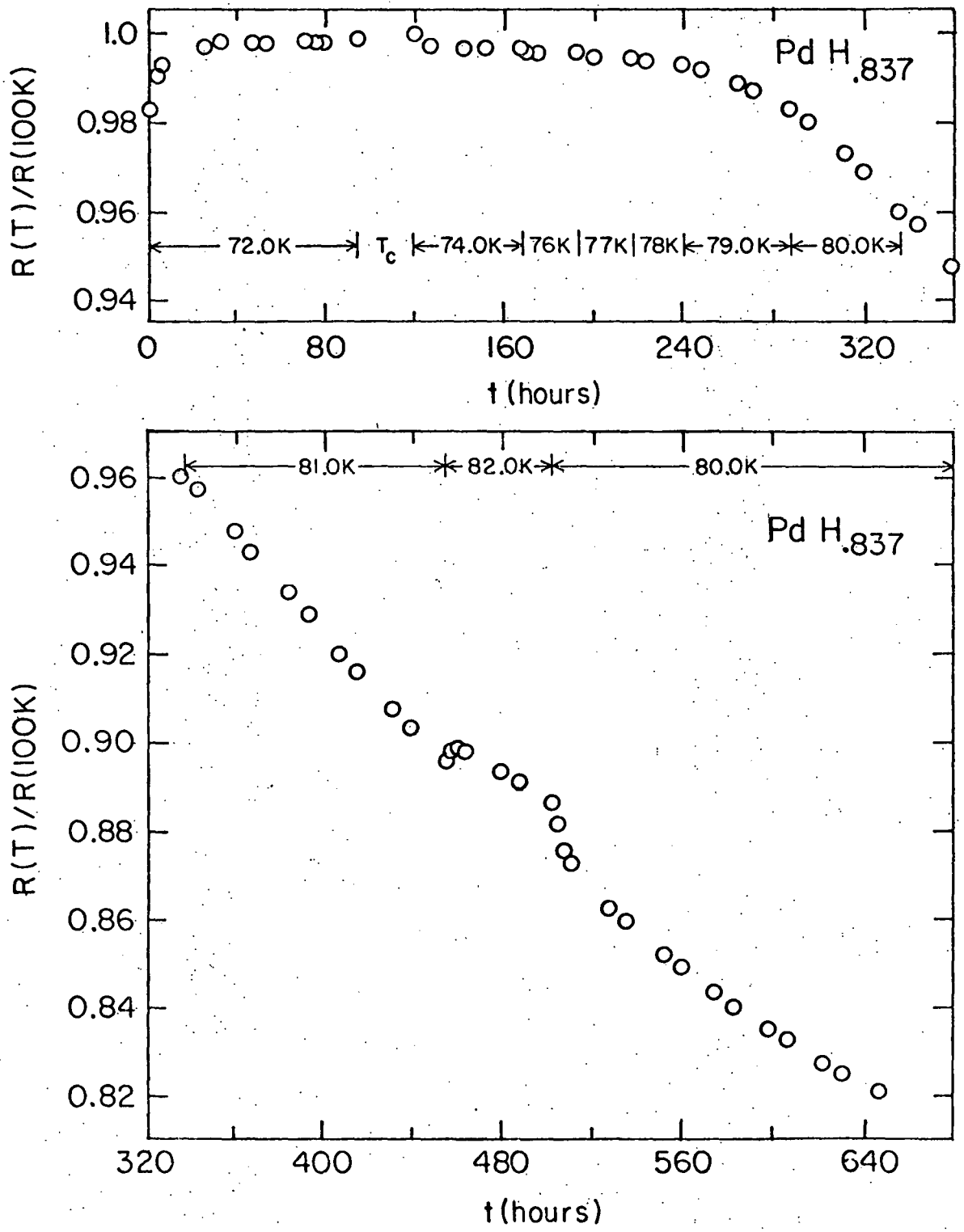
Pd H.837
R(T)/R(100K)
1.0
0.98
0.96
0.94
72.0K
T_c
74.0K
76K
77K
78K
79.0K
80.0K
0
80
160
240
320
t (hours)
Pd H.837
R(T)/R(100K)
0.96
0.94
0.92
0.90
0.88
0.86
0.84
0.82
81.0K
82.0K
80.0K
320
400
480
560
640
t (hours)

Figure 19. Superconducting transitions of $PdH_{0.837}$ in the disordered and ordered states.

(○) initial disordered T_c

(▲) SRO T_c, $R/R(100\ K) \approx 1.0$

(■) ordered T_c, $R/R(100\ K) \approx 0.82$

(▼) final disordered T_c.

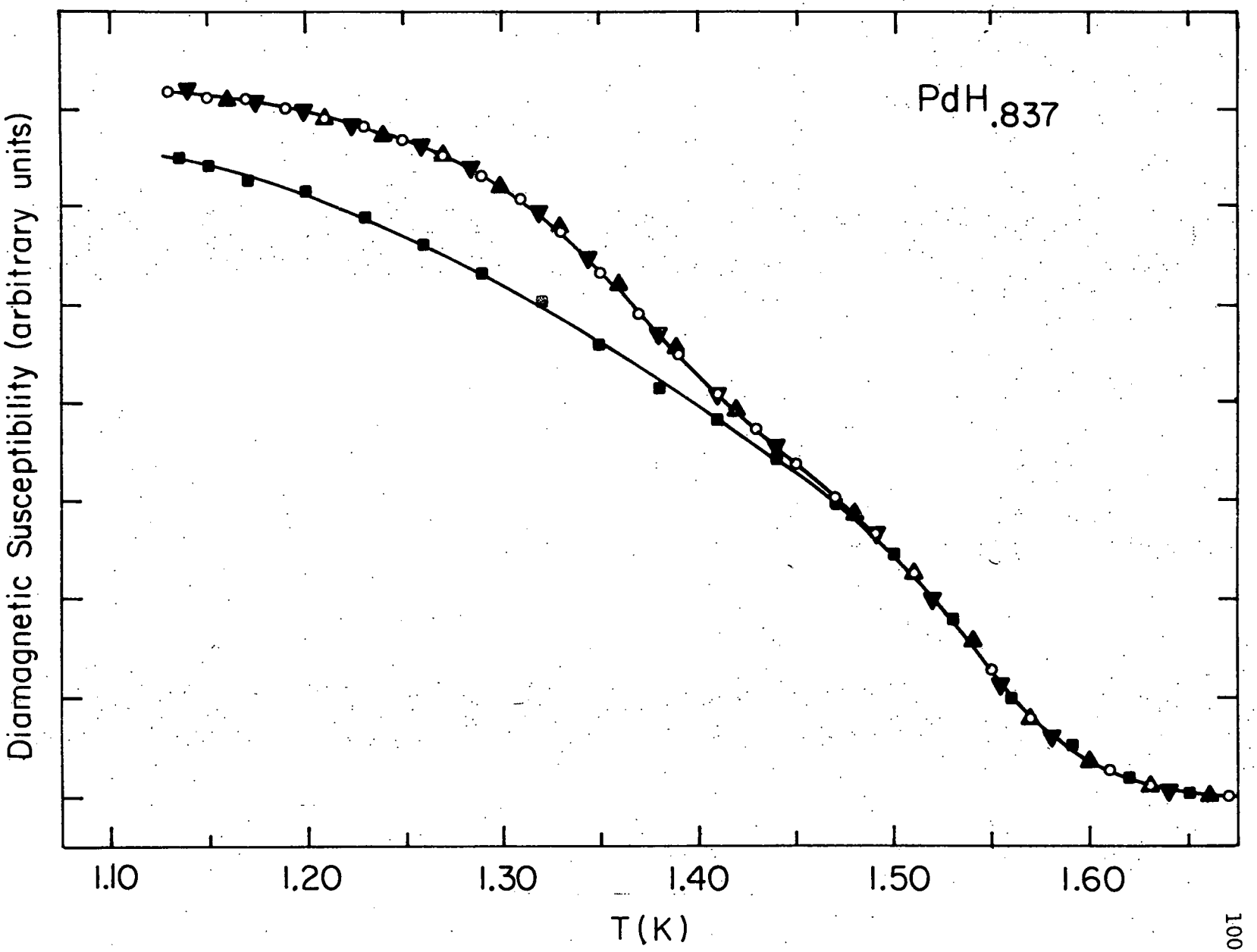
PdH.837
Diamagnetic Susceptibility (arbitrary units)
1.10
1.20
1.30
1.40
1.50
1.60
T(K)
100

with increasing temperature up to 82 K, at which temperature the rate again decreased (see Figure 18). The decrease was never as steep as in the $PdD_{0.817}$ sample, or in those observed by Ellis. Nonetheless, the resistance ultimately decreased by a large amount, indicating a significant degree of LRO.

After the resistance ratio had decreased to 0.82, the sample was quenched to 4.2 K and T_c of the ordered state was measured. It was found that the ordering process had split the transition, depressing the transition temperature of the low T_c, low concentration parts of the sample, but leaving unchanged that of the high T_c, high concentration parts (see Figure 19).

The most likely explanation of this splitting is the coexistence of both ordered δ-phase and disordered β-phase domains in this sample. There are two possible ways in which such a coexistence of phases might arise. First, the ordering process may consist of the piecemeal conversion of regions of β-phase material into regions of δ-phase material, with the splitting of the transition reflecting the fact that some regions had not yet been converted because we did not let the process go to completion. Alternatively, the concentration $x = 0.837$ may be large enough that it lies above the δ-phase portion of the phase diagram, and falls instead in a $\beta + \delta$ two-phase region. In this case, cooling the sample below $\sim$ 82 K would result in a phase separation, and hence a split transition. While we cannot rule out the first possibility entirely, we strongly favor the second explanation. The ordering of the $PdD_{0.817}$ sample produced no splitting of the superconducting transition, but instead produced a depression of the entire

transition, indicating that the entire bulk of the sample was ordering simultaneously, and that only the degree of order was increasing as the annealing progressed. It seems unlikely that the hydride sample would order region-by-region when the deuteride sample ordered uniformly.

When the $PdH_{0.837}$ sample was warmed to 100 K and then quenched to remeasure the disordered state T_c, it was found that the transition returned to its original form, as shown in Figure 19.

The third sample to be studied was a $PdD_{0.742}$ foil. Neutron diffraction data on a $PdD_{0.742}$ crystal[99] revealed only the elastic diffuse scattering associated with SRO, as described in a previous section. The behavior of the resistance of this sample during annealing, shown in Figures 20 and 21, is rather complex and difficult to interpret. Annealing the sample at 72 K produced a small decrease in resistance, similar to what one might expect if a very small portion of the sample were ordering in the δ-phase. The temperature was subsequently lowered in steps, and after each step there occurred an initial, rapid (1 - 2 hours) increase in resistance, followed by a slow decrease, until the temperature was dropped to 50 K and below, where there was little change in resistance. The initial, rapid increase in R whenever the temperature was dropped is reminiscent of the behavior of γ-phase material: the magnitude of the increase grows with decreasing T above 56 K, but is small or absent below 56 K, in much the same way that the peak in the equilibrium resistance vs. temperature for the γ-phase behaves. However, the slow decrease

Figure 20. Resistance ratio of $PdD_{0.742}$ sample during annealing process. R(100 K) = 8.003 mΩ.

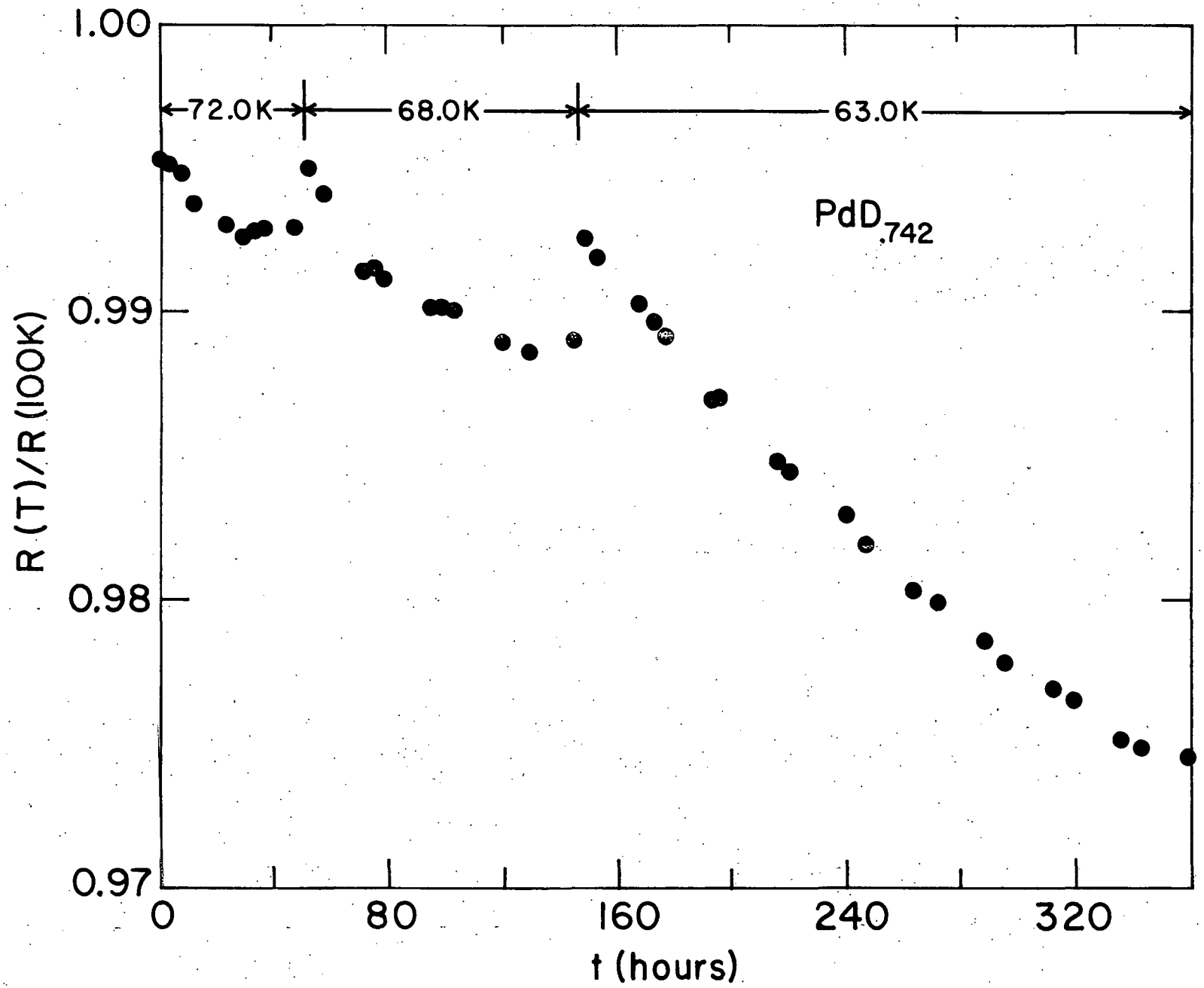
1.00
0.99
0.98
0.97
R (T)/R (100K)
72.0K
68.0K
63.0K
PdD.742
0
80
160
240
320
t (hours)

Figure 21. Further annealing of $PdD_{0.742}$ sample.

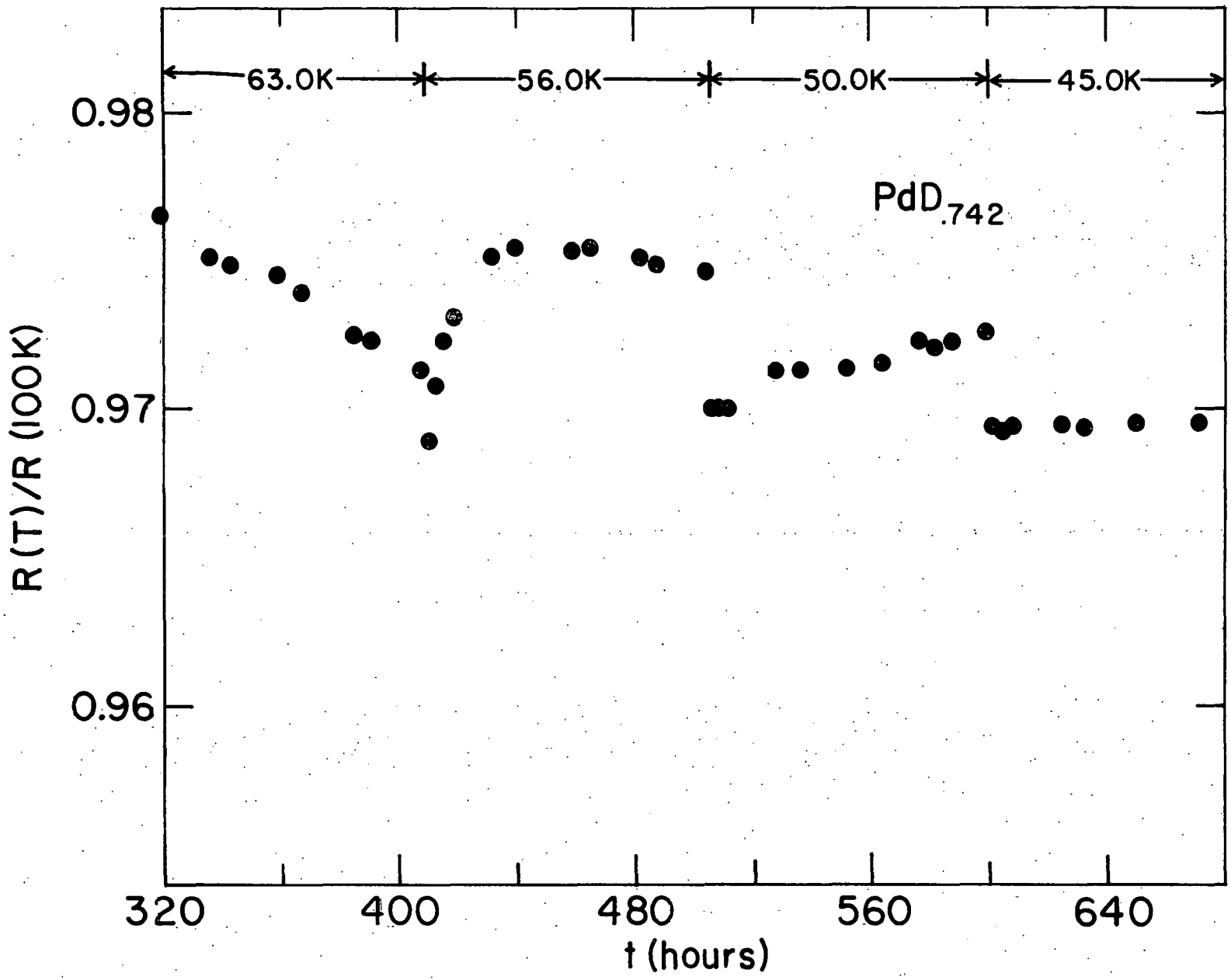
63.0K
56.0K
50.0K
45.0K
0.98
0.97
0.96
PdD.742
R(T)/R (100K)
320
400
480
560
640
t (hours)

in resistance which follows each increase is not typical of γ-phase samples, as it occurs at higher temperatures and over longer time intervals than the decreases observed in the γ-phase. As stated previously, the diffuse scattering observed in the neutron diffraction measurements of samples in this composition range is similar to that observed in the early ordering stages of the Ni_4Mo system. It is conceivable that the slow decrease in resistance which occurred at T = 63 K (see Figure 20) was due to the early stages of an ordering process which would, after a very long time, result in the formation of the $D1_a$ structure in this sample. A detailed diffraction study of samples in this concentration regime, made over long time periods, is needed to determine what sort of structural changes are occurring during annealing.

After about 650 hours of annealing, the resistance of the $PdD_{0.742}$ sample had decreased by only 2.5%, indicating that little, if any, LRO had developed. The sample was quenched to liquid He temperatures and T_c was measured. Surprisingly, the T_c was found to have increased by about 7.5%, from its disordered state value of 0.401 K to a new value of 0.431 K. The changes in T_{20} and T_{80} were also of this magnitude, reflecting the fact that the transition was essentially rigidly shifted upward in temperature by $\sim$ 30 mK. When the sample was disordered again by heating to 100 K, and then requenched to liquid He temperatures, the transition returned to its original value, as shown in Figure 22.

Discussion of Results

The $PdD_{0.817}$ and $PdII_{0.837}$ samples behaved as one would expect from the simple arguments advanced at the beginning of the chapter;

Figure 22. Superconducting transitions of $PdD_{0.742}$ in the disordered and ordered states.

(●) initial disordered T_c

(▲) ordered T_c, $R/R(100\ K) \approx 0.97$

(■) final disordered T_c.

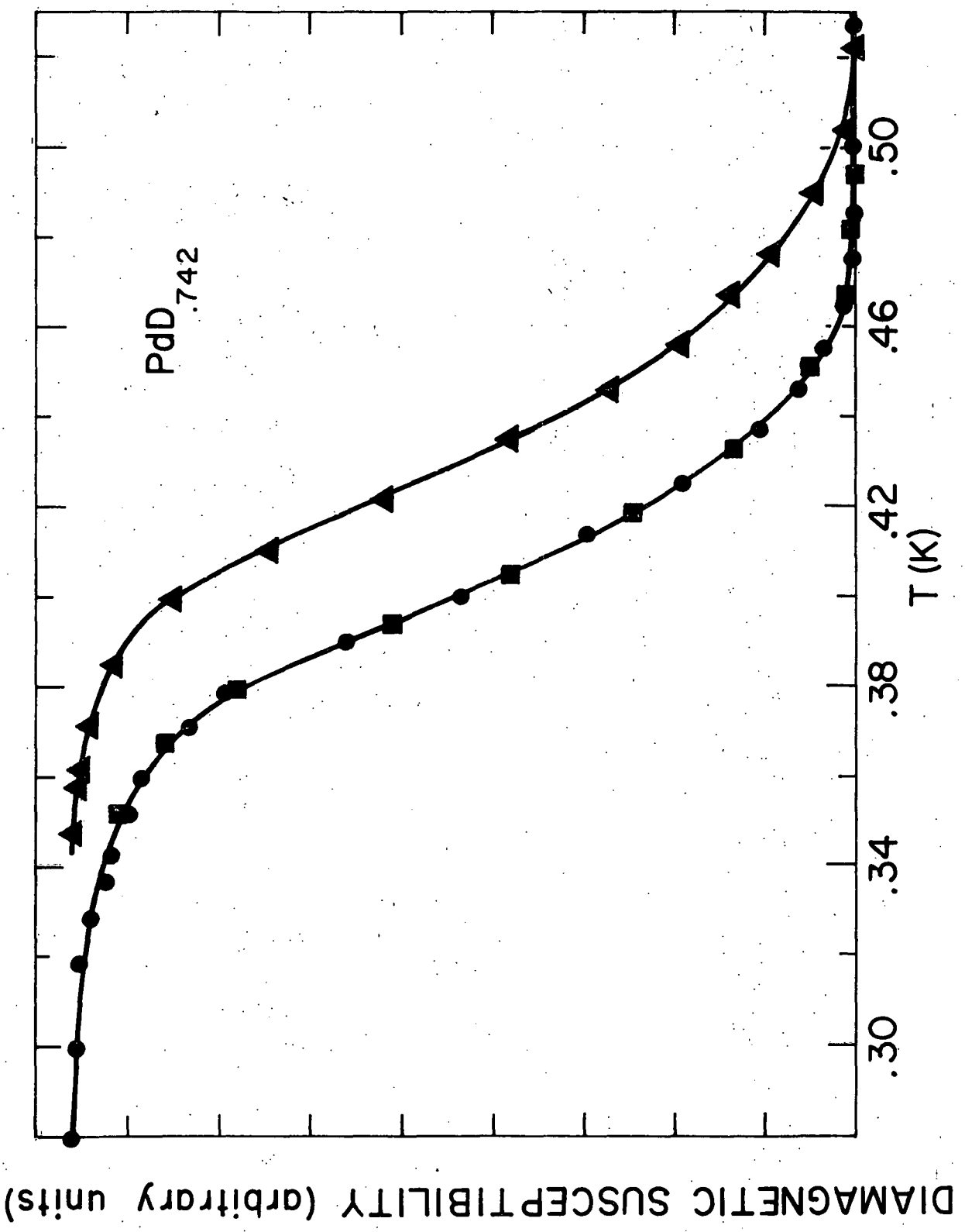
PdD.742
.30
.34
.38
.42
.46
.50
T (K)
DIAMAGNETIC SUSCEPTIBILITY (arbitrary units)

Table 1.

Temperatures at which samples attained 20% (T_{20}), 50% (T_c) and 80% (T_{80}) of maximum diamagnetism in the disordered and ordered state superconducting transitions.

Sample	Disordered State			Ordered State			Relative Change $(T^o-T^d)/T^d$		
	T^d_{20}(K)	T^d_c(K)	T^d_{80}(K)	T^o_{20}(K)	T^o_c(K)	T^o_{80}(K)	$\frac{\Delta T_{20}}{T_{20}}$	$\frac{\Delta T_c}{T_c}$	$\frac{\Delta T_{80}}{T_{80}}$
$PdD_{0.817}$	2.303	2.211	2.122	2.129	2.056	1.978	-7.6%	-7.0%	-6.8%
	(all T's ± 0.002 K)			(for R/R(100 K) $\approx$ 0.80)					
				2.073	2.008	1.944	-10.0%	-9.2%	-8.4%
				(for R/R(100 K) $\approx$ 0.57)					
$PdH_{0.837}$	1.543	1.436	1.332	1.543	1.436	1.332	0	0	0
	(all T's ± 0.002 K)			(for R/R(100 K) $\approx$ 1.0)					
				1.543	1.428	1.250	0	-0.6%	-6.2%
				(for R/R(100 K) $\approx$ 0.82)					
$PdD_{0.742}$	0.427	0.401	0.378	0.460	0.431	0.407	+7.7%	+7.5%	+7.7%
	(all T's ± 0.001 K)			(for R/R(100 K $\approx$ 0.97)					

the structural change produced by annealing depressed T_c by removing the instability that led to the structural change. The only surprise encountered was the splitting of the transition of the hydride sample upon ordering. This splitting is taken as indirect evidence that $PdH_{0.837}$ lies in a two-phase ($\beta + \delta$) region of the phase diagram. The δ-phase boundary must then lie in the concentration range $0.817 < x < 0.837$, as the transition of the $PdD_{0.817}$ sample was not split. Additional diffraction work is necessary to confirm this interpretation.

The $PdD_{0.817}$ transition and the low temperature part of the $PdH_{0.837}$ transition were both depressed by 9 - 10% of their disordered state values. The relative magnitude of this depression is similar to that observed in V_3Si when this material undergoes its martensitic transformation.[111] As the electron and phonon properties or the ordered, δ-phase of $PdH_x(D_x)$ are not yet known, we cannot ascribe the depression of T_c to any particular changes in these properties. The symmetry change (from FCC to body-centered tetragonal) produced by the ordering will result in a new, smaller Brillouin zone. This, in turn, will cause the new zone boundaries to intersect the electron and phonon dispersion relations at new points, resulting in the modification of these relations near the new zone boundaries.

A common result of such a symmetry change is the creation of new peaks in the electronic density of states caused by the flattening out of the bands near the new zone boundary. If these new peaks form in δ-phase $PdH_x(D_x)$ in such a way as to decrease the electronic density of states at the H(D) site, then a decrease in T_c would result, as discussed in Chapter III. NMR measurements of the effect

of ordering on the longitudinal relaxation time, T_1, may be able to detect such a decrease in the density of states. The absence of anomalous behavior in the magnetic susceptibility[23] near 50 K is not necessarily an indication that the electronic structure is unaffected by the ordering process, as the time scale on which these measurements were made (a few hours) was far too short to allow LRO to form. Similarly, the absence of any anomaly in the elastic constants[112] or Raman spectra[113] does not mean that the acoustic and optic phonon modes remain unchanged, as once again these samples were not given sufficient time to develop LRO. We might expect the phonon modes, particularly the optic modes, of the ordered state to be stiffer than those of the disordered state, on the general grounds that the restoring force (i.e., the force constant) is increased by the restoration of stability in the lattice brought about by the phase transition. The broad linewidths observed in the inelastic neutron scattering experiments on PdD_x,[18] attributed to the random distribution of vacancies, should also narrow when these vacancies order. Because the optic modes are so important to the superconductivity of $PdH_x(D_x)$, any changes in the optic mode spectrum may have a large effect on T_c. New inelastic neutron scattering experiments on the ordered, δ-phase of $PdD_{0.78}$, which are already under way,[114] should reveal any changes in the phonon spectrum produced by ordering.

The enhancement of T_c in the $PdD_{0.742}$ sample which the annealing produced was a surprise. In the context of our hand-waving arguments that increased stability leads to a decreased T_c, we must infer that somehow the instability of this sample was increased by the annealing

treatment. Any attempt to explain this T_c enhancement in terms of symmetry changes produced by the ordering is fraught with difficulty. Because we have only SRO present in this sample, we have no translational symmetry beyond that on a microdomain size scale. Thus a discussion of electron and phonon properties based on a change in the Brillouin zone is of dubious merit.

When the enhancement of T_c in $PdD_{0.742}$ and the depression of T_c in $PdD_{0.817}$ and $PdH_{0.837}$ are considered along with the neutron diffraction results, we claim that it is not necessary to know the details of what happens to the electrons and phonons during the annealing process. Instead, all of these results fit neatly into the more general theory of dynamic instabilities in high T_c superconductors advanced by Ngai and Reinecke.[115,116]

Ngai and Reinecke propose that, in an unstable material, the local ground-state configuration (electronic and/or ionic) is separated by a small energy difference and low potential barrier from one or more other possible configurations. The electrons and phonons in the material can induce transitions between these various local configurations, and the authors dub these transitions "local structural excitations" or LSE's.

The interaction of LSE's with phonons leads to several modifications of the phonon properties. In the Pd-H(D) system, Ngai and Reinecke show that LSE-phonon coupling can qualitatively account for the marked softness of the optic modes, the large mean-squared displacement of the H(D) vibrations, the anharmonicity of the optic modes, and the H(D)-Pd force constant difference. The phonon mode

softening induced by the LSE's will increase the electron-phonon coupling, and hence T_c. Additionally, the electron-LSE interaction can produce an attractive electron-electron interaction mediated directly by the LSE's, as well as that mediated by the phonons, further enhancing T_c. When the degree of lattice instability becomes too large, the lattice will undergo a structural transition which, the authors predict, will split the nearly degenerate energy levels, lowering one level below the others. The increased energy difference between the lower level and the upper levels suppresses LSE's from the lower to upper levels, and so leads to a reduction in T_c and a stiffening of the phonon frequencies.

The interpretation of the diffuse diffraction intensity from SRO-phase PdD_x as being due to coexistence of DO_{22} and Dl_a microdomains is consistent with the LSE model; the DO_{22} and Dl_a structures may represent two possible lattice configurations which are closely spaced in energy and which are competing to establish LRO. The PdD_x neutron diffraction data show that this type of diffuse scattering persists at high temperatures (up to 150 K), even at short annealing times (about 30 minutes), and at higher concentrations ($x = 0.78$), where it appears as a precursor to the formation of the δ-phase at lower temperatures.[99] Thus it seems likely that even in quenched, disordered samples there is a small amount of SRO present in the form of microdomains of DO_{22} and Dl_a structures. LSE's between these configurations may account for the unusual phonon properties of $PdH_x(D_x)$ mentioned above, and may also enhance T_c.

Annealing of high concentration (δ-phase) samples results in the diffuse scattering being replaced by the sharp superlattice line at (4/5, 2/5, 0).[99] In the model of Ngai and Reinecke, this could reflect the lowering in energy of the Dl_a configuration below that of the DO_{22} configuration, which would suppress the LSE's. This would have several consequences in the Ngai-Reinecke model: (1) T_c would be depressed, (2) the optic mode frequencies would be increased, and (3) the H(D)-Pd force constant difference would be decreased. We have already noted the depression of T_c upon formation of the δ-phase. The inelastic neutron scattering results will tell whether the optic mode frequencies increase in the δ-phase. Measurement of T_c vs. x for several δ-phase samples of PdH_x and PdD_x would shed some light on the third effect; if LSE's are responsible, at least in part, for the force constant difference, then the reverse isotope effect should be diminished (or perhaps even revert to normal) in the δ-phase, where the LSE's are suppressed.

The neutron diffraction results[99] show that annealing of lower concentration ($0.71 \lesssim x \lesssim 0.75$) samples produces a fivefold increase of the diffuse scattering intensity, but no change in the intensity distribution, which may imply the nucleation of more microdomains or the increase in order in the present microdomains. If this produces an enhancement of LSE's, then an increase in T_c would result, such as that seen experimentally. In this case, we might also expect a further softening of the optic phonon frequencies in the SRO-phase, detectable by inelastic neutron scattering. Theoretically, an increase in the magnitude of the reverse isotope effect would also result, but this

would be difficult to verify experimentally, as the T_c of PdH_x is vanishingly small in this concentration range.

In summary, the LSE model of Ngai and Reinecke can qualitatively account for the observed behavior of T_c in the ordered phases of $PdH_x(D_x)$. The relative change in T_c ($\sim \pm 10\%$) produced by annealing is of the same magnitude as the underestimation of T_c values obtained from current theoretical calculations on β-phase $PdH_x(D_x)$ described in Chapter III. Other than through the observed force constant difference, the effects of LSE's on the T_c of $PdH_x(D_x)$ have not been included in the present theories. Their inclusion should help bring the calculated values of T_c into closer agreement with experiment. Measurement of the phonon frequencies in the ordered phases will provide an additional test of the LSE model.

V. SUMMARY

The experimental work presented in Chapter III of this thesis demonstrates that the current theoretical treatment of superconductivity in $PdH_x(D_x)$, in simplifying the problem, has omitted some of the contributions to superconductivity in this system. In particular, an explanation of the reverse isotope effect based soley on the observed difference in force constants results in an underestimate of its magnitude. To bring the calculated magnitude of the reverse isotope effect into agreement with experiment, we suggest that the effect of zero-point motion of the H(D) atom on its electronic environment must be included as well. Experimental evidence of a difference in electronic structures of PdH_x and PdD_x is now emerging.

The inclusion of the electronic difference will increase the calculated magnitude of the reverse isotope effect, but will exacerbate the underestimation of T_c in PdH_x (the calculated values of T_c for PdD_x already being seriously underestimated). To increase these calculated T_c values, we believe that the coupling of conduction electrons to the acoustic mode vibrations of the H(D) atoms should be included.

The experimental work in Chapter IV shows that the ordering of H(D) atoms in substoichiometric $PdH_x(D_x)$ can have a sizeable effect on the superconducting transition. The formation of long range order in the δ-phase led to a reduction of T_c while the enhancement of short range order in a lower concentration sample led to an increase in T_c.

These findings agree with the qualitative trends predicted in the "local structural excitation" model advanced by Ngai and Reinecke. The effects of these excitations on the T_c of β-phase $PdH_x(D_x)$ have not been explicitly included in the current theoretical calculations. Their inclusion should also tend to increase the calculated values of T_c, bringing them into closer agreement with experiment. This LSE model represents an important step in trying to quantitatively deal with the effects of structural instabilities in superconductors. The experimental support which we find for this model gives us hope that an understanding of the relationship between instability and high T_c's is near at hand, and that such an understanding may lead to new advances in high temperature superconductivity.

REFERENCES

1. D. G. Westlake, C. B. Satterthwaite and J. H. Weaver, Physics Today 31, 32 (November 1978).

2. Topics in Applied Physics, Vol. 28, 29 - Hydrogen in Metals I, II, edited by G. Alefeld and J. Volkl (Springer-Verlag, New York, 1978).

3. T. Graham, Phil. Trans. R. Soc. 156, 415 (1866).

4. A. Maeland and T. B. Flanagan, J. Phys. Chem. 68, 1419 (1964).

5. J. Vuillemin, Phys. Rev. 144, 396 (1966).

6. F. M. Mueller, A. J. Freeman, J. O. Dimmock and A. M. Furdyna, Phys. Rev. B1, 4617 (1970).

7. G. G. Low and T. M. Holden, Proc. Phys. Soc. (London), 89, 119 (1966).

8. R. A. Webb, J. B. Ketterson, W. P. Halperin, J. J. Vuillemin and N. B. Sandesara, J. Low Temp. Phys. 32, 659 (1978).

9. J. E. Schirber and B. Morosin, Phys. Rev. B12, 117 (1975).

10. J. E. Worsham, Jr., M. K. Wilkinson and C. G. Shull, J. Phys. Chem. Solids 3, 393 (1957).

11. C. A. Mackliet and A. I. Schindler, Phys. Rev. 146, 463 (1966).

12. C. A. Mackliet, D. J. Gillespie and A. I. Schindler, Solid State Commun. 15, 207 (1974).

13. C. A. Mackliet, D. J. Gillespie and A. I. Schindler, J. Phys. Chem. Solids 37, 379 (1976).

14. M. Zimmermann, G. Wolf and K. Bohmhammel, phys. stat. sol.(a) 31, 511 (1975).

15. G. Wolf and M. Zimmermann, phys. stat. sol.(a) 37, 485 (1976).

16. J. M. Rowe, J. J. Rush, H. G. Smith, Mark Mostoller and H. E. Flotow, Phys. Rev. Lett. 33, 1297 (1974).

17. J. M. Rowe, personal communication.

18. C. J. Glinka, J. M. Rowe, J. J. Rush, A. Rahman, S. K. Sinha and H. E. Flotow, Phys. Rev. B17, 488 (1978).

19. M. R. Chowdhury and D. K. Ross, Solid State Commun. 13, 229 (1973).

20. J. D. Jorgensen, K. Sköld, A. Rahman, C. A. Pelizzari, H. E. Flotow, R. J. Miller, R. Standley and T. O. Brun, Conference on Neutron Scattering, Gatlinburg, Tennessee, June 6-10, 1976, Vol. I, p. 535.

21. A. Rahman, K. Sköld, C. Pelizzari, S. K. Sinha and H. E. Flotow, Phys. Rev. B14, 3630 (1976).

22. H. C. Jamieson and F. D. Manchester, J. Phys. F2, 323 (1972).

23. R. J. Miller, T. O. Brun and C. B. Satterthwaite, Phys. Rev. B18, 5054 (1978).

24. A. C. Switendick, Ber. Buns. Phys. Chem. 76, 535 (1972).

25. J. S. Faulkner, Phys. Rev. B13, 2391 (1976).

26. C. D. Gelatt, Jr., Jacquelyn A. Weiss and H. Ehrenreich, Solid State Commun. 17, 663 (1975).

27. J. Zbasnik and M. Mahnig, Z. Physik B23, 15 (1976).

28. G. Cubiotti and B. Ginatempo, J. Phys. C12, L551 (1979).

29. M. Gupta and A. J. Freeman, Phys. Rev. B17, 3029 (1978).

30. D. A. Papaconstantopoulos, B. M. Klein, E. N. Economou and L. L. Boyer, Phys. Rev. B17, 141 (1978).

31. D. A. Papaconstantopoulos, B. M. Klein, J. S. Faulkner and L. L. Boyer, Phys. Rev. B18, 2784 (1978).

32. D. E. Eastman, J. K. Cashion and A. C. Switendick, Phys. Rev. Lett. 27, 35 (1971).

33. F. Antonangeli, A. Balzarotti, A. Bianconi, E. Burattini, P. Perfetti and N. Nistico, Phys. Lett. 55A, 309 (1975).

34. L. E. Storm, personal communication.

35. C. L. Wiley and F. Y. Fradin, Phys. Rev. B17, 3462 (1978).

36. J. Bardeen, L. N. Cooper and J. R. Schrieffer, Phys. Rev. 106, 162 (1957).

37. N. W. Ashcroft, Phys. Rev. Lett. 21, 1748 (1968).

38. T. Schneider and E. Stoll, Physica 55, 702 (1971).

39. B. Baranowski, T. Skoskiewicz and A. W. Szafranski, Sov. J. Low Temp. Phys. 1, 296 (1975).

40. C. B. Satterthwaite and D. T. Peterson, J. Less-Common Met. 26, 361 (1972).

41. B. T. Matthias, T. H. Geballe and V. B. Compton, Rev. Mod. Phys. 35, 1 (1963).

42. M. F. Merriam and D. S. Schreiber, J. Phys. Chem. Sol. 24, 1375 (1963).

43. C. B. Satterthwaite and I. L. Toepke, Phys. Rev. Lett. 25, 741 (1970).

44. R. Caton and C. B. Satterthwaite, J. Less-Common Met. 52, 307 (1977).

45. T. Skoskiewicz, phys. stat. sol.(a) 11, K123 (1972).

46. T. Skoskiewicz, phys. stat. sol.(b) 59, 329 (1973).

47. T. Skoskiewicz, A. W. Szafranski, W. Bujnowski and B. Baranowski, J. Phys. C7, 2670 (1974).

48. J. E. Schirber and C. J. M. Northrup, Jr., Phys. Rev. B10, 3818 (1974).

49. R. J. Miller and C. B. Satterthwaite, Phys. Rev. Lett. 34, 144 (1975).

50. B. Stritzker, Z. Physik 268, 261 (1974).

51. C. G. Robbins, M. Ishikawa, A. Treyvaud and J. Muller, Solid State Commun. 17, 903 (1975).

52. C. G. Robbins and J. Muller, J. Less-Common Met. 42, 19 (1975).

53. See, for example, D. J. Scalapino, in Superconductivity, edited by R. D. Parks (Marcel Dekker, Inc., New York, 1969), p. 449.

54. G. M. Eliashberg, Sov. JETP 11, 696 (1960).

55. W. L. McMillan, Phys. Rev. 167, 331 (1968).

56. K. H. Benneman and J. W. Garland, in Superconductivity in d- and f-Band Metals, edited by D. H. Douglass, AIP Conference Proceedings, No. 4, 1972.

57. P. B. Allen and R. C. Dynes, Phys. Rev. B12, 905 (1975).

58. K. H. Benneman and J. W. Garland, Z. Physik 260, 367 (1973).

59. F. Heininger, E. Bucher and J. Muller, Phys. Kond. Materie 5, 243 (1966).

60. S. Auluck, Lett. Nuovo Cim. 7, 545 (1973).

61. J. E. Schirber, Phys. Lett. 46A, 285 (1973).

62. W. Buckel, A. Eichler and B. Stritzker, Z. Physik, 263, 1 (1973).

63. B. N. Ganguly, Z. Physik 265, 433 (1973).

64. H. Rietschel, Z. Physik B22, 133 (1975).

65. G. Sicking, Ber. Bunsenges. Phys. Chem. 76, 790 (1972).

66. J. C. H. Chiu and R. A. B. Devine, Solid State Commun. 22, 631 (1977).

67. A. Eichler, H. Wuhl and B. Stritzker, Solid State Commun. 17, 213 (1975).

68. L. Dumoulin, P. Nedellec, C. Arzoumanian, and J. P. Burger, phys. stat. sol.(b) 90, 207 (1978).

69. D. A. Papaconstantopoulos and B. M. Klein, Phys. Rev. Lett. 35, 110 (1975).

70. B. M. Klein and D. A. Papaconstantopoulos, J. Phys. F6, 1135 (1976).

71. B. M. Klein, E. N. Economou, and D. A. Papaconstantopoulos, Phys. Rev. Lett. 39, 574 (1977).

72. D. A. Papaconstantopoulos, personal communication.

73. Pd obtained from Materials Research Corporation, Orangeburg, N.Y.

74. J. C. Barton, F. A. Lewis and I. Woodward, Trans. Faraday Soc. 59, 1201 (1963).

75. R. J. Miller, Ph.D. Thesis, University of Illinois at Urbana-Champaign, 1976 (unpublished).

76. V. B. Ginodman, L. N. Zherikhina and A. V. Inyushkin, Sov. J. Low Temp. Phys. 5, 387 (1979)

77. U. Mizutani, T. B. Massalski, J. Bevk and R. R. Vandervoort, J. Phys. F7, L63 (1977).

78. J. S. Brown, Physics Lett. 51A, 99 (1975).

79. Natthi Singh, V. K. Jindal and K. N. Pathak, Phys. Rev. B18, 3271 (1978).

80. W. J. Venema, R. P. Griessen and H. L. M. Bakker, Bull. Am. Phys. Soc. 25, 247 (1980).

81. P. Jena, C. L. Wiley and F. Y. Fradin, Phys. Rev. Lett. 40, 578 (1978).

82. P. Jena, F. Y. Fradin and D. E. Ellis, Phys. Rev. B20, 3543 (1979).

83. J. P. Burger and D. S. MacLachlan, J. Physique 37, 1227 (1976).

84. B. T. Matthias, T. H. Geballe and V. B. Compton, Rev. Mod. Phys. 35, 1 (1963).

85. L. Testardi, Rev. Mod. Phys. 47, 637 (1975).

86. J. C. Phillips, Phys. Rev. Lett. 26, 543 (1971).

87. L. Testardi, Comments Solid State Phys. 6, 131 (1975).

88. D. M. Nace and J. G. Aston, J. Am. Chem. Soc. 79, 3623 (1957); ibid. 3627.

89. T. E. Ellis, Ph.D. Thesis, University of Illinois at Urbana-Champaign, 1978 (unpublished).

90. C. B. Satterthwaite, T. E. Ellis and R. J. Miller, Proc. Int. Conf. of Transition Metals, Toronto (August 1977).

91. S. Zepeda and F. D. Manchester, J. Low Temp. Phys. 4, 127 (1971).

92. I. S. Anderson, C. J. Carlisle and D. K. Ross, J. Phys. C11, L381 (1978).

93. I. S. Anderson, D. K. Ross and C. J. Carlisle, Phys. Lett. 68A, 249 (1978).

94. T. E. Ellis, C. B. Satterthwaite, M. H. Mueller and T. O. Brun, Phys. Rev. Lett. 42, 456 (1978).

95. C. B. Satterthwaite, R. W. Standley, R. C. Potter, M. H. Mueller, T. O. Brun, R. L. Hitterman and H. W. Knott, Bull. Am. Phys. Soc. 25, 181 (1980).

96. O. Blaschko, R. Klemencic, P. Weinzierl and O. J. Eder, Solid State Commun. 27, 1149 (1978).

97. O. Blaschko, R. Klemencic, P. Weinzierl and O. J. Eder, J. Phys. F9, L113 (1979).

98. O. Blaschko, R. Klemencic, P. Weinzierl, O. J. Eder and W. Just, to be published.

99. O. Blaschko, R. Klemencic, P. Weinzierl, O. J. Eder and P. von Blanckenhagen, to be published.

100. M. H. Mueller, personal communcation.

101. P. R. Okamoto and G. Thomas, Acta Met. 19, 825 (1971).

102. The ultra pure Pd foil was graciously provided by J. A. Mydosh of Kamerlingh Onnes Laboratory, Leiden.

103. Lake Shore Cryotronics, Columbus, Ohio, model GR-200A-(100).

104. Lake Shore Cryotronics, Columbus, Ohio, model Pt-102.

105. Ge-Au resistor supplied by B. Dodson of the University of Illinois.

106. Cryotronics, Inc., High Bridge, N.J., model 155B.

107. Data Precision, Danvers, Ma., model 3500.

108. Honeywell Co., Philadelphia, Pa., model 2783.

109. Keithley Instruments, Inc., Cleveland, Oh., model 148.

110. Roger P. Ries and B. Keith Moore, Rev. Sci. Inst. 41, 996 (1970).

111. M. Dayan, A. M. Goldman, C.-C. Huang, M. C. Chiang and L. E. Toth, Phys. Rev. Lett. 42, 335 (1979).

112. R. Sherman, H. K. Birnbaum, J. A. Holy and M. V. Klein, Phys. Lett. 62A, 353 (1977).

113. D. K. Hsu and R. G. Leisure, Phys. Rev. B20, 1339 (1979).

114. R. Klemencic, personal communication.

115. K. L. Ngai and T. L. Reinecke, Phys. Rev. B16, 1077 (1977).

116. K. L. Ngai and T. L. Reinecke, J. Phys. Chem. Solids 39, 793 (1978).

VITA

Robert Wendell Standley was born in [redacted] He received his secondary education at Lake Forest High School in Lake Forest, Illinois, graduating in June, 1970. He attended the California Institute of Technology for four years, graduating with a Bachelor of Science degree in physics in June, 1974. Since that time, he has attended the University of Illinois at Urbana-Champaign, where he received a Master of Science degree in physics in October, 1975. He was awarded a University Fellowship in physics for the academic years 1977-1978 and 1978-1979. He is a member of the American Physical Society, the American Association for the Advancement of Science, the Federation of American Scientists and the honor society of Phi Kappa Phi.